Fault-Tolerant Cooperative Control Design for a Team of Car-Like Vehicles with Actuator Faults and Fading Channels

by

Mahmoud Ali M. HUSSEIN

MANUSCRIPT-BASED THESIS PRESENTED TO ÉCOLE DE TECHNOLOGIE SUPÉRIEURE IN PARTIAL FULFILLMENT FOR THE DEGREE OF DOCTOR OF PHILOSOPHY
Ph.D.

MONTREAL, "SEPTEMBER 30, 2023"

ÉCOLE DE TECHNOLOGIE SUPÉRIEURE
UNIVERSITÉ DU QUÉBEC

BOARD OF EXAMINERS

THIS THESIS HAS BEEN EVALUATED

BY THE FOLLOWING BOARD OF EXAMINERS

Prof. Zhaoheng Liu, Thesis supervisor
Département de génie mécanique, École de technologie supérieure

Prof. Youmin Zhang, Thesis Co-supervisor
Department of Mechanical, Industrial, and Aerospace Engineering, Concordia University

Prof. Sheldon Andrews, Chair, Board of Examiners
Département des logiciels et TI, École de technologie supérieure

Prof. Henri Champliaud, Member of the Jury
Département de génie mécanique, École de technologie supérieure

Prof. Ya-Jun Pan, External Independent Examiner
Department of Mechanical Engineering, Dalhousie University

THIS THESIS WAS PRESENTED AND DEFENDED

IN THE PRESENCE OF A BOARD OF EXAMINERS AND THE PUBLIC

ON "AUGUST 29, 2023"

AT ÉCOLE DE TECHNOLOGIE SUPÉRIEURE

DEDICATION

To the memory of my mother, the great woman who dedicated her life to us

ACKNOWLEDGEMENTS

First, I would like to express my deep and sincere gratitude to my research supervisors Prof. Zhaoheng Liu and Prof. Youmin Zhang, for allowing me to do my Ph.D. research and providing invaluable guidance, continuous support, and encouragement throughout this research. Without their consistent assistance, great support, and insightful guidance, I would not have been able to complete this study project. I constantly feel inspired by their enthusiasm, diligence, and knowledge, and these qualities are the greatest gifts I could ever want to receive.

My sincere thanks also go to the jury members for their acceptance to evaluate my thesis and for their advice to improve this work.

Words are not enough to express my deepest feelings to my father, brothers, and sisters, who have given me unconditional and endless love.

Special thanks to my wife, Huda, and my children Ahmed, Amean, Adam, and Nour for their patience, support, and the sacrifice they had to make. Their support is the key ingredient for any achievements I have ever made.

Finally, my thanks would be incomplete if I do not mention my friends and colleagues who supported me directly or indirectly to achieve this research work.

Conception d’une commande coopérative tolérante aux fautes pour une équipe de véhicules de type automobile avec des défauts d’actionneurs et d’évanouissement de canaux

Mahmoud Ali M. HUSSEIN

RÉSUMÉ

Cette thèse de doctorat propose de nouvelles approches de contrôle coopératif tolérant aux fautes pour le groupe de véhicules de type automobile soumis à des pannes d’actionneurs, à des canaux de communication évanescents et à des perturbations externes. Dans cette étude, l’accent est mis sur les défauts des actionneurs car ceux-ci jouent un rôle clé dans la stabilité des systèmes physiques et peuvent avoir un impact significatif sur les systèmes de contrôle et provoquer des accidents catastrophiques lorsqu’ils subissent des défaillances. Les défaillances des actionneurs peuvent résulter du vieillissement ou de la détérioration de leurs composants, ce qui conduit à une éventuelle distorsion ou à une perte d’efficacité de l’actionneur.

Cette thèse vise à approfondir l’étude de l’impact des défauts de l’actionneur sur la stabilité des systèmes de commande en réseau, en tenant compte des canaux à affaiblissement et des perturbations externes, tout en considérant des problèmes liés à l’actionneur qui n’ont pas été abordés dans les études relatives. À cette fin, trois approches coopératives tolérantes aux fautes ont été développées et validées par des simulations numériques et des tests expérimentaux en temps réel en utilisant la dernière version du Quanser self-driving car QCar.

La première approche est le contrôle de formation tolérant aux fautes distribuées (CFTFD), qui vise à contrôler un groupe de véhicules semblables à des voitures, soumis à des fautes d’actionneurs additives. Dans la conception du CFTFD, nous prenons en compte la dynamique des véhicules réels et traitons le problème des défaillances partielles et graves des actionneurs. En outre, nous fournissons des solutions au problème de formation de réaffectation pour les véhicules sains en présence d’un ou de plusieurs véhicules présentant des défauts d’actionneurs graves/complets. Le CFTFD que nous proposons peut réduire la charge de calcul due à la mise en œuvre de l’algorithme de contrôle de manière distribuée par chaque véhicule et fournit un système globalement fiable contre les changements soudains qui peuvent survenir dans les actionneurs au cours de la mission de formation. Le schéma CFTFD est conçu sur la base d’un observateur à mode glissant d’ordre élevé pour détecter et isoler les défauts additifs des actionneurs, qui sont superposés aux signaux de commande, et l’algorithme de super-torsion pour compenser l’impact de ces défauts d’actionneur. Les preuves rigoureuses sont fournies pour garantir l’efficacité de la CFTFD proposée en présence des défauts étudiés. Les résultats expérimentaux ont démontré l’efficacité du CFTFD en fournissant une réponse plus rapide à l’apparition de défauts et de bonnes performances dans la gestion des défauts partiels et graves des actionneurs par rapport aux études récemment rapportées.

La deuxième est l’approche du contrôle coopératif tolérant aux fautes (CCTF). L’objectif de cette approche est de contrôler une équipe de véhicules de type automobile soumis à des défaillances multiplicatives et additives des actionneurs en présence d’informations de voisinage

estompées. La motivation de cette étude provient de l'observation que les agents échangent des informations sur des réseaux sans fil, qui introduisent intrinsèquement un évanouissement aléatoire des signaux transmis. Dans le contrôle coopératif des systèmes en réseau avec une largeur de bande de communication restreinte, l'interaction continue entre les agents voisins augmenterait inévitablement la charge de transmission du réseau et limiterait l'application pratique du système. Il est donc important d'étudier comment garantir la convergence des membres de l'équipe vers la trajectoire souhaitée en présence de défauts de l'actionneur à l'aide de données contaminées. Dans la conception du CCTF, nous avons tout d'abord étudié l'impact du problème des canaux d'évanouissement sur les performances des véhicules de type automobile. Nous avons ensuite étudié l'impact de l'apparition simultanée de canaux d'évanouissement et de défauts de l'actionneur. La CCTF est conçue sur la base de la technique du mode glissant terminal intégral, connue pour sa réactivité, sa robustesse et sa stabilité dans des conditions inconnues.

À notre connaissance, aucune des études existantes n'a fait état de résultats sur le problème des défauts d'actionneur avec des informations de voisinage évanouies. Il s'agit de la première tentative d'étude de l'apparition simultanée de canaux d'évanouissement et de défauts d'actionneurs pour une équipe de véhicules de type automobile. Les performances du CCTF sont validées avec succès par des expériences en temps réel.

Enfin, dans la troisième approche, le contrôle coopératif adaptatif tolérant aux défauts (CCATD), nous étudions davantage le problème des canaux d'évanouissement et les défauts de l'actionneur en présence de perturbations externes. Le CCATD est développé sur la base du contrôle en mode glissant terminal rapide non singulier afin d'accélérer le suivi du consensus et la convergence de l'ensemble du système. Ce contrôleur est conçu pour gérer à la fois les défauts multiplicatifs et additifs des actionneurs ainsi que l'aléa multiplicative du canal d'évanouissement. L'impact sur la performance de l'équipe de l'effacement des informations de voisinage et des défauts des actionneurs avec des perturbations externes est étudié. La théorie de la stabilité de Lyapunov démontre que le contrôleur peut garantir une bonne performance du système global indépendamment de ces problèmes. En outre, la synchronisation des véhicules peut être assurée. Par rapport aux méthodes de contrôle tolérantes aux faute existantes, la méthode que nous proposons a une structure simple et peut être facilement mise en œuvre dans la pratique. Des simulations sont fournies pour valider les résultats théoriques.

Mots-clés: Contrôle tolérant aux fautes, détection et diagnostic des défaillances, contrôle coopératif, défaut de l'actionneur, canal de communication à évanouissement, robots mobiles, véhicule de type automobile.

Fault-Tolerant Cooperative Control Design for a Team of Car-Like Vehicles with Actuator Faults and Fading Channels

Mahmoud Ali M. HUSSEIN

ABSTRACT

This doctoral thesis proposes novel fault-tolerant cooperative control approaches for a team of car-like vehicles subject to actuator faults, fading communication channels, and external disturbances. In this study, the focus is more on the actuator faults due to the fact that actuators play a key role in the stability of physical systems and can significantly impact control systems and result in catastrophic accidents when they experience some failures. Actuator faults can result from the aging or deterioration of actuator components, leading to the actuator's eventual bias or loss of effectiveness.

This thesis aims to further investigate the impact of the actuator faults on the stability of networked control systems taking into account fading channels and external disturbances while considering problems related to the actuators that have not been addressed in the relative studies. To this end, three fault-tolerant cooperative control approaches have been developed for this purpose and validated in numerical simulations and real-time experimental tests using the latest Quanser self-driving car QCar platform.

The first approach is the Distributed Fault-Tolerant Formation Control (DFTFC) which aims to control a group of car-like vehicles subject to additive actuator faults. In the design of the DFTFC, we consider the dynamics of the actual vehicles and address both the partial and severe actuator faults problem. Moreover, we provide solutions to the re-assignment formation problem for healthy vehicles in the presence of one or more vehicles with severe/complete actuator faults. Our proposed DFTFC can reduce the computation load due to the implementation of the control algorithm in a distributed manner by each vehicle and provides an overall reliable system against the sudden changes that may occur to the actuators during the formation mission. The DFTFC scheme is designed based on a High-Order Sliding Mode (HOSM) observer to detect and isolate additive actuator faults, which are superimposed on the control signals, and the super-twisting algorithm to compensate for the impact of such actuator faults. The rigorous proofs are provided to guarantee the efficacy of the proposed DFTFC in the presence of faults under investigation. The experimental results demonstrated the effectiveness of the DFTFC in providing a faster response to the occurrence of faults and good performance in handling both partial and severe actuator faults as compared to the recently reported studies.

Second is the Fault-Tolerant Cooperative Control (FTCC) approach. The objective of this approach is to control a team of car-like vehicles subject to multiplicative and additive actuator faults with the presence of faded neighborhood information. The motivation for this study stems from the observation that agents exchange information over wireless networks, which inherently introduce random fading to the transmitted signals. In the cooperative control of networked systems with a restricted communication bandwidth, continuous interaction between neighboring agents would inevitably increase the network transmission load and limit the practical application

of the system. It is thus important to investigate how to ensure the convergence of the team members to the desired trajectory in the presence of actuator faults using contaminated data. In the design of the FTTC, first, we investigated the impact of fading channels problem on the performance of car-like vehicles. Then, we studied the impact of the simultaneous occurrence of fading channels and actuator faults. The FTCC is designed based on the integral terminal sliding mode (ITSM) technique, which is known for its responsiveness, robustness, and stability in unknown conditions.

To the best of our knowledge, non of the existing studies reported results on the actuator faults problem with faded neighborhood information. This is the first attempt to investigate the simultaneous occurrence of fading channels with actuator faults for a team of car-like vehicles. The performance of the FTTC is successfully validated in real-time experiments.

Finally, in the third approach, Adaptive Fault-Tolerant Cooperative Control (AFTCC), we further investigate the fading channels problem and actuator faults with the presence of external disturbances. The AFTCC is developed based on the Non-singular Fast Terminal Sliding Mode Control (NFTSMC) to speed up the consensus tracking and convergence of the entire system. This controller is developed to handle both the multiplicative and additive actuator faults as well as the multiplicative randomness of the fading channel. The impact of faded neighborhood information and actuator faults with external disturbance on team performance is carefully analyzed. It is demonstrated by the Lyapunov stability theory that the controller can guarantee good performance of the overall system regardless of these issues. Furthermore, the synchronization of vehicles can be ensured. In comparison with existing fault-tolerant control methods, our proposed method has a simple structure and can be easily implemented in practice. Simulations are provided to validate the theoretical results.

Keywords: Fault-tolerant control, fault detection and diagnosis, cooperative control, actuator fault, fading communication channel, mobile robots, car-like vehicles.

TABLE OF CONTENTS

Page

LIST OF TABLES

LIST OF FIGURES

LIST OF ALGORITHMS

LIST OF ABBREVIATIONS

AFTC	Active Fault-Tolerant Control
DFTFC	Distributed Fault-Tolerant Formation Control
FDD	Fault Detection and Diagnosis
FTCC	Fault-Tolerant Cooperative Control
HOSM	High-Order Sliding Mode
IMU	Inertial Measurement Unit
ITSM	Integral Terminal Sliding Mode
MAS	Multi-Agent System
MIMO	Multiple Input and Multiple Output
NAV Lab	Networked Autonomous Vehicles Laboratory
NCS	Networked Control System
NFTSMC	Non-singular Fast Terminal Sliding Mode Control
PFTC	Passive Fault-Tolerant Control
PWM	Pulse Width Modulation
QCar	Quanser self-driving car
STC	Super-Twisting Control
UAV	Unmanned Aerial Vehicle
WMR	Wheeled Mobile Robot

LIST OF SYMBOLS

τ_i	Control torque of i^{th} vehicle
M	Symmetric and positive definite matrix
V	Coriolis and centrifugal forces
λ_L	Lagrangian constant
v_i	Linear velocity of i^{th} vehicle
ω_i	Steering velocity of i^{th} vehicle
p_i	Actual position of i^{th} vehicle
p_i^v	Desired position of i^{th} vehicle
u_o	Collision avoidance control law
τ_{Ni}	Nominal control torque of i^{th} vehicle
τ_{fi}	Faulty control torque of i^{th} vehicle
τ_{reconf}	Fault-tolerant control law
$\Delta\vartheta_i$	Additive actuator fault of i^{th} vehicle
Γ_i	Estimated magnitude of actuator fault
R_ϕ	Rotation matrix
$S^\star$	Formation pattern
J_i	Transformation matrix
ε_1	Position tracking error
ε_2	Velocity tracking error

$p_j^\star$	Faded neighborhood information of position
$\omega_j^\star$	Faded neighborhood information of velocity
s	Sliding surface
L_m	Laplacian matrix
γ_i	Multiplicative actuator fault
Δ_{ij}	Distance between the i^{th} follower and its neighbor j
Δ_{iL}	Distance between the i^{th} follower and the leader

CHAPTER 1

INTRODUCTION

1.1 Research Problem

The cooperative control problem of unicycle mobile robots has been widely investigated over the past decade (Sun, Wang, Shang & Feng, 2009; Kostić, Adinandra, Caarls, van de Wouw & Nijmeijer, 2010; Sadowska *et al.*, 2011). Various control strategies have been developed to address the cooperative control problem for mobile robots, including the leader-follower approach (Tanner, Pappas & Kumar, 2004; Mesbahi & Hadaegh, 1999), behavior-based control (Balch & Arkin, 1998; Lawton, Beard & Young, 2003), virtual vehicle approach (Beard, Lawton & Hadaegh, 2001; Ren & Beard, 2004b), artificial potentials (Liu & Passino, 2006; Leonard & Fiorelli, 2001) and graph theory strategies (Lafferriere, Williams, Caughman & Veerman, 2005; Fax & Murray, 2004).

To our knowledge, however, few studies addressed the cooperation problem for car-like vehicles. Nonetheless, this is an important topic to explore, as it pertains to a broader category of robots than unicycle-type robots. Hence, more investigation is needed for autonomous and safe driving of future autonomous cars in realistic conditions.

Cooperative control is closely related to consensus control. It is said that a consensus has been reached when all the vehicles in the team agree on a variable value of interest. All vehicles exchanging information across a network topology must have a consistent view of all the data necessary for cooperation to succeed. In the literature, there have been several results related to cooperative control problems for mobile robots based on consensus theory under fault-free conditions (Olfati-Saber & Murray, 2004; Ren & Beard, 2005; Feng & Zheng, 2019; Zou, Su, Li, Niu & Li, 2019; Yu & Ji, 2018).

However, in practice, faults in networked systems are more likely to occur in one of the agents' components, i.e., actuators, sensors, etc., and that can not be prevented. A fault is an unpermitted divergence of at least one of the system's distinctive properties from the acceptable, typical, standard state (Isermann, 2005). In some cases, a fault does not affect a robot's overall performance, but it can eventually lead to its failure to complete the assigned task. A fault may be small in magnitude or hidden and thus undetectable. Actuator faults are typically defined as the difference between the expected and actual output of the actuator. They can result from the aging or deterioration of actuator components, leading to the actuator's eventual bias or loss of effectiveness (Kamel, Yu & Zhang, 2020). Although actuators significantly impact control systems when they undergo some failures, which can cause instability in the coordination of the entire system and lead to catastrophic accidents, the accommodation problem for networked systems with actuator faults is not yet fully studied. Few works can be found on fault-tolerant control problems for networked systems in (Semsar-Kazerooni & Khorasani, 2010; Shen, Jiang, Shi & Zhao, 2014; Panagi & Polycarpou, 2011; Khodabandeh, Kharrati & Hashemzadeh, 2021). It is, therefore, imperative to further investigate the effects of the actuator fault occurrence on the system's performance to achieve cooperative tasks.

Fault diagnosis algorithms are commonly used to solve the fault problem in a wide range of applications. These algorithms are referred to as Fault Detection and Diagnosis (FDD) schemes/algorithms. The FDD schemes are classified based on redundancy into two main types: hardware-based FDD redundancy and software-based FDD redundancy. In hardware redundancy, the process components are first replicated using identical components. The measurements are taken between the outputs of any component, and it's redundant to indicate any signal (fault) that exceeds the threshold of normal system operation. This method has the reliability of isolating faults, but it requires more space for extra components and more costs for maintenance. Thus, its use is limited to a few applications, such as power plants and flight systems. The analytical redundancy methods implement the mathematical model of the system in software that is running in parallel with the physical model and excited by the same input. In this manner, the behavior of the process is monitored in real-time. The difference between the physical and software models produces a residual signal if any deviation from the desired behavior exists. That signal gives an indication of the fault occurrence, and it needs a further process in the residual evaluation process to extract the information about that fault. However, It is important to mention that most of the FDD algorithms have been developed for the networked system with the assumption that there is no loss of information among team members during the mission.

With the rapid growth of computer network technology, an increasing amount of system data is exchanged via communication networks. During the transfer of information over the communication medium, a portion of the energy could be transformed randomly into heat energy or absorbed by the communication medium. In addition, the signal amplitude may fluctuate due to interference from the external environment, resulting in signal distortion. This phenomenon is called fading channel (Shen & Qu, 2019).

In real-world applications, the fading problem is a significant channel-induced phenomenon in wireless networks caused by refraction, reflection, and diffraction during propagation (Elia, 2005). Fading damages the transmitted data, i.e., position, velocity, etc., which is critical for the control design of the networked systems. Thus, it is important to consider the effect of fading channels on the cooperative control of networked systems (Panagou, Stipanović & Voulgaris, 2015; Li & Niu, 2019). Although the research in networked systems with fault-tolerant controls has received more attention in the last decade, recent studies show that some important issues are still unresolved. The challenge here is to compensate for actuator faults at various severity levels in order to complete the team's mission regardless of severity. Furthermore, addressing actuator faults is necessary when communication networks are unreliable.

Motivated by the above-mentioned discussions, this research addresses the cooperative control problem for a team of car-like vehicles subject to actuator faults and fading channels. Specifically, we design a fault-tolerant control scheme that enables each vehicle to detect, diagnose, and accommodate actuator faults by itself with/without the presence of fading channels. As a result, the team can continue the mission with a predefined geometric pattern and achieve the desired task.

1.2 Research Objectives

The objective of this study is to design a reliable networked control system that can accomplish cooperative tasks in fault-free and fault conditions. In fault conditions, it is assumed that any vehicle in the team formation can be subjected to either partial or severe actuator faults while exchanging information with other vehicles over fading communication channels. The goal of the developed algorithms is to control the faulty vehicles with partial actuator faults to complete the mission with the rest of the team members. In the case of a severe actuator fault, the faulty vehicle is excluded from the team formation, allowing the remaining members to complete the mission.

1.3 Thesis Outlines

This research is organized into six chapters, including the introduction chapter. The structure of the remaining chapters can be summarized as follows: Chapter 2 introduces the state-of-the-art of existing literature on robotic systems with fault-tolerant control methods. Chapter 3 introduces a Distributed Fault-Tolerant Formation Control (DFTFC) scheme based on a virtual vehicle approach. With the proposed controller, we can avoid the risk of a system failure due to the fault of the leaders, reduce the computation load due to the implementation of the control algorithm in a distributed manner by each robot, and have an overall reliable system against the sudden changes that may occur to the actuators during the formation mission. The DFTFC scheme consists of a High-Order Sliding Mode (HOSM) observer that detects and isolates additive actuator faults, which are superimposed on the control signals, and the super-twisting algorithm designed to compensate for the impact of such types of actuator faults. Theoretically, despite the uncertainties, it is proven that a second-order sliding manifold can be reached in a finite time; this implies that the fault estimate exponentially converges to the real fault magnitude (Davila, Fridman & Levant, 2005). In our study, we divided the methodology into two stages. Stage 1: Designing a distributed formation controller based on the virtual vehicle approach under fault-free conditions, and Stage 2: Designing a distributed fault-tolerant formation controller for the entire system with the assumption that a partial or severe actuator fault condition could occur in any one of the team formation members during the mission.

Chapter 4 addresses the Fault-Tolerant Cooperative Control (FTCC) problem for leader-follower networks in the presence of actuator faults and fading channels. First, we design the FTCC under the effect of a fading channel using the sliding mode control technique. The tracking variables cannot be properly calculated with fading channel conditions. To overcome this issue, the information exchanged over the fading channel is utilized to evaluate the error of tracking variables. Using this strategy not only increases the precision of the controller's design but also provides a practical solution to the consistency problem of leader-follower networks with channel fading. Second, we develop an FTCC approach under the influence of fading channels and actuator faults. Specifically, the multiplicative and additive actuator faults are considered in this study. The FTCC for such fault cases is designed based on the Integral Terminal Sliding Mode (ITSM) technique, which is known for its responsiveness, robustness, and stability in unknown conditions.

Chapter 5 investigates fading channels, actuator faults, and external disturbances as part of the cooperative control problem for networked control systems. We develop an adaptive cooperative control based on Non-singular Fast Terminal Sliding Mode Control (NFTSMC) for a team of car-like vehicles that allows each vehicle to compensate for the impact of faults if they exist and continue the mission with the rest of the team members. First, we develop adaptive fault-tolerant cooperative control in the presence of fading channels and external disturbances. Second, we develop an adaptive fault-tolerant cooperative control design under the influence of fading channels, actuator faults, and external disturbances. The proposed controller is based on NFTSMC as it can overcome the singularity in the consensus tracking problem and provide fast convergence rates. Chapter 6 introduces the conclusion and recommendations for future work.

CHAPTER 2

BACKGROUND AND LITERATURE REVIEW

Networked control systems have received considerable attention in the past decade due to their wide range of applications in mobile robots, satellite formation, unmanned aerial vehicles, and so on (Wang, Zeng & Cong, 2016). While these applications are different in their mission, the fundamental cooperative control strategies are almost similar. This chapter introduces an overview of some of the most important cooperative control methods for wheeled mobile robots, fault detection and diagnosis algorithms, and fault-tolerant control methods reported in the literature.

This chapter is organized as follows. A discussion of motion control problems for car-like vehicles is presented in Section 2.1. The modeling of a nonholonomic car-like vehicle is described in Section 2.2. Moreover, the cooperative control of mobile robots is addressed in Section 2.3. In Section 2.4, coordination strategies are presented. The coordination and formation control approaches are discussed in Section 2.5. Furthermore, Section 2.6 covers the fault detection and diagnosis algorithms for distributed control systems. The methods for fault-tolerant control that were proposed in the relevant studies are discussed in Section 2.7. A summary of the originality of the thesis and contributions is presented in Section 2.8, which includes a review of studies that addressed actuator and communication faults in formation control systems and an assessment of their progress and limitations. Finally, Section 2.9 introduces the development of the experimental setup.

2.1 Motion Control Problem of Car-Like Vehicles

In robotics, motion autonomy is the capability of a robot to execute a specified movement without external intervention. It is an important issue in robotics. The degree of motion autonomy can vary significantly depending on the circumstances. For example, acquiring motion autonomy is easier for a manipulator arm working on an assembly line (a known, precise, and highly predictable workspace) than for a planetary rover. One of our primary research objectives is motion autonomy, particularly for car-like vehicles. Control of car-like vehicles is a critical control problem that must be addressed in order for any task to be completed. The nonlinear dynamics dominating the robotic vehicles' motion complicate the problem even more. The control design is thus challenging and is complicated by the lack of a precise model, which is essential for the model-based approach to control design. A common approach to solving a robotic system's motion control problem is using an abstract robot model, such as a rigid body kinematic model. A typical motion control objective is to steer the robot to follow a given trajectory or a pre-defined geometric path. As a result, the motion control problem of robotic vehicles has been thoroughly investigated, with proposed control approaches mainly categorized as trajectory tracking and path-following schemes. Trajectory tracking schemes enable the robotic vehicle to converge on a reference trajectory constrained in time. On the other hand, the path-following scheme allows the robotic vehicle to follow a given geometric path at a specified speed, regardless of the time constraints.

2.2 Modeling of Nonholonomic Car-Like Vehicle

2.2.1 Kinematic modeling

A nonholonomic mobile robot is one that is incapable of moving in the lateral direction and can only move perpendicular to the driving wheels' axis. Nonholonomic robots are capable of operating in a wide variety of application domains, including search and exploration, surveillance, transportation, and tracking of military targets. The nonholonomic system could be described by nonholonomic constraints, which most often appear in mechanical systems where some constraints are placed on the motion. A nonholonomic constraint is defined as a constraint that is not integrable and contains time derivatives of a system's generalized coordinates $q = (x, y, \phi, \psi)$, where (x, y) are the position of the vehicle, ϕ is the orientation of the car body and ψ is the steering angle. Wheeled mobile robots typically exhibit nonholonomic restrictions due to the condition of rolling without slipping between the wheels and the ground. The two nonholonomic constraints subject to the driving wheels of the vehicle shown in Figure 2.1 can be described as follows:

$$
\begin{aligned}
\dot{x}\sin(\phi) - \dot{y}\cos(\phi) &= 0 \\
\dot{x}\sin(\phi+\psi) - \dot{y}\cos(\phi+\psi) - L\dot{\phi}cos(\psi) &= 0,
\end{aligned}
\tag{2.1}
$$

From the nonholonomic constraints, the kinematics model of the wheeled mobile robot can be

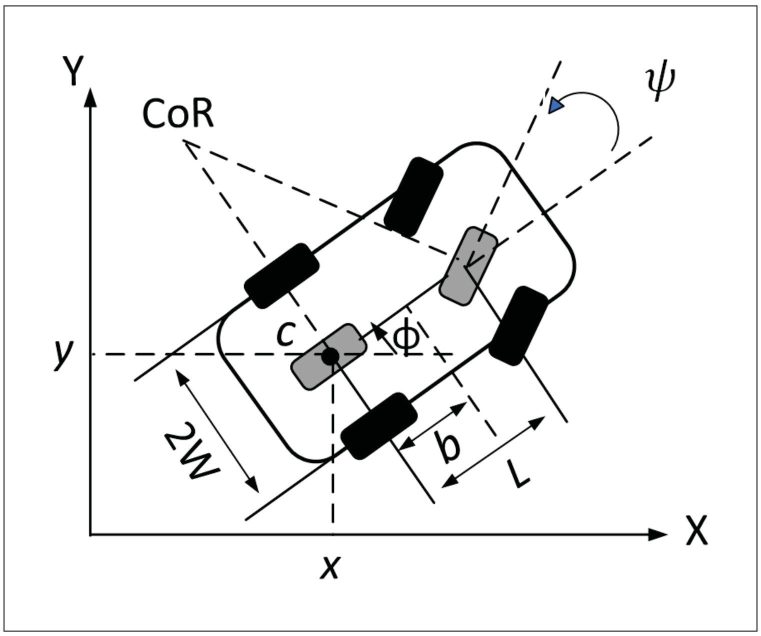

Figure 2.1 Car-like vehicle reference frame and parameters.

expressed as follows:

$$
\begin{aligned}
\dot{x} &= v\cos(\phi), \\
\dot{y} &= v\sin(\phi), \\
\dot{\phi} &= v\frac{tan(\psi)}{L}, \\
\dot{\psi} &= \omega,
\end{aligned}
\tag{2.2}
$$

where v and ω are the linear and steering velocities of the vehicle, respectively. L is the distance between the front and rear axles.

2.2.2 Dynamic modelling

The dynamics of the car-like vehicle with generalized coordinates $q \in R^n$ and subject to k constraints can be given by the following relation:

$$M(q)\ddot{q} + V(q, \dot{q})\dot{q} = B(q)\tau - A^T(q)\lambda_L, \tag{2.3}$$

where $M(q) \in R^{n\times n}$ is a symmetric and positive definite matrix, $V(q, \dot{q}) \in R^{n\times n}$ is the Coriolis and centrifugal forces, $\tau \in R^r$ is the input vector. $B(q) \in R^{n\times r}$ is the transformation matrix, $A(q) \in R^{k\times n}$ is the matrix associated with the constraint, $\lambda_L \in R^k$ is the Lagrangian constant, where

$$M = \begin{bmatrix} m & 0 & I_c \sin(\phi) & 0 \\ 0 & m & -I_c \cos(\phi) & 0 \\ I_c \sin(\phi) & -I_c \cos(\phi) & I_b & I_w \\ 0 & 0 & I_w & I_w \end{bmatrix},$$

$$V = \begin{bmatrix} 0 & 0 & -I_c\dot{\phi}\cos(\phi) & 0 \\ 0 & 0 & -I_c\dot{\phi}\sin(\phi) & 0 \\ 0 & 0 & 0 & 0 \\ 0 & 0 & 0 & 0 \end{bmatrix}, B = \begin{bmatrix} \cos(\phi_) & 0 \\ \sin(\phi_) & 0 \\ L\sin(\psi_)\cos(\psi) & 0 \\ 0 & 1 \end{bmatrix},$$

$$A^T(q)\lambda = A^T(q)\begin{bmatrix} \lambda_1 \\ \lambda_2 \end{bmatrix},$$

where $m = m_c + 4m_w$, $I_c = (L-b)m_c + 2Lm_w$, $I_b = m_c(L-b)^2 + 4W^2 m_w + I_{b_{zz}} + 4I_{w_{zz}}$, m_c and m_w are the vehicle and wheel masses, respectively, I_w is the moment of inertia of each wheel with a motor about the wheel axis. $I_{b_{zz}}$ is the moment of inertia of the vehicle body about the z-axis passing through the vehicle's center of mass. $I_{w_{zz}}$ is the moment of inertia of the wheel about the z-axis passing through the wheel centroid.

It is assumed that the vehicles in a formation mission are identical with the same parameters. The system in (2.3) can be simplified for control purposes as follows.

First, we introduce a full rank matrix $S(q)$, which has a set of linear independent vector that is obtained by spanning the null space of $A(q)$, i.e.,

$$S^T A^T = 0. \tag{2.4}$$

From (2.4), one can find auxiliary vector $\bar{\omega} \in R^{n-m}$ such that

$$\dot{q} = S\bar{\omega}, \tag{2.5}$$

where

$$S = \begin{bmatrix} \cos\phi & 0 \\ \sin\phi & 0 \\ \frac{tan(\psi)}{L} & 0 \\ 0 & 1 \end{bmatrix}, \bar{\omega} = \begin{bmatrix} v & w \end{bmatrix}^T. \tag{2.6}$$

Substituting (2.5) into (2.3), we can obtain the reduced dynamic form that will be used later for the control design as

$$\bar{M}(q)\dot{\bar{\omega}} + \bar{V}(q,\dot{q})\bar{\omega} = \bar{B}(q)\tau, \tag{2.7}$$

where

$$\bar{M}(q) = S^T M S, \quad \bar{V} = S^T(M\dot{S} + VS), \quad \bar{B} = S^T B.$$

2.2.3 Control of car-like vehicle

Many control algorithms have been proposed in the context of the kinematic control problem without considering the car-like vehicle's dynamic model. Murray & Sastry (1993) examined methods for steering systems with nonholonomic limitations between arbitrary configurations.

In his early works, Brockett derived optimal controllers for a class of canonical systems where the input vector fields and Lie brackets are tangent to the configuration manifold. Based on Brockett's findings, Murray & Sastry (1993) constructed suboptimal trajectory paths for non-canonical systems and investigated systems requiring more than one bracketing degree to achieve controllability. They employed sinusoids with integrally connected frequencies in order to produce motion at a certain bracketing level. Preliminary researchers in Egerstedt, Hu & Stotsky (2001) addressed the problem of controlling wheel-based mobile platforms using two model-independent solutions. Both solutions rely on the virtual vehicle control method. In Lamiraux & Lammond (2001), a steering control method is proposed to provide smooth paths under curvature constraints for a car-like vehicle. Steering is integrated into a global motion planning scheme with obstacles. Throughout the study, the car is viewed as a 4-D system from a kinematic perspective and as a 3-D system from a geometric perspective. Kumar & Sukavanam (2008) developed a trajectory-tracking concept based on the kinematics of a four-wheeled mobile robot. The trajectory is described as a time-indexed path in a plane containing both its position and orientation. Nonholonomic constraints are considered in the control design of mobile robots. During the design process of controllers, the kinematic equation is transformed into a chained form in order to facilitate the development of controllers. Following that, a backstepping tracking controller based on the robot's kinematic model is derived.

Nevertheless, certain tracking errors may occur due to high-speed motion, heavy weights, external disturbances, and system uncertainties when the kinematics model is used without considering the dynamic model. However, the major issue with controllers that incorporate dynamics and kinematics is their complexity in comparison to controllers that use only kinematics. The complexity arises from the presence of some unknown parameters and parametric uncertainties, such as lateral and longitudinal slipping. Several of these parameters are unknown. Thus, the controller should be enhanced so that unknown parameters can be estimated and identified.

2.3 Cooperative Control of Wheeled Mobile Robots

A cooperative multi-agent system is made up of agents that can work together to accomplish a common goal. In this sense, such a control problem is referred to as cooperative control, which emphasizes the agents' cooperative function during operation. Controlling the formation of multiple agents can be thought of as a unique cooperative operation. During the execution of a mission, the goal of formation is to maintain a specific shape with constant relative distances between the agents. As a result, the two most important characteristics of a formation configuration are shape and location. A formation is a group of agents linked together by their controller specifications, which specify the relationship each agent must have with its neighbors. Agent interconnections are represented as edges in a directed acyclic graph (Tanner *et al.*, 2004). A group of robots can form a variety of formations, the most common of which are lines, triangles, diamonds, and so on. Aside from the shape, each robot in the team must occupy a specific position in the formation. According to Balch & Arkin (1998), there are three major techniques for determining team formation structure: unit-center-referenced, leader-referenced, and neighbor-referenced, as shown in Figure 2.2.

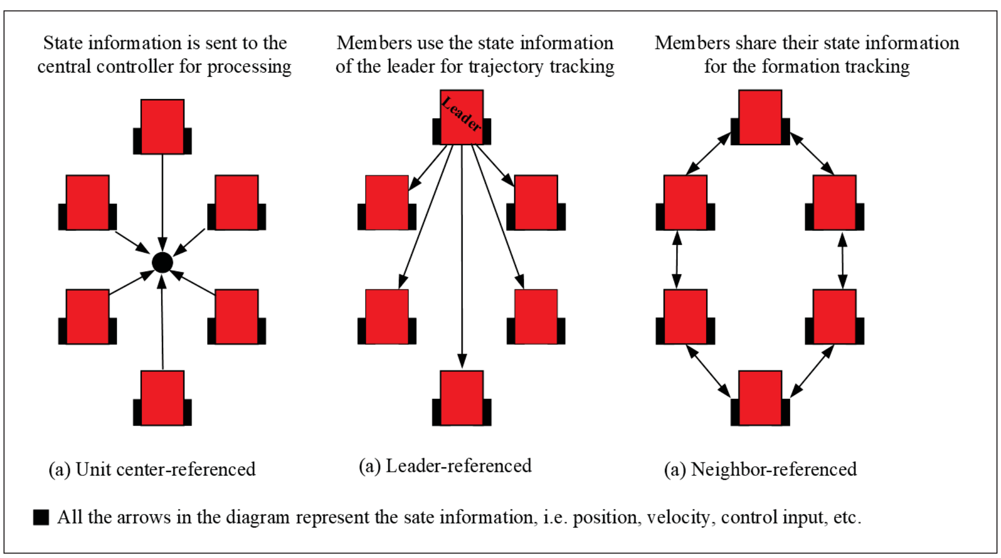

Figure 2.2 Different techniques for team formation structure.

2.4 Coordination Strategies

Coordination is a collective behavior for a group of dynamic agents working together in the same environment to form a particular shape known as the formation to reach a common goal (Gautam & Mohan, 2012). A flock of birds is an example of collective behavior (Reynolds, 1987). Reynolds created a computer animation that simulates the motion of a flock of birds. Each bird or particle in the computer animation behaves independently in the environment where each particle should consider two behaviors: collision avoidance with each other and getting together while flying. Reynold published more papers; for instance, in (Reynolds, 1999), he represented the motion of autonomous objects in computer animation, and in (Reynolds, 2000), he presented a strategy for coordinating large groups of autonomous objects interacting with each other and with their environment. In Balch & Hybinette (2000), a new behavior-based approach was introduced to the flocking study to assign a position for each robot in the group formation. The robots are not located at particular positions but are attracted to the closest locations in the pre-designed geometrical configuration.

In literature, the coordination strategy can be implemented in two control paradigms: the centralized, decentralized, or hybrid paradigm. In the centralized system, one controller performs all the computations required for each robot to meet the control goals (Kanjanawanishkul, 2011). Although this method has optimal decisions in coordinating robots, it requires a high computation capability due to the large flow of information. Great dependence on a single controller makes it not robust for the coordination of multi-mobile robots. In the decentralized method, each team member makes its computations and makes control decisions independently. This method, as compared with centralized control, has the flexibility of adding more robots to the system without having any complexity in the computations. Many studies on the coordination of multi-agent systems considered one of these control approaches. For instance, Pane, Fuady & Mutijarsa (2013), proposed overtaking behavior and collision avoidance techniques for a multi-robot system based on centralized control. The overtaking module is used to get the broken robot‘s ID and send it to the followers in order to avoid collision with the faulty robot. Huang, Farritor, Qadi & Goddard (2006) proposed a centralized localization and control method for highway safety applications such as maneuver safety barrels in the work zones. The group has inexpensive and limited sensors in which the robots follow the leader that performs the complex operations for navigation over a long distance. The proposed algorithm allows followers to have simple computations, fewer sensors, and inexpensive cost; therefore, it is suited for high-risk missions. In Chang & Tsai (2014), a differential geometry technique has been applied to investigate the stability of decentralized formation controllers for mobile robots based on their relative distance measurements between them. The convergence of the system was proved by simulation. Andreasson, Dimarogonas, Sandberg & Johansson (2014) developed a nonlinear consensus protocol of first and second-order dynamics to analyze the distributed control protocol for single and double integrators of dynamical systems. Proportional–Integral methodology was adopted to attenuate the disturbances in the network of fixed communication topology. The proposed protocol asymptotically solves the average consensus in the absence of disturbances. An algorithm for coordination of centralized weakly mobile robots is presented in (Xu & Song, 2010). The algorithm combines the centralized and decentralized strategies for each robot. The algorithm enables the robots to use the local sensors and make decisions in the presence of obstacles or any external disturbances. In Ren & Beard (2004a), a decentralized control scheme was proposed to construct the formation for spacecraft. The synchronization of the spacecraft's motion is achieved over a low-bound channel communication between neighbors.

2.5 Coordination and Formation Control Approaches

As of today, the vast majority of existing control formation architectures rely on either centralized or distributed techniques to coordinate and manipulate a group of dynamic agents. In a centralized control system, these agents are controlled by a powerful core unit. A unit such as this can be a robot in the formation capable of significant computations or a ground control station with powerful communications and computing capabilities (De La Cruz & Carelli, 2006). This system can gather data from all members, optimize vehicle coordination, track mission completion, and accommodate individual vehicle faults. Consequently, centralized control refers to a system that has global information, a centralized organization, and a high computing capacity.

Conversely, the centralized approach is less robust, more expensive, and more vulnerable to failure. Furthermore, as the number of robots increases, centralized control becomes ineffective due to communication limitations. The centralized control system is, therefore, not suitable for real-time missions.

Distributed control, on the other hand, is developed to solve these issues; each robot communicates and shares its information with the others as part of the overall mission. It has numerous benefits, including scalability, the ability to tolerate individual faults, reduced communication loads, and increased computational power of robots.

The formation control can be viewed as a unique cooperative operation. The formation aims to maintain a predefined shape with constant relative distances between agents while executing the mission. As a result, the shape and location of a formation configuration are critical characteristics. The common approaches used to make a certain formation pattern are classified as virtual-based structure, behavior-based control, artificial potential approach, leader-follower, and graphical approach (Zhang & Mehrjerdi, 2013).

2.5.1 Virtual structure approach

The virtual structure formation-based control that involves a team of robots treats the desired geometrical shape as one rigid object in which each robot is treated as a node. For example, Lewis & Tan (1997) presented one of the pioneering works. They proposed the virtual structure approach to maintain the geometrical patterns of robots during their motion. The same control strategy was applied to ground vehicles using a fuzzy logic controller in (Ren & Beard, 2004b). A number of studies have demonstrated the effectiveness of the virtual control technique in providing precise formations and maintaining them during maneuvers (Guanghua, Deyi, Wenyan & Peng, 2013). Preliminary researchers Egerstedt & Hu (2001) presented a virtual leader strategy for coordinating a given nonphysical point. Following that, both the agents and the virtual leader maintained the desired formation while tracking the reference trajectory of the virtual leader. Zohar, Ailon & Guterman (2012) designed a control algorithm based on the virtual vehicle concept and the flatness property. Their study examined two main configurations: rigid formations and platoons or convoy-like formations. The controller allows members to split, merge, and maneuver during the group motion to avoid collisions. According to Do & Pan (2007), unicycle mobile robots are controlled using a virtual structure in conjunction with a path-tracking approach, which enables the formation shape to be changed. The virtual structure approach, however, has the disadvantage of centralized decisions in the implementation of all computations and communications to coordinate between the robots, which could result in the failure of the entire system.

2.5.2 Behavior-based method

The observations of animals inspired this approach. It is a simplification of observed natural behaviors. Studies of flocking and shoaling show the behavior of the animals toward their desire to maximize the chance of detecting predators and foraging for food simultaneously. Robotics researchers benefited from the formation behavior in nature and developed similar formation tactics for robots. Each robot is employed with several behaviors to accomplish a specific task, i.e., keeping formation, avoiding the obstacle, tracking trajectory, and seeking the goal. For example, Balch & Arkin (1998) proposed reactive behavior for different types of team formation. The behavior of each formation type is integrated with other navigational behaviors to enable the vehicles to reach their goals, avoid obstacles, and keep their relative positions in the formation. Lee & Chwa (2018) presented an algorithm for decentralized behavior-based formation control that depends solely on the position of neighboring robots. It is proposed to use an escape angle to prevent collisions between the objects. The scholars in Monteiro & Bicho (2010) proposed a method for generating behaviors for a team of unmanned vehicles moving in an unknown environment with a prescribed geometrical shape. A behavior-based approach is presented in (Xu, Zhang, Zhu, Chen & Yang, 2014a) for a swarm robot formation control. The authors investigated several behaviors relevant to two typical formation control problems: initial formation and formation control in cluttered environments. A classification-based search method is introduced in the first problem in order to generate an arbitrary formation with lower computational complexity. The second problem involves the application of a behavior-based method to navigate in an unknown environment. In general, the behavior-based approach requires less communication between robots. Therefore, it is effective in guiding robots in an unknown environment. However, it has issues with the difficulty of analyzing the dynamics model; thus, the convergence to the predefined geometric formation cannot always be guaranteed.

2.5.3 Leader-follower control method

In this control strategy, one or more robots are designed to be leaders while the rest follow the leader. The leader has a predefined trajectory that is possibly given by the high-level layer in the coordination control architecture. For trajectory tracking, followers use leaders' positions and orientations as a reference to their positions while moving. Several studies introduced this approach for the coordination of autonomous vehicles. For example, Das *et al.* (2002) designed two control methods, $l - \phi$, and $l - l$ control, based on the feedback linearization method. The $l - \phi$ controller maintains the desired relative distance and the relative orientation between the leader and follower robot. In the $l - l$ strategy, the controller keeps the relative positions between one follower and two leaders in a system of three robots to enable the follower to track the leaders. Other techniques have been proposed to follow the leader-follower control approach in the literature, i.e., feedback linearization (Mariottini, Morbidi, Prattichizzo, Pappas & Daniilidis, 2007), backstopping (Li, Xiao & Cai, 2005), and sliding mode control (Defoort, Floquet, Kokosy & Perruquetti, 2008; Sanchez & Fierro, 2003). The leader-follower method has strength in its simplicity and reliability of controlling a multi-robot system. However, this strategy lacks the presence of a feedback controller, which makes the leader's motion independent of followers, and that maximizes the possibility of having a failure to the team structure when navigating in an unknown environment.

2.5.4 Artificial potential fields

The concept of this control strategy was first introduced in 1986 (Khatib, 1986). A primary objective of this approach is to determine the interaction forces between neighboring agents and to enforce the inter-agent spacing between them using artificial potentials. This approach was originally presented for path planning of a robot manipulator, and then it was used for trajectory tracking in the mobile robots' community. However, the local minima that depends on the structure of the obstacle is the main drawback of this method. For instance, when the robot runs into a U-shaped obstacle and becomes trapped in this type of configuration, the robot cannot get out of the obstacle, and, in this case, it is called the robot's cyclic behavior.

Many variations and improvements are proposed to the behavior of a potential field in local minima and reduced oscillations of robots in narrow places (Khatib & Chatila, 1995; Zhang, Shen, Wang & Wang, 2010). For instance, Khatib & Chatila (1995) invented an extended potential field method for the manipulator. Two assumptions were added to the basic approach: 1) the rotational potential field and 2) the task potential field. The former assumption considers the repulsive force as a function of the robot's position and orientation as measured from the obstacle to that robot. The latter is based on the instantaneous robot velocity. By applying both assumptions, smoother tracking of the trajectory can be obtained. In practice, this method is widely used for obstacle avoidance and multi-robot formation due to its simplicity in the implementation with low calculations. Therefore, it can be easily applied to real systems.

2.5.5 Graph-based method

A graph is used to model the behavior and interaction of dynamical systems as nodes for the agents and edges for the information flowing between the agents. A graph depicts the topology of a communication network that shows the constraints associated with the connections between nodes. To reach the stability of the distributed system, the communication topology and the dynamics of the agents are integrated to achieve the cooperative control goal. In Fax & Murray (2004), the graph theory is used to demonstrate the relationship between communication topology and the formation stability for a team of autonomous vehicles. The authors used the Laplacian matrix to examine the graph theory's impact on the formation's stability. Finally, the study demonstrated that convergence could be achieved when two conditions are met: a stable information flow and a stable vehicle controller.

In Olfati-Saber & Murray (2004), consensus algorithms for large-scale systems with fixed and dynamic communication networks were investigated. In this study, the direct links of communication are created for the graph topology with the consensus protocol. Then, the convergence analysis based on the Lyapunov function is proposed for the agreement protocol. In Xiao & Wang (2006), the state consensus problem was investigated with a switching network and varying time delays of the information flow. The study showed that the consensus is reached when the time delays, weighting factors, and communication topology are time-invariant, and the communication topology also has spanning trees. Ren (2007) investigated a consensus algorithm with a time-varying state for autonomous vehicles where only part of the vehicles has access to that varying state, and those vehicles do not have direct access to all vehicles in the team. Graph theory is applied to analyze the consensus algorithm for both state and time-varying states. Mengji, Kaiyu & Li (2014) introduced the frequency domain method to a system with double integrator dynamics to solve the consensus problem for N-robots with directed topologies (graph theory) and non-uniform time delays. Under sufficient, the consensus is reached. When all values of the time delays are bounded, the non-uniform delays won't influence the stability of the consensus. In Dong, Xi, Lu & Zhong (2014), a formation control protocol is proposed for a time-invariant linear system with higher order to construct the desired team structure based on graph theoretical analysis. The convergence is achieved under necessary and sufficient conditions. In Qiao & Sipahi (2015), a consensus control protocol is applied to three centralized mobile robots with a communication time delay between the central computer and the robots. The consensus protocol is established based on graph theory, input-output linearization, and some uncertainties associated with the control. The proposed algorithm was successfully tested and achieved consensus in both numerical simulation and real-time experimental works. Cepeda-Gomez & Perico (2015) proposed a consensus protocol with double integrator dynamics for a system that has multiple subsystems with communication time delays. The convergence of robots to the desired formation was validated by numerical simulation.

2.5.6 Formation tracking problem

Formation tracking aims to construct a desired geometric shape for a team of robots while following a reference point. Formation tracking can be divided into path following and trajectory tracking. In the path following, the robot must reach and follow the path without any time constraint. While in trajectory tracking, the path is tracked with a restricted time dependence. The path following is more flexible than trajectory tracking, i.e., a smooth convergence to the desired path, and unstable zero dynamics are easier to remove.

The leader-follower approach is a good example of using a trajectory-tracking strategy. A leader-follower motion strategy has been used to study mobile robots' localization and control motion problems. Mariottini *et al.* (2007) applied this motion strategy and is distinguished from relative studies by its use of a feedback controller to ensure system stability.

The path-following strategy can be divided into two categories: (i) the coordinated path strategy and (ii) the virtual structure strategy (Kanjanawanishkul, 2011). In a coordinated path-following strategy, every member of the team is assigned a parametrized reference path such that when all parameters are synchronized, the entire team follows the predefined path. A virtual structure has a virtual leader that has the map trajectory for reaching the target, and other robots are instructed to follow his coordinates. As an example, in Egerstedt & Hu (2001), a coordination model for non-holonomic robots is proposed based on a virtual structure strategy. A study was conducted to determine whether robots accurately track their references or if there is some bounded error in the tracking process. Ghommam, Mehrjerdi, Saad & Mnif (2010) proposed a combination of a path following and virtual structure strategy to create the predefined formation. According to their model, each robot shares its state with the rest of the team. By considering the time derivative of the parameter as input to the controller, the motion of the formation is synchronized.

2.5.7 Collision free coordination

There have been several approaches to obstacle avoidance in the literature that have been applied to cooperative control systems for collision avoidance while navigating in static or dynamic environments. For instance, in Fujimori, Teramoto, Nikiforuk & Gupta (2000), a cooperative collision avoidance technique was proposed for unmanned vehicles. This technique was first tested on two robots and then extended to more robots. It was ensured by considering the geometric paths of robots as cooperative behavior to avoid obstacles while tracking their paths. It is mentioned in Guy *et al.* (2009) that a local obstacle avoidance algorithm can be used to avoid collisions between agents. According to the authors, the approach could handle multiple scenarios with a large number of heterogeneous agents in a few milliseconds in real-time simulation. A Lyapunov method based on collision-free dynamics with a unicycle model was introduced in (Kostic, Adinandra, Caarls & Nijmeijer, 2010). The method allows the formation of the agents to vary over time. In Rezaee & Abdollahi (2013), the rotational potential field is proposed to enable robots to reach their desired goals without colliding with obstacles in accordance with the principle of repulsive and attractive forces. Chen & Sun (2016) developed a distributed optimal control method for reaching consensus while avoiding obstacles at the same time. Simulations were used to demonstrate the proposed approach.

2.5.8 Inter-vehicle communication

Coordination and communication are extremely important components of a multi-robot system in order to achieve the intended results. The primary purpose of communication is to coordinate robot actions in order to prevent conflicts. Furthermore, robots can share sensory information to communicate information about their environment, for example, when they perform exploration tasks. In addition, robots can exchange physical information, such as position, velocity, etc., to form geometric shapes. Communication in multi-agent systems can be classified into three categories: communication range, communication topology, and communication bandwidth. The communication range is the maximum distance that two team members can communicate. The communication range has three principal cases: (i) implicit communication, where the robots communicate by observing other team members' behavior when direct communication does not exist. (ii) Local communication, where robots can only communicate with other robots that are located nearby. (iii) Global communication where every member can broadcast his state information to all members in the team formation (Zhang & Mehrjerdi, 2013). The communication topology is represented by either a bidirectional or unidirectional interconnection structure among teammates. This topology can either be static or dynamic when the relationship between members changes arbitrarily (Kanjanawanishkul, 2011). However, systems that need global information access to each subsystem may suffer from a lack of scalability. The less coordination for multiple robots is needed, the better it can be scaled to larger numbers.

2.6 Fault Detection and Diagnosis Algorithms in Distributed Control Systems

Safety and continuous operation are key issues when developing distributed FDD algorithms. Several research groups have been fascinated by the various fault diagnostic approaches for distributed systems. In the context of large-scale linear time-invariant systems, decentralized filter detection has been proposed in (Shankar, Darbha & Datta, 2002). The subsystems are equipped with a bank of interacting filters for preventing the propagation of faults as soon as they occur. In Patton *et al.* (2007), a fault tolerance strategy for distributed systems is provided with the assumption that the communication channel has unlimited bandwidth to simplify the computations necessary for controlling the subsystems. Their results proved that a coordination function in a distributed structure could compensate for the effects of faults on the system. In another study, a robust decentralized FDD module for actuator faults was developed using a sliding mode observer (Yan & Edwards, 2008). A fault estimation process was conducted in real-time using the features of the observer. Similarly, Ferrari, Parisini & Polycarpou (2009) designed a distributed FDD scheme for stationary large-scale nonlinear systems. In each subsystem, there is a local fault detector, which detects a fault in the corresponding neighbor based on measurements made by the subsystem and information received from the neighbors.

Various other strategies have been applied in cooperative control systems to develop distributed fault detection and diagnosis algorithms. An FDD scheme based on local interaction methodology has been presented for the formation of UAV leader-follower pairs (Lechevin, Rabbath & Earon, 2007). Despite demonstrating the proposed algorithm's effectiveness in detecting simultaneous faults of actuators and communication loss, this method had limitations as it did not address the reconfiguration problem for the formation of multiple vehicles under communications constraints. In Daigle, Koutsoukos & Biswas (2007), a distributed FDD approach was applied for the formation of unmanned systems. Bond graphs were used to describe the system model's components, sensors, and actuators. Among this study's limitations was that only a single fault could be detected and isolated by the fault diagnosis scheme. Moreover, the diagnosis scheme does not provide detailed information about these systems' cooperation behavior. This resulted in the scheme being able to isolate only simple faults. Fagiolini, Babboni & Bicchi (2009) designed a distributed misbehaving detection method for monitoring the motion of multiple mobile robots. A local observer on each robot uses information sensed from neighbors and measurements received from other observers to determine whether a robot has misbehaved manner during the time of the operation. Various control approaches have been considered in some studies to address the FDD problem. Azizi & Khorasani (2011) developed a hierarchical framework consisting of three fault recovery levels in order to study the actuator fault accommodation cooperatively in the formation flight of unmanned aerial vehicles. Meskin & Khorasani (2009a) provided an algorithm for detecting faults in multiple satellite systems during formation flight in which fault actuators are mitigated. Three architectures of FDD control were investigated: decentralized, centralized, and distributed-based control.

It is important to emphasize that most of the aforementioned techniques and related research in the distributed FDD problem for multi-agent systems assume perfect information flow between robots. In some studies, however, the fault detection problem has been shown to occur due to imperfect communication during satellite formation flight using the centralized FDD algorithm (Meskin & Khorasani, 2009b), resulting in increasing computation and communication loads as the number of team members increases. In networked control systems with quantization problems, Ghasemi, Askari Marnani & Menhaj (2017) used similar control approaches, but the information was exchanged between a central monitoring system and local units. It is worth mentioning that both studies in (Meskin & Khorasani, 2009b) and (Ghasemi *et al.*, 2017) applied their proposed approaches to linear systems, which limits their solutions to only a few systems in practice. A fault diagnosis algorithm for large-scale nonlinear systems with certain communicated information has been developed in (Zhang, 2010) and (Zhang & Zhang, 2011). Although both studies considered the constraints of communication that certain information is communicated between subsystems, the nonlinear models were not general. In conclusion, motivated by the above considerations, we propose solutions to the distributed FDD algorithms that detect and isolate any robot with actuator failures from the system whenever there is a perfect or imperfect communication link between robots with a general degree of nonlinearity in the system dynamics.

2.7 Fault-Tolerant Control Methods

Fault-Tolerant Control Systems (FTCSs) have recently gained substantial attention because of their significant role in maintaining the safety of modern technological systems via configured redundancy (Zhang & Jiang, 2008). In addition to performing regular control functions, FTCS is a physical control system that is capable of maintaining system safety in case of faults. An FTCS can be physically represented as a Multiple Input and Multiple Output (MIMO) system. It possesses similar inputs to traditional controllers, such as set points and control system error signals. However, it contains inputs that a traditional controller rarely has, comprising measurements from the monitoring systems and safety requirements. Two types of FTCSs are studied in the literature: Passive Fault-Tolerant Control Systems (PFTCs) and Active Fault-Tolerant Control Systems (AFTCs). The PFTCs are found to be robust against a class of pre-defined faults (Eterno, Weiss, Looze & Willsky, 1985). It compensates for the effect of anticipated faults with no need for online fault information such as time, magnitude, or type of fault. However, it requires hardware redundancy, i.e., multiple actuators, sensors, etc., to replace the faulty component. In contrast to PFTC, AFTCs request the online fault information from the FDD algorithm to accommodate the fault by synthesizing or switching to pre-computed control law online (Zhang & Chamseddine, 2012; Blanke, Kinnaert, Lunze, Staroswiecki & Schröder, 2006). The design objectives for AFTCs include the transient and steady-state performance of the system not only under normal operations but also under fault conditions. It is important to point out that the system behavior emphasis in these two modes of operation can be significantly different. During normal operations, more emphasis should be placed on the quality of the system's behavior. However, system survival with an acceptable (probably degraded) performance becomes a predominant issue in the presence of a fault.

Several review studies on FTCSs design methods have been carried out, and various effective design techniques are provided for different applications in (Boskovic, Prasanth & Mehra, 2007; Isermann & Raab, 1993; Ji, Zhang, Biswas & Sarkar, 2003), including fault-tolerant control schemes for mobile robots (Stancu, Codres & Puig, 2016). One such study presented FDD and fault-tolerant control with a sensor fault accommodation scheme as presented by (Zhang, Polycarpou & Parisini, 2001). A sliding mode FTCS using a fault hiding approach based on the kinematic model of a nonholonomic mobile robot is introduced in (Stancu *et al.*, 2016). A fault-tolerant controller design method is presented in (Carvalho Leite, Schäfer & de OLiveira e Souza, 2012) as a two-step procedure to provide alternative steering and reuse the nominal controller in a way that resembles a crab-like driving mode. Three fault modes are injected (one, two, and three failed steering joints) in real wheeled planetary rovers to evaluate the response of the non-reconfigured and reconfigured control systems when faced with these faults.

The critical issue in AFTCs is the limited time available for the FDD and the control system reconfiguration (Zhang & Jiang, 2006). Also, in the event of failure, efficient utilization and management of redundancy (in hardware, software, and communication networks), stability, transient performance, and guaranteed steady-state performance are important issues to consider in the design of AFTCs. Another important criterion for judging the suitability of a control method for AFTCS is its ability for the implementation to maintain an acceptable (nominal or degraded) performance in the impaired system in an online real-time setting (Zhang & Jiang, 2006). In this regard, the reconfigurable controller should be designed automatically with little trial-and-error or human interactions, and the methods selected must provide a solution even if the solution is not optimal.

Furthermore, in the study of FTCS, specifications for the system stability fall into three durations of system operations: (i) fault-free period (ii) transient period during the reconfiguration and

(iii) steady-state period after the reconfiguration. Moreover, as in any practical control system, robustness in stability and performance are also extremely important. For stability robustness, the feedback controllers must be designed to stabilize the closed-loop system in the presence of uncertainties. This is a well-investigated area on its own in control engineering (Zhou, Doyle, Glover *et al.*, 1996), and this issue has not been addressed extensively in AFTCs.

In the field of wheeled mobile robotics (WMR), the subject of faults occurring in wheeled locomotion has attracted significant attention because of its vital impact on the functionality of such robots (Rubio, Valero & Llopis-Albert, 2019). A robust adaptive fault-tolerant control approach for WMR has been resolved that deals with time-varying unknown control gain and parametric/non-parametric uncertainties of WMR, together with output constraints and actuation/propulsion failures (Wu, Yang & Ye, 2014). A hybrid fault adaptive control method is designed to accommodate partial faults and degradation for two-wheel drive (2WD) robots in (Ji *et al.*, 2003). A hierarchical-control accommodation framework is developed to determine a suitable control strategy to accommodate the isolated fault. It is revealed that for a small degradation in actuation effort, a robust controller achieves fault accommodation without significant loss of performance.

However, FTCSs for networked systems have not been fully investigated. The study presented by (Thumati, Dierks & Sarangapani, 2012), proposed a FTCS for a group of WMRs. Faults are mitigated by including an additional term in the basic control law that is a function of unknown fault dynamics and is retrieved by a neural network. This work primarily deals with how to accommodate the faults of the team members, but the team reconfiguration was not included. In Chamseddine, Zhang & Rabbath (2012), the FTCS problem for a team of UAVs is considered. Based on a trajectory re-planning approach, a formation recovery algorithm is proposed. In the fault-free case, each vehicle's trajectory is planned using a differential flatness method. When an actuator fails, a formation supervisor issues a centralized command to all UAVs to re-plan their trajectories within the physical limitations of the faulty vehicle. Xu, Yang, Jiang, Zhou & Zhang (2014b) introduced an adaptive FTC algorithm for a team of UAVs affected by actuator faults. The fault is modeled as a disturbance that affects the system. This fault is estimated by an observer, which is then accommodated by a compensator integrated into the regular controller. The reconfiguration, however, is not taken into account. More relative studies have been recently reported and can be found in (Xu, Yang, Huang, Shu & Wang, 2019; Yazdjerdi & Meskin, 2020; Khodabandeh *et al.*, 2021; Li, Dong, Li & Tong, 2023).

From the above discussions, the problems of the FTCSs for networked systems can be summarized as follows:

1. Most of the developed FTCS algorithms focus on communication faults.

2. The main challenge is to design a fault-tolerant cooperative controller that is computationally simple, reliable, and robust.

3. Many FTC control methods are designed based on the kinematics model of differential drive vehicles, ignoring the actual dynamics of the physical vehicles. Due to this limitation, the proposed controllers cannot be implemented in real vehicles.

4. Most of the FTC control methods are developed for differential drive vehicles, which are highly sensitive to slight changes in wheel velocity. Small differences in the relative velocities of the wheels can have a significant effect on the trajectory of the robot. There is a challenge synchronizing the drive motors due to slight differences in the motors, differences in friction in the drive trains, and differences in friction between the wheels and the ground.

5. The developed FTC methods can not handle severe actuator faults that may occur in any one of the team members. In other words, the performance of the FTC methods is limited to some level of faults; as the severity level arises, the entire system becomes more vulnerable to damage.

6. It is important to note that many of the proposed approaches have not been validated in real-time experiments.

2.8 Originality of the Thesis and Contributions

This thesis addresses the fault-tolerant cooperative control problem for a team of car-like vehicles that are subject to fading channels, actuator faults, and external disturbances. The methodology developed in this research work compensates for the effects of the faults for individual vehicles as well as for the whole team formation. The main contributions of this thesis can be summarized as follows:

In Article 1:

1. Comparing to recently reported results introduced in (Xu *et al.*, 2019; Yazdjerdi & Meskin, 2020; Khodabandeh *et al.*, 2021; Li *et al.*, 2023), our proposed DFTFC is more feasible for implementation in real vehicles. It provides a faster response to the occurrence of faults and better performance in handling both partial and severe actuator faults. In addition, it is faster in converging the vehicles to their reference trajectories after the occurrence of the faults, as demonstrated in the videos of our experimental results in (NAV Lab YouTube Channel, 2022).

2. None of the recently reported studies solved the reconfiguration of the team formation in the presence of severe/complete actuator faults in any vehicle. In this study, we addressed this limitation and proposed a re-assignment task mechanism based on the Simplex algorithm. This algorithm is integrated with the DFTFC to ensure the convergence of the team to the desired formation pattern. As mentioned earlier, the faulty vehicle with severe faults is excluded by the DFTFC, and with the developed re-assignment algorithm, the remaining vehicles are assigned to their desired positions p_i^v. The theoretical analysis for the implementation of the re-assignment algorithm with the DFTFC has been carefully analyzed in Section 3.3. The pseudocode for the proposed DFTFC algorithm with the re-assignment task mechanism is introduced in Section 3.4.

3. In contrast to the existing studies, the proposed DFTFC scheme is implemented in real car-like vehicles to validate the efficacy of the proposed controller in the presence of actuator fault conditions.

In Article 2:

1. This work introduces the first results for a team of car-like vehicles subject to simultaneous actuator faults and faded neighborhood communication information. The fading channel's effect and the vehicle dynamics' nonlinearity are carefully analyzed, providing guidelines for the fault-tolerant control design.

2. Compared to the existing studies in (Ren & Chen, 2015) and (Li, Niu & Cao, 2022), the settling time function in our study relies only on design parameters rather than the initial states, which restricts the practical application since the vehicles' information variables may not be accurately measured as they are often distorted by noises and disturbances.

3. The proposed methodology is implemented in real vehicles using the latest Quanser self-driving car (QCar) platform to validate the controller's performance in the presence of faults under investigation.

In Article 3:

1. To the best of the authors' knowledge, the problem of the simultaneous occurrence of the fading channel and actuator faults for networked systems has not been reported. This study introduces the first results of the cooperative control problem, considering the effect of fading channel and actuator fault with the presence of external disturbances.

2. In the developed adaptive control, the adaptive mechanism is able to modify the gain of sliding mode control automatically. This provides an advantage over a constant control gain in that the sliding mode control can function properly without prior knowledge of uncertainties and disturbances in the system.

3. As compared to existing fault-tolerant control methods, our developed control has a simple structure and can be readily implemented in practice.

2.9 Development of Experimental Setup

To successfully implement the proposed approaches in real-time experiments, the testbed includes two QCars, each with a 9-axis Inertial Measurement Unit (IMU), servo motors, and a Jetson TX2 processor and others, as illustrated in Figure 2.3 and Figure 2.4. The vehicles receive the commands from the PC and map them into the Pulse Width Modulation (PWM) to power the motors. Once the motors respond to the control signals, the onboard processor receives the IMU measurements and sends data through wireless communication Wi-Fi to the PC to generate the appropriate PWM signals for the motion along the reference trajectory. The specifications of the QCar are introduced in Table 2.1.

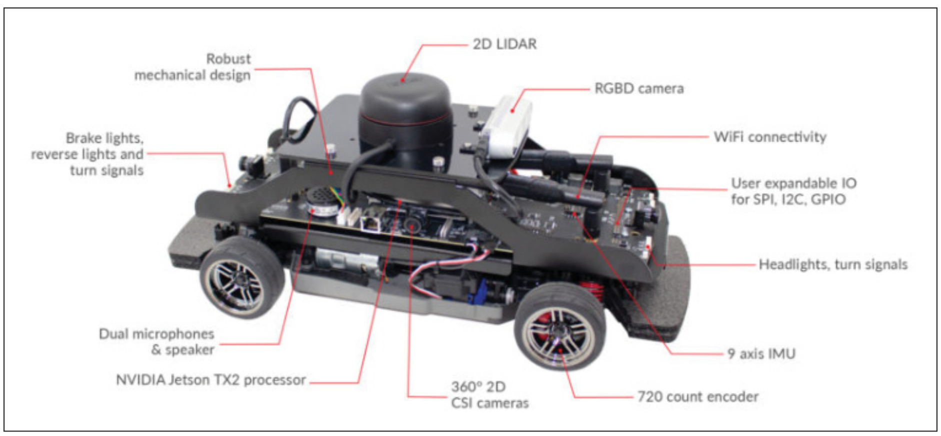

Figure 2.3 QCar platform .

Table 2.1 Specifications of QCar

Dimensions	$39\times 21 \times 21$ cm
Weight with batteries	2.7 Kg
Operation time	2 hours 11m
Onboard computer	NVIDIA Jetson TX2
Encoders	720 count motor encoder
IMU	9 axis IMU sensor
Connectivity	Wifi 802.11a/b/g/n/ac 867Mbpswith dual antennas

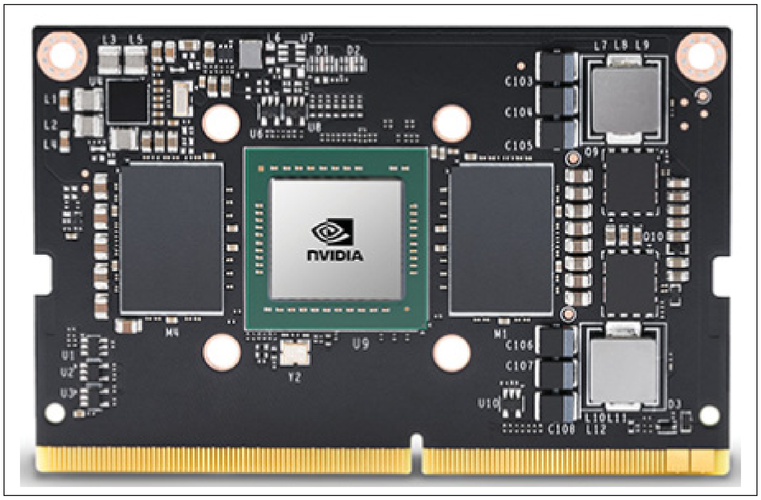

Figure 2.4 NVIDIA Jetson TX2 processor.

CHAPTER 3

DISTRIBUTED FAULT-TOLERANT FORMATION CONTROL DESIGN VIA HIGH-ORDER SLIDING MODE FOR A TEAM OF CAR-LIKE VEHICLES

Mahmoud Hussein[1], Youmin Zhang[2], Zhaoheng Liu[3]

[1] Departement of Electrical Engineering, École de technologie supérieure,
1100 Notre-Dame Ouest, Montréal, Québec, Canada H3C 1K3
[2] Department of Mechanical, Industrial, and Aerospace Engineering, Concordia University,
1455 De Maisonneuve Blvd. W. Montréal, Québec, Canada H3G 1M8
[3] Département de Génie Mécanique, École de technologie supérieure,
1100 Notre-Dame Ouest, Montréal, Québec, Canada H3C 1K3

Article submitted for publication to IEEE Transactions on Intelligent Vehicles in May 2023.

Abstract

This study introduces a distributed fault-tolerant formation control scheme for a team of car-like vehicles with actuator faults. The proposed controller includes a fault diagnostic scheme using a high-order sliding mode observer and a reconfigurable controller based on the super-twisting algorithm. The results showed that by the proposed controller, each robot could detect, diagnose, and accommodate actuator faults by itself. Two control strategies are proposed: 1) When a vehicle is exposed to a partial fault, the controller accommodates the fault and enables the vehicle to continue the mission with the rest of the team members in the formation. Furthermore, it allows healthy vehicles to re-adjust their motion and move in the way for compensating the reduced capability of the faulty vehicle with degraded performance in the formation mission; 2) In severe fault conditions, the proposed controller excludes the faulty vehicle and re-assigns its task to the rest of the healthy members to complete the mission. The re-assignment task for the team formation is formulated as an optimal assignment problem and is solved by the Simplex algorithm. The experimental tests have been conducted on the latest Quanser self-driving car (QCar) platform to verify the effectiveness of the proposed algorithm and ensure its capability to avoid accidents between team members.

Keywords: Actuator faults, Fault-tolerant control, order sliding mode, Car-like vehicle, Mobile robot, Super-twisting algorithm.

3.1 Introduction

The need for ensuring the reliability and safety of the networked control systems (NCSs) has evolved due to the complexity of these systems (Wang *et al.*, 2016). With increasing complexity and interconnectedness, the risk of having a fault in one or more components of the entire system increases. In practice, faults in NCSs are more likely to occur in one of the agents' components, i.e., actuators, sensors, etc., and that can not be prevented. A fault is defined as an unpermitted divergence of at least one of the system's distinctive properties from the acceptable, typical, standard state (Isermann, 2005). The fault in such defective situations is difficult to detect and isolate. In addition, it is hard to develop strategies for restoring the system to normal operation without using the concept of fault-tolerant control (FTC).

FTC is one of the most advanced control techniques that ensures acceptable performance when some component failures are encountered in dynamic systems (Zhang & Jiang, 2008). Moreover, it maintains the overall system's stability and provides a better response in both fault-free and fault scenarios. Two types of FTC are studied in the literature: passive fault-tolerant control (PFTC) and active fault-tolerant control (AFTC) (Wang, 2020). The PFTC is found to be robust against a class of pre-defined faults. It compensates for the effect of anticipated faults with no need for online fault information such as time, magnitude, or type of fault. In contrast to PFTC, AFTC requests the online fault information from the fault detection and diagnosis (FDD) algorithm to eliminate the effect of fault by synthesizing or switching to pre-computed control law in an online manner (Zhang & Chamseddine, 2012). The design objectives for AFTC include the transient and steady-state performance of the system not only under normal operations but also under fault conditions. It is important to point out that the system behavior emphasis in these two modes of operation can be significantly different. During normal operations, more emphasis should be placed on the quality of the system's behavior. However, system survival with an acceptable (probably degraded) performance becomes a predominant issue in the presence of a fault (Zhang & Jiang, 2003). Many studies on the FTC design methods have been carried out, and various effective design techniques are provided for different applications (Zhu, Li, Huang, Dong & Cai, 2023; Zhang, Sun, Liu, Lv & Deng, 2021; Pei *et al.*, 2023) including fault-tolerant control schemes against actuator faults for mobile robots (Jin, Zhao, Wang, Zhao & Dong, 2019; Alshorman *et al.*, 2020).

In this study, we further investigate the impact of the actuator faults on the stability of NCSs, considering issues that have not been addressed in the related studies. It is important to point out that actuators can significantly impact control systems and result in catastrophic accidents when they experience some failures. Actuator faults are typically defined as the difference between the expected and actual output of the actuator. They can result from the aging or deterioration of actuator components, leading to the actuator's eventual bias or loss of effectiveness (Kamel *et al.*, 2020). Several developed FTC methods for NCSs to compensate for the impact of the actuator faults, including bias and loss of effectiveness, can be found in (Semsar-Kazerooni & Khorasani, 2010; Shen *et al.*, 2014; Panagi & Polycarpou, 2011; Yang, Staroswiecki, Jiang & Liu, 2011; Kamel, Yu & Zhang, 2018). Recently, more related studies have been reported in (Xu *et al.*, 2019; Yazdjerdi & Meskin, 2020; Khodabandeh *et al.*, 2021; Li *et al.*, 2023). However, these recent studies have some limitations that can be summarized as follows:

1. The FTC control methods are designed based on the kinematics model of differential drive vehicles, ignoring the actual dynamics of the physical vehicles. Thus, the proposed controllers are inapplicable to real vehicles. Although the study introduced in (Li *et al.*, 2023) considered the dynamics of differential drive robot in the design of the FTC, the proposed controller has not been validated in real-time experiments. In addition, the authors did not address the complete/severe actuator faults issue that represents severe damage to the actuators' components. In practice, when the actuators are subjected to such fault conditions, they will be invalid for use. It is not safe for the entire system to keep such faulty vehicles in team formation. Otherwise, the entire system will be damaged.

2. The FTC control methods are developed for differential drive vehicles, which are highly sensitive to slight changes in wheel velocity. Small differences in the relative velocities of the wheels can have a significant effect on the trajectory of the robot. There is a challenge synchronizing the drive motors due to slight differences in the motors, differences in friction in the drive trains, and differences in friction between the wheels and the ground.

3. The developed FTC methods can not handle severe actuator faults that may occur in any one of the team members. In other words, the performance of the FTC methods is limited to some level of faults; as the severity level arises, the entire system becomes more vulnerable to damage.

4. None of the above-mentioned studies proposed solutions to exclude the vehicles with a severe/complete actuator failure and ensure the safety of the remaining vehicles to complete the team mission.

In this paper, we aim to overcome these limitations and fill the gap in the research by developing a distributed fault-tolerant formation control (DFTFC) scheme for a team of car-like vehicles. In the design of the DFTFC, we consider the dynamics of the actual vehicles and address both the partial and severe actuator faults problem. Moreover, we provide a solution to the formation re-assignment problem for healthy vehicles in the presence of one or more vehicles with severe/complete actuator faults. Our proposed DFTFC can reduce the computation load due to the implementation of the control algorithm in a distributed manner by each vehicle and provides an overall reliable system against the sudden changes that may occur to the actuators during the formation mission, regardless of the severity of the faults. The DFTFC scheme is designed based on a high-order sliding mode (HOSM) observer to detect and isolate additive actuator faults, which are superimposed on the control signals, and the super-twisting algorithm to compensate for the impact of such actuator faults. The rigorous proofs are provided to guarantee the efficacy of the proposed DFTFC in the presence of faults under investigation. In our study, we divided the methodology into two stages. Stage 1: Designing a distributed formation controller based on the virtual vehicle approach under fault-free conditions, and Stage 2: Designing a distributed fault-tolerant formation controller for the entire system with the assumption that a partial or severe actuator fault conditions may occur in any one of the team members during the team mission. The severity level of the fault can be defined as presented in (Kamel *et al.*, 2018). In the partial fault condition, the proposed controller allows the faulty vehicle to accommodate the fault and continue the mission with the rest of the healthy ones. While in the severe fault condition, the controller excludes the faulty one from the formation and notifies the rest of the team members to reconfigure their formation to a specific pattern and continue functioning for the rest of the mission.

The main contributions of this study can be summarized as follows:

1. Comparing to recently reported results in (Xu *et al.*, 2019; Yazdjerdi & Meskin, 2020; Khodabandeh *et al.*, 2021; Li *et al.*, 2023), our proposed DFTFC is more feasible for implementation in real vehicles. It provides a faster response to the occurrence of faults and better performance in handling both partial and severe actuator faults. In addition, it is faster in converging the vehicles to their reference trajectories after the occurrence of the faults, as demonstrated in the videos of our experimental results in (NAV Lab YouTube Channel, 2022).

2. None of the recently reported studies solved the reconfiguration of the team formation in the presence of severe/complete actuator faults in any vehicle. In this study, we addressed this limitation and proposed a re-assignment task mechanism based on the Simplex algorithm. This algorithm is integrated with the DFTFC to ensure the convergence of the team to the desired formation pattern. As mentioned earlier, the faulty vehicle with severe faults is excluded by the DFTFC, and with the developed re-assignment algorithm, the remaining vehicles are assigned to their desired positions p_i^v. The theoretical analysis for the implementation of the re-assignment algorithm with the DFTFC has been carefully analyzed in Section 3.3. The pseudocode for the proposed DFTFC algorithm with the re-assignment task mechanism is introduced in Section 3.4.

3. In contrast to the existing studies, the proposed DFTFC scheme is implemented in real car-like vehicles to validate the efficacy of the proposed controller in the presence of actuator fault conditions.

The remainder of the paper is organized as follows. Section 3.2 presents the dynamic model and problem statement. Section 3.3 introduces the distributed fault-tolerant formation control design. Section 3.4 introduces the pseudocode for the proposed DFTFC algorithm with the re-assignment task mechanism. The experimental results and analysis are provided in Section 3.5. Finally, the conclusion and future work are presented in Section 3.6.

3.2 Dynamic Model and Problem Statement

3.2.1 Vehicle dynamic model

Consider a team of car-like nonholonomic vehicles having a pair of front steering wheels and a pair of rear wheels. A car-like vehicle uses Ackermann's steering principle to create a center of rotation (CoR) along the axis of the rear wheels. As depicted in Figure 2.1, the kinematic model of the vehicle can be simplified to that of a bicycle model as presented in (Hu, Zhang & Rakheja, 2021). The vehicle's position (x, y) is defined by the coordinates of the midpoint of the rear axle c, and the heading angle ϕ is the orientation of the vehicle with respect to the longitudinal axis. ψ is the steering angle of the front wheels. L is the distance between the front and rear axles. b is the distance from the center of mass to the rear axle.

In this study, the kinematic model of i^{th} vehicle is modeled as presented in Eq. (2.2). The dynamics of i^{th} vehicle with generalized coordinates $q_i \in R^n$ and subject to k constraints can be given by the following relation:

$$M(q_i)\ddot{q}_i + V(q_i, \dot{q}_i)\dot{q}_i = B(q_i)\tau_i - A^T(q_i)\lambda_i, \tag{3.1}$$

where $M(q_i) \in R^{n\times n}$ is a symmetric and positive definite matrix, $V(q_i, \dot{q}_i) \in R^{n\times n}$ is the Coriolis and centrifugal forces, $\tau_i \in R^r$ is the input vector. $B(q_i) \in R^{n\times r}$ is the transformation matrix, $A(q_i) \in R^{k\times n}$ is the matrix associated with the constraint, $\lambda_i \in R^k$ is the Lagrangian constant, where

$$M = \begin{bmatrix} m & 0 & I_c\sin(\phi_i) & 0 \\ 0 & m & -I_c\cos(\phi_i) & 0 \\ I_c\sin(\phi_i) & -I_c\cos(\phi_i) & I_b & I_w \\ 0 & 0 & I_w & I_w \end{bmatrix},$$

$$V = \begin{bmatrix} 0 & 0 & -I_c\dot{\phi}\cos(\phi_i) & 0 \\ 0 & 0 & -I_c\dot{\phi}\sin(\phi_i) & 0 \\ 0 & 0 & 0 & 0 \\ 0 & 0 & 0 & 0 \end{bmatrix}, B = \begin{bmatrix} \cos(\phi_i) & 0 \\ \sin(\phi_i) & 0 \\ L\sin(\psi_i)\cos(\psi_i) & 0 \\ 0 & 1 \end{bmatrix},$$

$$A^T(q_i)\lambda_i = A^T(q_i)\begin{bmatrix} \lambda_{i1} \\ \lambda_{i2} \end{bmatrix},$$

where $m = m_c + 4m_w$, $I_c = (L-b)m_c + 2Lm_w$, $I_b = m_c(L-b)^2 + 4W^2m_w + I_{bzz} + 4I_{wzz}$, m_c and m_w are the vehicle and wheel masses, respectively, I_w is the moment of inertia of each wheel with a motor about the wheel axis. I_{bzz} is the moment of inertia of the vehicle about the z-axis. I_{wzz} is the moment of inertia of the wheel about the z-axis.

It is assumed that the vehicles in a formation mission are identical with the same parameters. The system in (3.1) can be simplified for control purposes as follows.

First, we introduce a full rank matrix $S_i(q_i)$, which has a set of linear independent vector that is obtained by spanning the null space of $A(q_i)$, i.e.,

$$S_i^T A^T = 0. \tag{3.2}$$

From (3.2), one can find auxiliary vector $\bar{\omega}_i \in R^{n-m}$ such that

$$\dot{q}_i = S_i \bar{\omega}_i, \tag{3.3}$$

where

$$S_i = \begin{bmatrix} \cos\phi_i & 0 \\ \sin\phi_i & 0 \\ \frac{tan(\psi_i)}{L} & 0 \\ 0 & 1 \end{bmatrix}, \bar{\omega}_i = \begin{bmatrix} v_i & w_i \end{bmatrix}^T. \tag{3.4}$$

Substituting (3.3) into (3.1), we can obtain the reduced dynamic form that will be used later for the control design as:

$$\bar{M}(q_i)\dot{\bar{\omega}}_i + \bar{V}(q_i, \dot{q}_i)\bar{\omega}_i = \bar{B}(q_i)\tau_i, \tag{3.5}$$

where

$$\bar{M}(q_i) = S_i^T M S_i, \quad \bar{V} = S_i^T (M\dot{S}_i + V S_i), \quad \bar{B} = S_i^T B.$$

3.2.2 Control objectives

The overall control goal is to maintain the stability of the team formation in the presence of partial or severe actuator faults. Hence, we design a distributed fault-tolerant formation controller that achieves the convergence of all vehicles' positions p_i to their desired ones p_i^v and satisfies this condition $\lim_{t\to\infty} \left\| p_i - p_i^v \right\| \to 0$ with the following assumption.

Assumption 1. *There is no loss of information among team members during the mission.*

Remark 1. *This assumption is important in synthesizing a controller that relies on the state information of the local agent "ith vehicle" and its neighbors in achieving cooperative tasks.*

Therefore, in this study, we assume that the exchanged information between team members exists all the time with no communication issues occurring during the team mission.

3.3 Distributed Fault-Tolerant Formation Control Design

The fault-tolerant formation control design is folded into two stages as illustrated in Figure 3.1:

3.3.1 Stage 1: Designing distributed formation controller based on virtual vehicle approach under fault-free conditions

In this stage, the virtual vehicle approach is applied to establish the pre-defined team formation based on the posture and orientation of the virtual vehicle. Each vehicle fixes its location in the formation as related to the virtual vehicle's position so all team members can achieve the desired formation together. The strength of the controller we propose is that it is distributed; the i^{th} vehicle communicates with its local neighbors rather than with the entire formation. By the positional relationship, the kinematic model of the i^{th} vehicle becomes as follows:

$$\begin{bmatrix} \dot{x}_i^v \\ \dot{y}_i^v \\ \dot{\phi}_i^v \end{bmatrix} = \begin{bmatrix} \bar{B}_v \\ B_o \end{bmatrix} \begin{bmatrix} v_i \\ \dot{\phi}_i \end{bmatrix}, \tag{3.6}$$

where

$$\bar{B}_v = \begin{bmatrix} cos\phi_i & -l_{xi}sin\phi_i - l_{yi}cos\phi_i \\ sin\phi_i & l_{xi}cos\phi_i - l_{yi}sin\phi_i \end{bmatrix}, B_o = \begin{bmatrix} 0 & 1 \end{bmatrix},$$

and (x_i^v, y_i^v) is the desired position of the i^{th} vehicle in the formation relative to the virtual vehicle, ϕ_i^v is the desired heading angle of i^{th} vehicle. (l_{xi}, l_{yi}) is the relative distance between the i^{th} vehicle and the virtual vehicle. To achieve the control goal, we choose the consensus

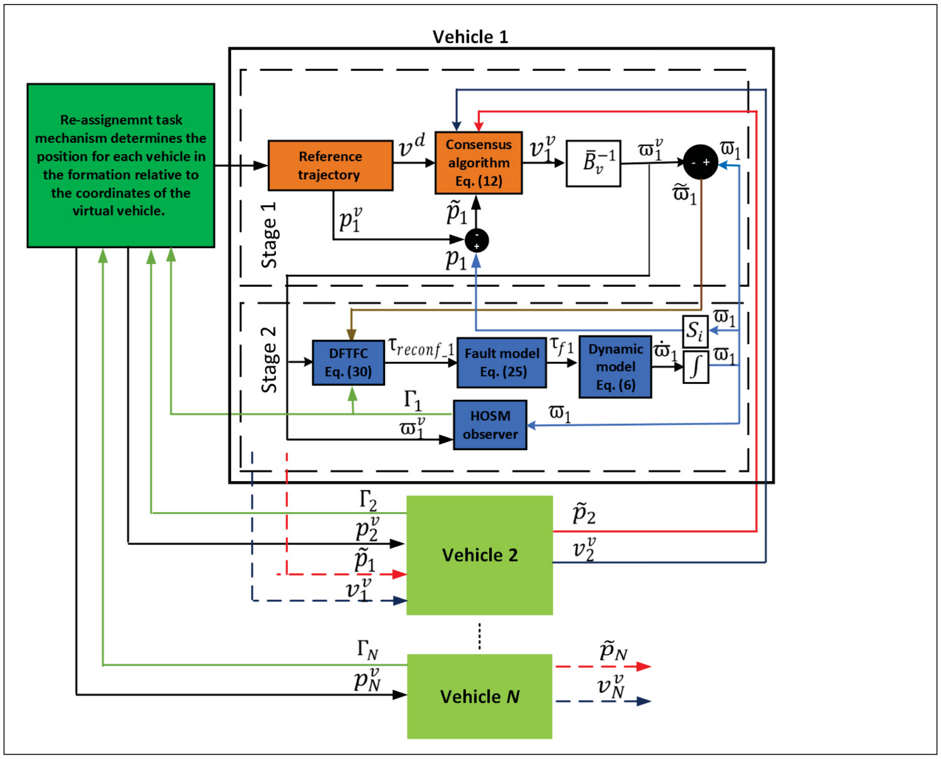

Figure 3.1 Overall system structure

algorithm as introduced in (Yoshioka & Namerikawa, 2008).

$$
\begin{aligned}
v_i^v &= v^d - K_c \sum_{j \in N} a_{ij}(p_i - p_i^v) - (p_j - p_j^v) \\
&= v^d - K_c \sum_{j \in N} a_{ij}(\tilde{p}_i - \tilde{p}_j),
\end{aligned}
\tag{3.7}
$$

where v_i^v is the velocity of the i^{th} vehicle such that $v_i^v = [\dot{x}_i^v, \dot{y}_i^v]^T$, v^d is the desired velocity of the formation. $a_{ij} = 1$ if vehicle i receives information from vehicle j and 0 otherwise. K_c is a positive control gain.

In real systems, it is important to consider collision avoidance techniques in the design of the formation controller. The artificial potential approach is an effective technique to avoid collisions between members. Here, we use the artificial potential function introduced by (Tanner & Kumar,

2005) as follows:

$$U_i = \sum_{j \in N} U_{ij}, \tag{3.8}$$

$$U_{ij} = \frac{D}{d_{ij}} + log \left\| d_{ij} \right\|. \tag{3.9}$$

Then, the collision avoidance control law u_o can be given by

$$u_o = - \nabla U_i | \sum_{j \in N} a_{ij} K_o (v_i^v - v_j^v)|, \tag{3.10}$$

where $K_o > 0$, d_{ij} is the relative distance between two neighboring vehicles, D is controller gain which is selected to satisfy that $D > 2((x_i^d)^2 + (y_i^d))^2)^{\frac{1}{2}} + R_o$ where R_o is the largest radius of the vehicles. With the collision avoidance algorithm in (3.10), the consensus algorithm can be given by:

$$v_i^v = v^d - K_c \sum_{j \in N} a_{ij}((\tilde{p}_i - \tilde{p}_j) - \nabla U_i | K_o \sum_{j \in N} a_{ij}(v_i^v - v_j^v)|. \tag{3.11}$$

From (3.6) and (3.11), the formation controller applied to system (3.5) can be written as:

$$\begin{bmatrix} v_i & \dot{\phi}_i \end{bmatrix}^T = \bar{B}_v^{-1} v_i^v. \tag{3.12}$$

3.3.2 Stage 2: Designing distributed fault-tolerant formation controller (DFTFC) based on the controller in Stage 1

Before proceeding to the controller design, we first need to apply the HOSM observer to estimate the states of the system and generate the residual signal that represents the magnitude of the fault acting on the actuator.

3.3.2.1 Second order sliding mode observer

Considering the system in (3.5), let us introduce new variables $\chi_{1i} = [v_i, \omega_i]^T$, $u_i = \tau_{Ni}$, then (3.5) can be rewritten in the state space form as follows:

$$\begin{aligned} \dot{\chi}_{1i} &= \chi_{2i} = \bar{\omega}_i, \\ \dot{\chi}_{2i} &= f_i(t, \chi_{1i}, \chi_{2i}, u_i), \\ h_i(t) &= \chi_{2i}. \end{aligned} \tag{3.13}$$

The function $f_i(.)$ in (3.13) can be replaced by

$$f_i(t, \chi_{1i}, \chi_{2i}, u_i) = \bar{M}^{-1}[u_i - \bar{V}\chi_{2i}]. \tag{3.14}$$

In the case of faults, the system (3.13) is not exactly known and should be identified in practice. Then the following relationship holds:

$$\hat{f}_i(t, \chi_{1i}, \hat{\chi}_{2i}, u_{fi}) = \bar{M}^{-1}[u_i + \Delta\vartheta_i - \bar{V}\hat{\chi}_{2i}], \tag{3.15}$$

where $u_{fi} = u_i + \Delta\vartheta_i$, $\hat{\chi}_{2i}$ is the estimated velocity of i^{th} vehicle. As introduced in (Shtessel, Edwards, Fridman & Levant, 2014) one can determine the approximated representation of the model as follows:

$$\begin{aligned} \dot{\hat{\chi}}_{1i} &= \hat{\chi}_{2i}, \\ \dot{\hat{\chi}}_{2i} &= \hat{f}_i(t, \chi_{1i}, \hat{\chi}_{2i}, u_{fi}), \\ h_i(t) &= \hat{\chi}_{2i}. \end{aligned} \tag{3.16}$$

It is known that the HOSM observer has the following form (Davila *et al.*, 2005):

$$\begin{aligned} \dot{\hat{\chi}}_{1i} &= \hat{\chi}_{2i} + z_{1i}, \\ \dot{\hat{\chi}}_{2i} &= \hat{f}_i(t, \chi_{1i}, \hat{\chi}_{2i}, u_{fi}) + z_{2i}, \end{aligned} \tag{3.17}$$

where $\hat{\chi}_{1i}, \hat{\chi}_{2i}$ are the state estimates, z_{1i} and z_{2i} are the correction variables of the form

$$\begin{aligned} z_{1i} &= K_{1i}|\tilde{\chi}_{1i}|^{0.5} sign(\tilde{\chi}_{1i}), \\ z_{2i} &= K_{2i} sign(\tilde{\chi}_{1i}), \end{aligned} \tag{3.18}$$

where the observer parameters K_{1i} and K_{2i} can be defined later during the tuning process.

From (3.18), we have $\tilde{\chi}_{1i} = \chi_{1i} - \hat{\chi}_{1i}$; and similarly, we can write $\tilde{\chi}_{2i} = \chi_{2i} - \hat{\chi}_{2i}$, then the error dynamics can be given by the following relationship:

$$\begin{aligned} \dot{\tilde{\chi}}_{1i} &= \tilde{\chi}_{2i} - z_{1i}, \\ \dot{\tilde{\chi}}_{2i} &= \bar{M}^{-1}[\Delta\vartheta_i - \varepsilon_i] - z_{2i}, \end{aligned} \tag{3.19}$$

where $\varepsilon_i = \bar{V}(\chi_{2i} - \hat{\chi}_{2i})$, we can rewrite the second equation in (3.19) as in (Davila *et al.*, 2005)

$$z_{2eq} = \bar{M}^{-1}[\Delta\vartheta_i - \varepsilon_i], \tag{3.20}$$

where z_{2eq} is the equivalent input signal corresponding to the discontinuous signal z_{2i}. However, it is important to implement a filter to reduce the noise resulting from the unmodeled effects in the experiments; therefore, the fifth-order low-pass filter $F(s)$ can be applied to handle this issue as follows:

$$F(s) = \frac{b_l}{1 - as^{-1} - as^{-2} - as^{-3} - as^{-4} - as^{-5}}, \tag{3.21}$$

where a and b_l are constants to be chosen later during the experimental tuning.

Then, the additive fault $\Delta\vartheta_i$ can be detected once occurred from the input signal z_{2eq} which gives an estimation to the fault $\Delta\hat{\vartheta}_i$ as follows:

$$\Delta\hat{\vartheta}_i = \ell_i(t) * \bar{M} z_{2eq}, \tag{3.22}$$

where $\ell_i(t)$ is the impulse response of the implemented filter and $*$ is the convolution product. From (3.22), the residual signal $r_{ii}(t)$ can be used to detect the partial and severe faults according to the following condition:

$$r_{ii}(t) = \begin{cases} 0 & \text{if } |\Delta\hat{\vartheta}_i| < T_i \\ 1 & \text{if } |\Delta\hat{\vartheta}_i| > T_i. \end{cases} \tag{3.23}$$

Remark 2. *The residual signal $r_{ii}(t)$ is useful to detect the occurrence of the actuator faults. It mainly depends on the estimated fault $\Delta\hat{\vartheta}_i$ that is derived in Eq. (3.22). $r_{ii}(t)$ is simply obtained by comparing $\Delta\hat{\vartheta}_i$ with the suitable threshold T_i selected based on the amplitude of the noise present in the system. If $\Delta\hat{\vartheta}_i < T_i$, then $r_{ii}(t) = 0$, which indicates that no fault is detected in the actuators, so the system is functioning under normal conditions. However, when $\Delta\hat{\vartheta}_i > T_i$, then $r_{ii}(t) = 1$, which indicates that the fault is detected in the i^{th} actuator, and the information of the estimated fault $\Delta\hat{\vartheta}_i$ is directly sent to the controller to take the appropriate action against this fault. The implementation of the $r_{ii}(t)$ in the system can be clearly observed in Eqs. (3.29) and (3.31).*

3.3.2.2 Fault-tolerant controller design

In this section, we design a fault-tolerant controller for a team of vehicles based on the formation controller in (3.12) and assume that the additive faults are bounded constant or periodic unknown signals acting on the control signal τ_{Ni} due to some mechanical or electrical faults. Then, the faulty control signal τ_{fi} can be written as follows:

$$\tau_{fi} = \tau_{Ni} + \Delta\vartheta_i, \tag{3.24}$$

where τ_{Ni} is the nominal torque input signal and $\Delta\vartheta_i \in R^2$ is the additive actuator fault. In the presence of actuator faults, Eq. (3.5) becomes:

$$\bar{M}\dot{\bar{\omega}}_i + \bar{V}\bar{\omega}_i = \tau_{fi}. \tag{3.25}$$

Now, we design the proposed fault-tolerant controller by first defining the error variable for vehicle i as follows:

$$e_i = \bar{\omega}_i - \bar{\omega}_i^d. \tag{3.26}$$

Taking the time derivative of (3.26) and substituting in (3.25) yields:

$$\begin{aligned} \dot{e}_i &= \dot{\bar{\omega}}_i - \dot{\bar{\omega}}_i^d \\ &= \bar{M}^{-1}(\tau_{fi} - \bar{V}\bar{\omega}_i) - \dot{\bar{\omega}}_i^d. \end{aligned} \tag{3.27}$$

The aim is to drive the error variables and their derivatives to zero. The super-twisting controller (STC) is used to avoid the chattering and compensate for the effects of the actuator faults. The STC has the following form (Derafa, Benallegue & Fridman, 2012):

$$\begin{aligned} \dot{\sigma}_i &= -\alpha_i |e_i|^{0.5} sign(e_i) + \epsilon_i, \\ \dot{\epsilon}_i &= -\beta_i sign(e_i), \end{aligned} \tag{3.28}$$

where α_i and β_i are positive gains to be defined later. The signum function $sign(e_i)$ can be defined as:

$$sign(e_i) = \begin{cases} 1 & \text{if} \quad e_i > 0 \\ 0 & \text{if} \quad e_i = 0 \\ -1 & \text{if} \quad e_i < 0. \end{cases}$$

From (3.27) and (3.28), the proposed fault-tolerant controller can be derived as:

$$\tau_{reconf-i} = \bar{M}\bar{u}_i + \bar{V}\bar{\omega}_i - \Gamma_i, \tag{3.29}$$

where $\tau_{reconf-i}$ is the reconfigured torque input, and $\bar{u}_i$ is defined as:

$$\bar{u}_i = \dot{\bar{\omega}}_i^d - \alpha_i |e_i|^{0.5} sign(e_i) - \beta_i \int_0^t sign(e_i) d\tau, \tag{3.30}$$

where Γ_i is provided by the HOSM observer, it represents the estimated magnitude of the fault acting on the faulty actuator.

$$\Gamma_i = \begin{bmatrix} r_{ii} & 0 \\ 0 & r_{ii} \end{bmatrix} \begin{bmatrix} \Delta\hat{\vartheta}_{li} \\ \Delta\hat{\vartheta}_{ri} \end{bmatrix}. \tag{3.31}$$

Theorem 1. *Consider the dynamic model of the system in (3.25), for any initial conditions $\sigma_i(0)$, the super-twisting control (3.29) ensures the convergence of (3.26) to zero in finite time if the controller gains are chosen as:*

$$\alpha_i > 2\sqrt{|\dot{\gamma}_i|}, \tag{3.32}$$
$$\beta_i > \frac{(K^2+1)\,|\dot{\gamma}_i|}{2K},\ K > 0. \tag{3.33}$$

Proof. To reach the convergence in finite time, first, we substitute the proposed controller (3.29) into the system (3.27) and yield:

$$\begin{aligned} \dot{e}_i &= -\alpha_i|e_i|^{0.5}sign(e_i) + \epsilon_i, \\ \dot{\epsilon}_i &= -\beta_i sign(e_i) + \dot{\gamma}_i, \end{aligned} \tag{3.34}$$

where $\gamma_i = \bar{M}^{-1}(\Delta\vartheta_i - \Delta\hat{\vartheta}_i)$ is the error between the real and estimated injected faults.

Then, let us consider the following Lyapunov function:

$$V_i = \sum_{i=1}^{N} \xi_i^T \overline{P}_i \xi_i, \tag{3.35}$$

where $\xi_i = [\xi_{i1} \quad \xi_{i2}]^T = [|e_i|^{0.5}sign(e_i) \quad \epsilon_i]^T$, $\overline{P}_i$ is a positive definite matrix, continuous and differentiable everywhere except on $e_i = 0$. $\overline{P}_i$ matrix is selected as:

$$\overline{P}_i = \begin{bmatrix} 2\bar{b}(\beta_i + 2\bar{b}^2) & -2\bar{b}^2 \\ -2\bar{b}^2 & \bar{b} \end{bmatrix}, \tag{3.36}$$

where $\bar{b}$ is a strictly positive constant.

The time derivative of ξ_i is computed as:

$$\dot{\xi}_i = \frac{1}{2|\xi_{i1}|}(\overline{A}_i\xi_i + B_i\dot{\gamma}|\xi_{i1}|), \tag{3.37}$$

with

$$\overline{A}_i = \begin{bmatrix} -\alpha_i & 1 \\ \\ -2\beta_i & 0 \end{bmatrix}, \quad \text{and} \quad B_i = \begin{bmatrix} 0 \\ \\ 1 \end{bmatrix}. \tag{3.38}$$

Hence, computing the derivative of (3.35) using (3.37) yields:

$$\begin{aligned} \dot{V}_i &= \sum_{i=1}^{N} \dot{\xi}_i^T \overline{P}_i \xi_i + \xi_i^T \overline{P}_i \dot{\xi}_i \\ &\leq \frac{1}{2|\xi_{i1}|} \sum_{i=1}^{N} \xi_i^T \left((\overline{A}_i^T \overline{P}_i + \overline{P}_i \overline{A}_i)\xi_i + 2\dot{\gamma}_i |\xi_{i1}| B_i^T \overline{P}_i \xi_i \right), \end{aligned} \tag{3.39}$$

Since the time derivative of γ_i is bounded, then the following inequality holds:

$$2\dot{\gamma}_i |\xi_{i1}| B_i^T \overline{P}_i \xi_i \leq \dot{\gamma}_i^2 C_i^T C_i \xi_i + \overline{B}_i \overline{P}_i \xi_i, \tag{3.40}$$

where $C_i = \begin{bmatrix} 1 & 0 \end{bmatrix}$ and $\overline{B}_i = \overline{P}_i B_i B_i^T$. By substituting (3.40) into (3.39) one has:

$$\begin{aligned} \dot{V}_i &\leq \frac{1}{2|\xi_1|} \sum_{i=1}^{N} \xi_i^T \overline{A}_i^T \overline{P}_i \xi_i + \xi_i^T \overline{P}_i \overline{A}_i \xi_i + \xi_i^T \dot{\gamma}_i^2 C_i^T C_i \xi_i + \xi_i^T \overline{B}_i \overline{P}_i \xi_i \\ &\leq -\frac{1}{|\xi_1|} \sum_{i=1}^{N} \xi_i^T \overline{Q}_i \xi_i, \end{aligned} \tag{3.41}$$

where

$$\begin{aligned} \overline{Q}_i &= -\frac{1}{2} \left(\overline{A}_i^T \overline{P}_i + \overline{P}_i \overline{A}_i + \dot{\gamma}_i^2 C_i^T C_i + \overline{P}_i B_i B_i^T \overline{P}_i \right) \\ &= \begin{bmatrix} \beta_i (2\overline{b}\alpha_i - 4\overline{b}^2) + 4\overline{b}^3 \alpha_i - \dot{\gamma}_i^2 - 4\overline{b}^2 & -\overline{b}^2 \alpha_i \\ \\ -\overline{b}^2 \alpha_i & \overline{b}^2 \end{bmatrix}, \end{aligned} \tag{3.42}$$

It can be seen that $\overline{Q}_i$ is a symmetric positive-definite matrix if

$$\begin{aligned} \alpha_i &> 2\overline{b}, && (3.43) \\ \beta_i &> 0.5 * \overline{b}(\alpha_i - 2\overline{b}) + \frac{\dot{\gamma}_i^2}{2\overline{b}(\alpha_i - 2\overline{b})}. && (3.44) \end{aligned}$$

Remark 3. *$\dot{\gamma}_i$ is given as a function of the estimated fault $\Delta\hat{\vartheta}_i$. In many systems, the occurrence of a fault is unexpected and unknown; therefore, it is not possible to detect it without using a fault detection and diagnosis algorithm. Hence, we have used HOSM observer as a fault diagnosis algorithm to detect and estimate the fault for the controller design, which uses this online information to make a suitable decision in response to the fault. The controller makes a decision that eventually ensures the completion of the team mission as desired. Therefore, by the HOSM observer, $\dot{\gamma}_i$ will be known, and then α_i can be simply selected according to the conditions in Eq. (3.32) and Eq. (3.43).*

Once again, by choosing $\overline{b} = \sqrt{|\dot{\gamma}_i|}$ and $\alpha_i - 2\overline{b} = K\sqrt{|\dot{\gamma}_i|}$, the conditions in (3.43) become the conditions in (3.32). Verifying these conditions ensures that $\dot{V}_i$ is negative definite. Moreover, (3.41) gives

$$\dot{V}_i \leq -\frac{1}{|\xi_1|}\lambda_{min}\{\overline{Q}_i\}\, \|\xi_i\|_2^2\,, \tag{3.45}$$

while V_i is bounded, then the following formula is obtained as follows:

$$\sqrt{\frac{V_i}{\lambda_{min}\{\overline{P}_i\}}} \leq \|\xi_i\|_2 \leq \sqrt{\frac{V_i}{\lambda_{max}\{\overline{P}_i\}}}. \tag{3.46}$$

Since $|\xi_1| \leq \|\xi_i\|_2$, Eq. (3.45) implies the following relationship:

$$\dot{V}_i = -\sqrt{\frac{\lambda_{min}^2\{\overline{Q}_i\}V_i}{\lambda_{max}\{\overline{P}_i\}}}. \tag{3.47}$$

Finally, based on Lyapunov theory (Moreno & Osorio, 2008), the maximal convergence time is computed as:

$$T_i^c \leq \frac{2\sqrt{\lambda_{max}\{\overline{P}_i\}V_i(0)}}{\lambda_{min}\{\overline{Q}_i\}}, \tag{3.48}$$

where $V_i(0)$ is the initial value of V_i. This completes the proof. □

3.4 Re-assignment Task Mechanism in the Severe Fault Conditions

The re-assignment problem can be formulated mathematically as follows:

Definition 3.1. *Consider a team of vehicles $R_i = \{R_1, R_2, ..., R_N\}$, navigating in a known environment, and the position of vehicle i is represented by $p_i \in \mathbb{R}^2$ and $p = [p_1, p_2, ..., p_N]^T$. The team goal is to organize and distribute themselves with a minimum total distance in a known formation pattern that is denoted by $p^v = [p_1^v, p_2^v ..., p_N^v]^T$.*

To achieve the re-assignment task for the formation problem, we define a set of points that form a formation pattern described by $S^\star = [S_1^\star, S_2^\star, ..., S_N^\star]^T$ and in this regard, the realization of a particular pattern represented as a function of $S^\star$ with the application of translation $\bar{p}^v$ and the rotation ϕ can be defined as follows:

$$p^v = 1_N \otimes \bar{p}^v + (I_N \otimes R_\phi)S^\star, \tag{3.49}$$

with

$$R_\phi = \begin{bmatrix} cos\phi & -sin\phi \\ sin\phi & cos\phi \end{bmatrix}.$$

where 1_N is a vector of all elements equal to 1, and $\otimes$ is the Kronecker product. To assign each vehicle one role in the formation, we define a set of assignment variables $x_{ij}, i, j \in \{1, ..., N\}$ such that when $x_{ij} = 1$ that means vehicle i is assigned a role j in the formation, otherwise $x_{ij} = 0$. Given the formation, the total distance (cost) needed to move vehicle i to position p_i^v in the formation can be presented by $\| p_i - p_i^v\|_2^2$.

Then, the minimum total cost can be introduced as an optimal assignment problem of the following form:

$$min \sum_{i=1}^{N} \sum_{j=1}^{N} x_{ij} \parallel p_i - p_i^v \parallel_2^2 . \tag{3.50}$$

Equation (3.50) ensures the optimal assignment for each robot to reach its designated position. The strategy of the proposed DFTFC scheme in Section 3.3 with the re-assignment task mechanism for multiple vehicles is summarized in Algorithm 1.

Algorithm 3.1 Pseudocode for the proposed DFTFC algorithm

for *each robot* **do**
    measure $\Delta\hat{\vartheta}_i$ by the HOSM observer
    while $\Delta\hat{\vartheta}_i > T_i$ **do**
        calculate $\bar{\omega}_i$;
        if $\bar{\omega}_i \leq 0.65\bar{\omega}_{Ni}$ **then**
            apply the control law (3.29)
            send $\hat{\vartheta}_i$ to every healthy vehicle
            elseif $\bar{\omega}_i > 0.65\bar{\omega}_{Ni}$, **then**
              Motors are switched off to leave the team formation
              Send 0 to team members to form a new formation;
            else send 1 and continue the mission
        end if
    end while
end for
for *each healthy vehicle in the formation* **do**
    receive N_{Ri} from each robot
    if *all the elements of* N_{Ri} *equals 1* **then**
        keep tracking the reference trajectory p_i^v
        elseif one or more of the received elements in N_{Ri} are zero, **then**
        apply the optimal assignment problem
        find the cost matrix
        apply the Simplex algorithm
        assign to the corresponding slot
    end if
end for

3.5 Experimental Results and Analysis

In this section, we demonstrate the effectiveness of our proposed control scheme on the latest Quanser self-driving car (QCar) platform. The experiments have been conducted in the Networked Autonomous Vehicles Laboratory (NAV Lab) at Concordia University. All the experimental test videos of the QCar performed in this study can be viewed on (NAV Lab YouTube Channel, 2022).

3.5.1 Experimental setup

As shown in Figure 3.2, the experimental testbed includes two QCars, each with a 9-axis inertial measurement unit (IMU), servo motors, and a Jetson TX2 processor. The vehicles receive the commands from the PC and map them into the pulse width modulation (PWM) to power the motors. Once the motors respond to the control signals, the onboard processor receives the IMU measurements and sends data through wireless communication Wi-Fi to the PC to generate the appropriate PWM signals for the motion along the pre-defined trajectory. In the experiments, the two vehicles are required to form a line formation while tracking the reference path of the virtual vehicle. The proposed controller was examined under two actuator fault scenarios: partial and severe faults on the QCar platform.

The physical parameters of the vehicles are given as follows: m_c = 2.3 kg, m_w = 0.23 kg, L = 0.2 m, $2W$ = 0.1 m, I_{bzz} = 0.015 kg m^2, I_{wzz} = 0.002 kg m^2.

The gains of the control laws are selected as follows: K_c = diag(2, 2), K_o = diag(0.5, 0.5), α_i = diag(3.4, 3.4), β_i = diag(2.6, 2.6). The fifth-order low-pass filter is used to eliminate the high switching frequencies produced by the HOSM observer. Therefore, the filter is applied in our study to eliminate the components of the high frequencies of the observer signals and obtain a suitable residual signal. This filter has two parameters that have positive values, and they are selected in this study as a = 0.24 and b_l = 3.35. The reference trajectory of the virtual vehicle is given as $\dot{x}$ = 1.35cos(0.5t) and $\dot{y}$ = 1.35sin(0.5t).

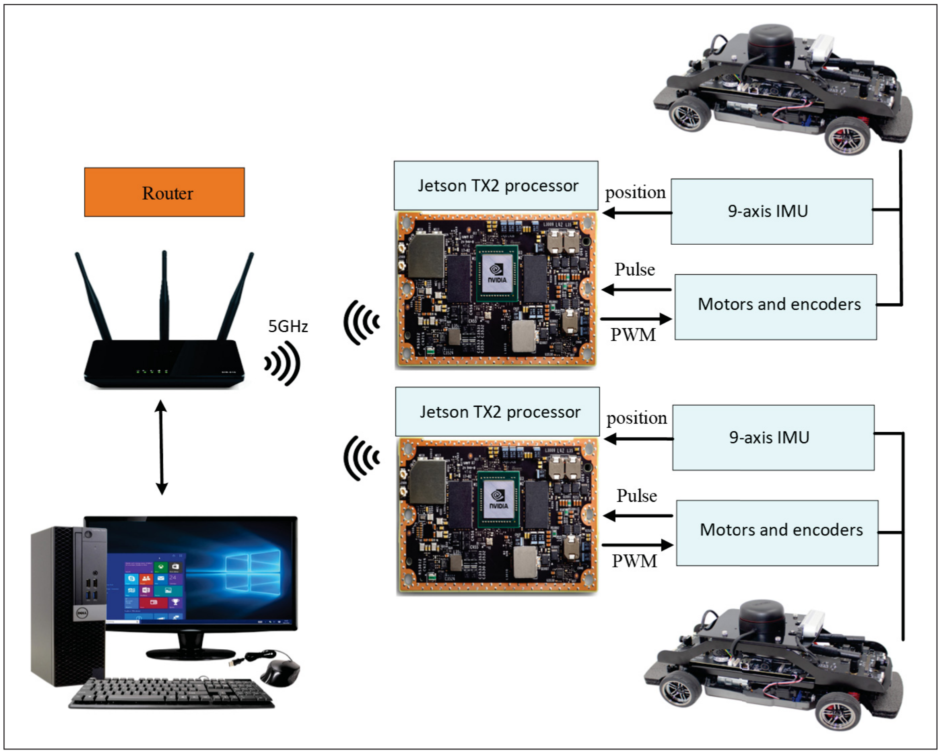

Figure 3.2   QCar experimental setup

3.5.2 Experimental results analysis of Scenario 1

In this scenario, the left motor of Vehicle 1 is subjected to a constant fault of -0.1 (N.m) at $t = 15$s. The fault signal is approximately 40% of the maximum control signal applied to the left motor. As illustrated in Figure 3.3, the fault affected the vehicle's motion for a few seconds before getting back to its reference trajectory. This figure shows two QCar vehicles moving in a line formation while tracking the coordinates of the virtual vehicle. The dashed dark line is the reference trajectory of Vehicle 2, while the red line is for the reference path of Vehicle 1. The green and blue lines describe the motion of Vehicles 1 and 2, respectively. Clearly, it can be seen that, under the influence of the fault, the proposed controller was capable of accommodating the fault in Vehicle 1. As a result, both vehicles remained stable and continued the mission successfully.

Figure 3.4 shows the trajectory tracking errors and illustrates that the proposed DFTFC can successfully accommodate the faults and achieve the tracking in a finite time. Figure 3.5 shows the linear velocities and steering angles of the two vehicles. Figure 3.5(a), presents the performance of the proposed DFTFC in compensating for the impact of the fault in a few seconds, allowing Vehicle 1 to move with an acceptable reduced velocity with Vehicle 2. In addition, the DFTFC reduced the velocity of Vehicle 2, as shown in Figure 3.5(b), to move within the same capability as faulty Vehicle 1 and maintain the pre-defined formation for the task.

Following the occurrence of the fault, the steering angles of the vehicles remained stable for the entire mission, as shown in Figures 3.5(c) and 3.5(d). This illustrates the effectiveness of the controller in maintaining the desired formation despite the presence of such a fault condition. Moreover, the two vehicles moved within approximately the same velocities and orientations, which is necessary for the maintenance of the formation, as depicted in Figures 3.5 and 3.6.

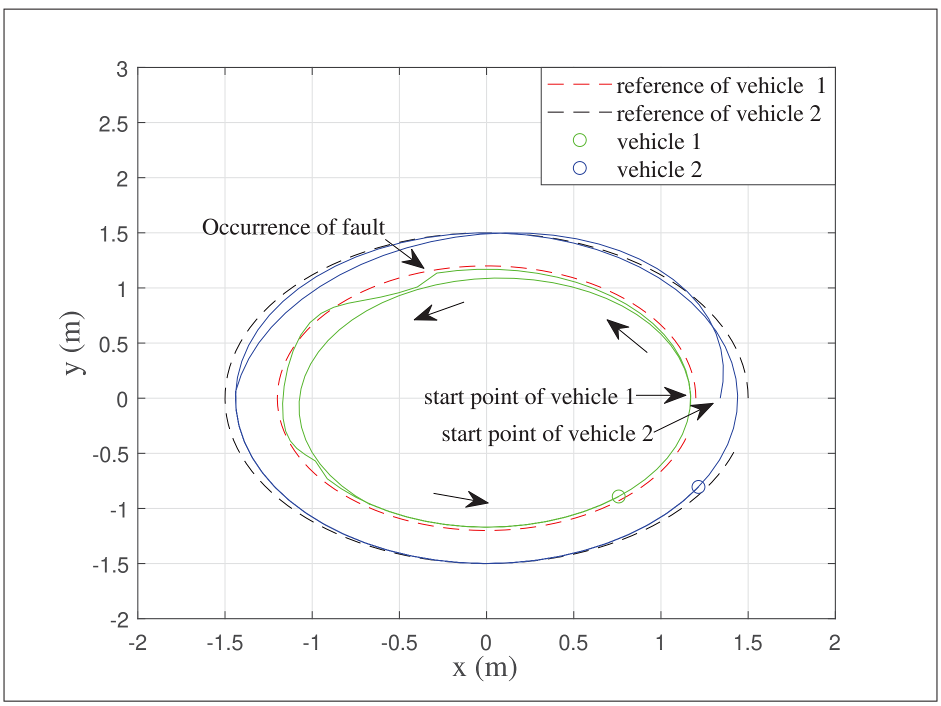

Figure 3.3 Actual trajectories of two vehicles with the partial fault scenario at t = 15s using the proposed DFTFC

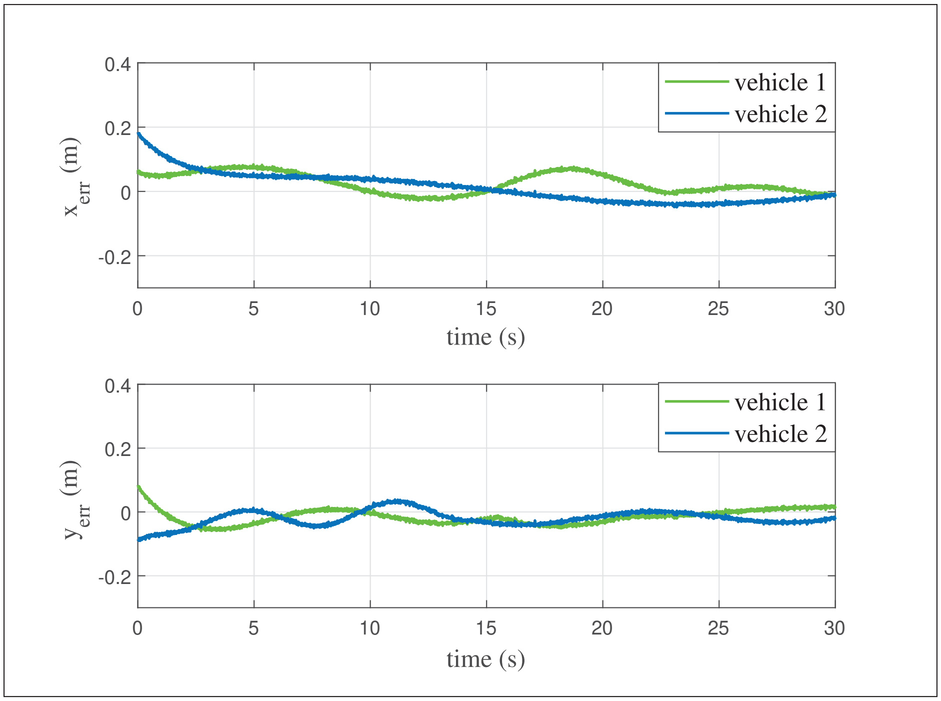

Figure 3.4 Trajectory tracking errors for vehicle 1 and vehicle 2

3.5.3 Experimental results analysis of Scenario 2

In Scenario 2, a severe fault of $-0.18 \sin \omega t$ (N.m) is injected at $t = 12$s to the left actuator of Vehicle 2. The fault signal is about 70% of the control signal applied to the left actuator. That has a severe impact on the performance of the motor. It is well known that the harmonics arise in the generated torques due to some mechanical or electrical failures. Therefore, these effects are modeled as a sinusoidal signal acting on the faulty motor. It is obvious in Figure 3.7 that the proposed controller allowed Vehicle 1 to continue the mission and excluded Vehicle 2 from the team formation. In addition, Figure 3.8 demonstrates the effectiveness of the DFTFC in handling severe faults. It can be seen from Figure 3.8(b) and Figure 3.8(d) that the controller excluded Vehicle 2 and enabled Vehicle 1 to avoid collision with Vehicle 2 and complete the mission as shown in Figures 3.8(a) and Figure 3.8(c).

However, it is worth mentioning that the comparative results of our experimental work with the reported results are discussed based on two main considerations: First is the reliability of the

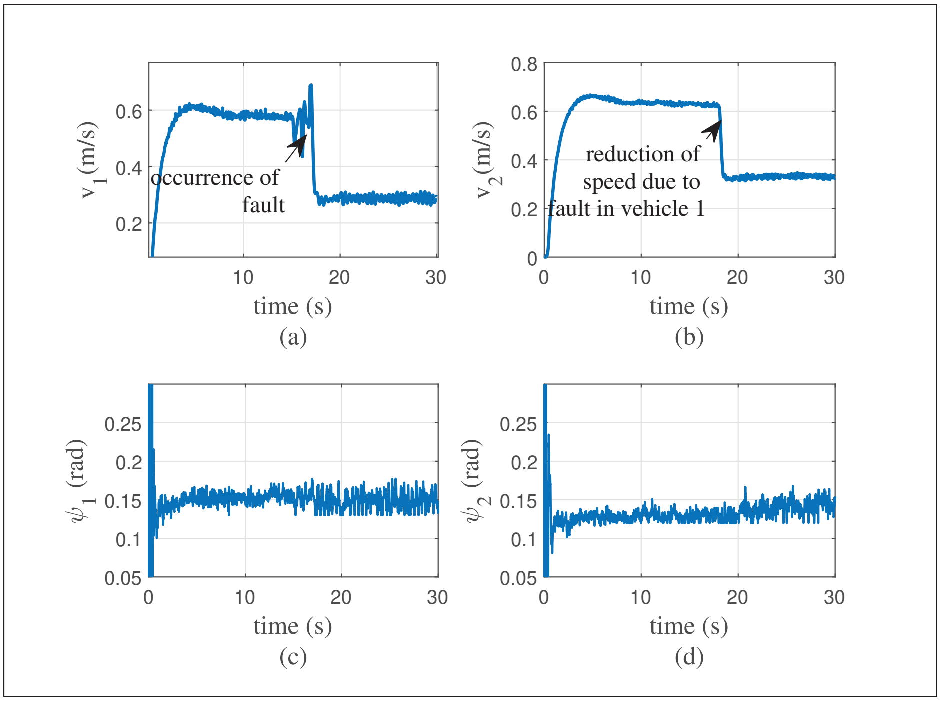

Figure 3.5 The linear velocity and steering angle of vehicle 1 and vehicle 2 (Scenario 1)

proposed controller to be implemented in practical applications. The authors of studies (Xu *et al.*, 2019; Yazdjerdi & Meskin, 2020; Khodabandeh *et al.*, 2021) discussed the impact of the actuator faults problem for multi-agent systems based on kinematic models ignoring the actual vehicle dynamics in their studies, making their proposed approaches not applicable to physical systems. Although the study introduced in (Li *et al.*, 2023) considered the actual dynamics of the robots, the experimental results have not been conducted. The study included only numerical simulations of differential drive robots, which are highly sensitive to slight changes in wheel velocity. Small differences in the relative velocities of the wheels can have a significant effect on the trajectory of the robot. Second is The capability of the proposed approaches in handling severe/complete actuator faults. None of the aforementioned studies addressed severe/complete actuator faults. Hence, their proposed controls will inevitably fail to protect the system from damage in the presence of such fault conditions.

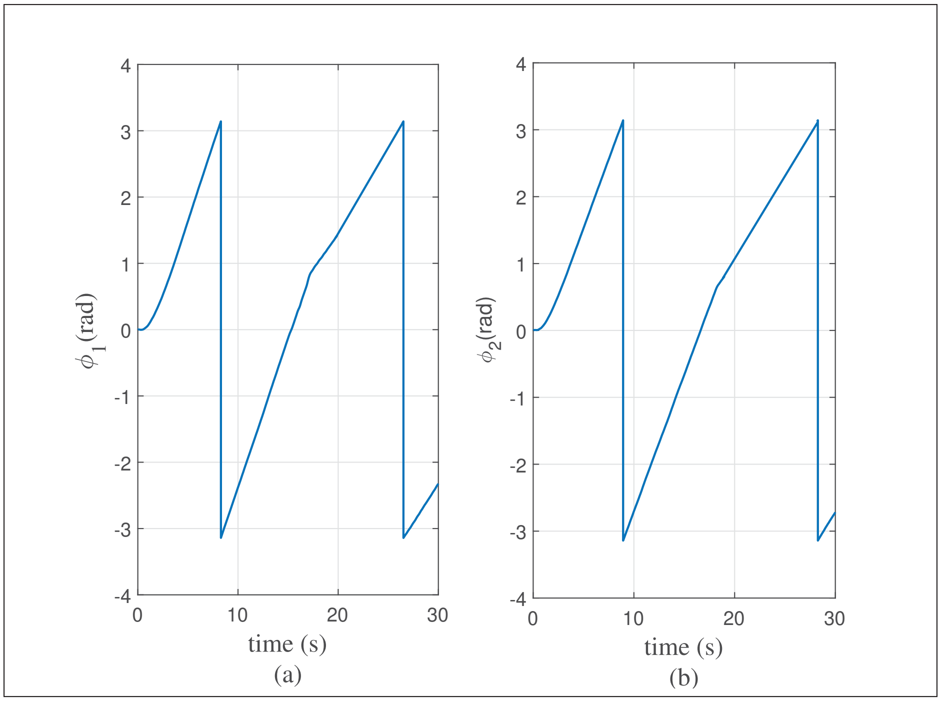

Figure 3.6 The heading angle of vehicle 1 and vehicle 2

By Comparing our experimental results with those reported in (Xu *et al.*, 2019; Yazdjerdi & Meskin, 2020; Khodabandeh *et al.*, 2021; Li *et al.*, 2023), it is evident that our controller is more reliable to be implemented in real systems. It has demonstrated its capability to handle both partial and severe faults, as shown in Figures 3.3-3.8. Particularly, Figures 3.3 and 3.7 illustrate the behavior of the vehicles before and after the occurrence of faults. It can be observed that the controller provided a fast response to the faults and successfully accommodated all actuator faults, regardless of their severity, which cannot be achieved by other controllers proposed in relative studies.

3.6 Conclusion and Future Work

In this paper, we have addressed the fault-tolerant formation control problem for a team of car-like vehicles subject to actuator faults. The super-twisting algorithm is used with the HOSM to monitor the operation status of the actuators and send any fault information to the controller. The proposed fault-tolerant controller ensures the completion of the mission in the presence of

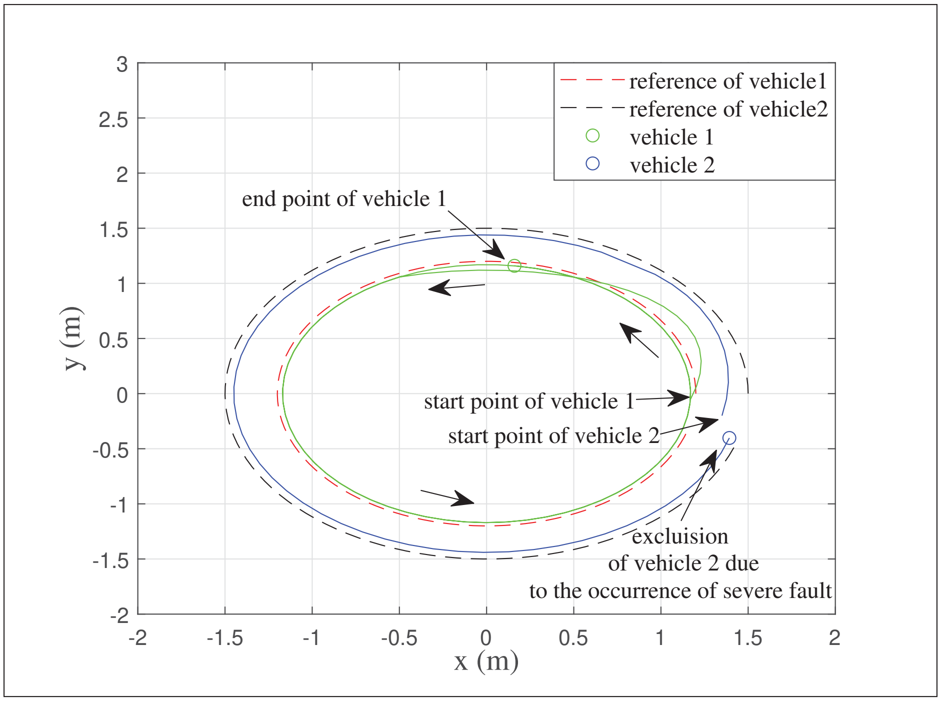

Figure 3.7 Actual trajectories of two vehicles with the severe fault scenario at t = 15s using the proposed DFTFC

such fault conditions. The experimental results demonstrate the effectiveness of the proposed methodology with two fault scenarios. Future work includes the investigation of simultaneous actuator and communication faults for multiple vehicles.

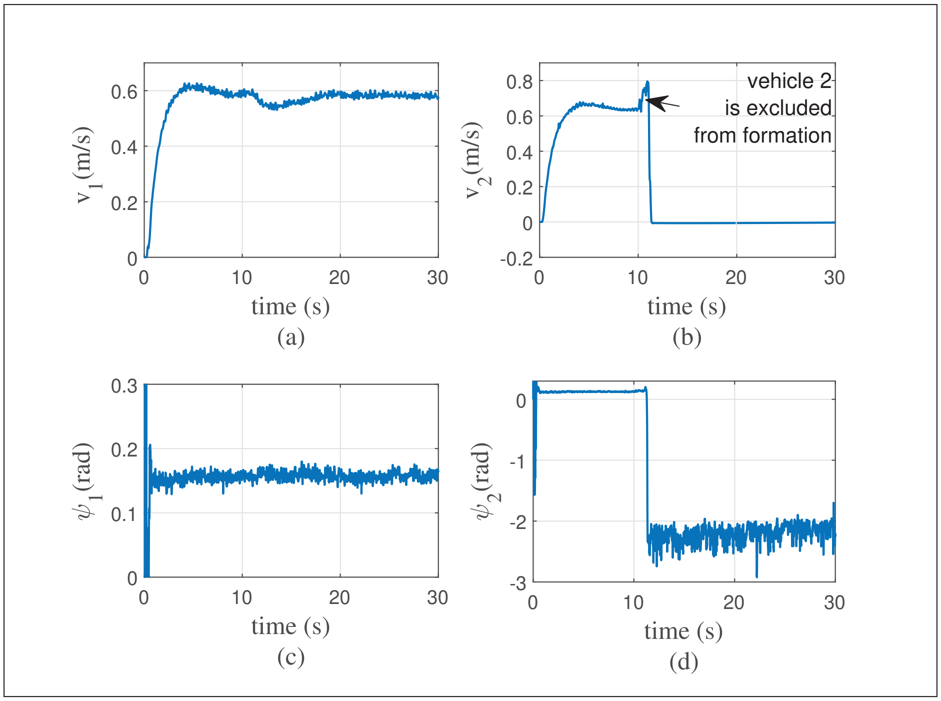

Figure 3.8 The linear velocity and steering angle of vehicle 1 and vehicle 2 (Scenario 2)

CHAPTER 4

FAULT-TOLERANT COOPERATIVE CONTROL DESIGN FOR CAR-LIKE VEHICLES SUBJECT TO ACTUATOR FAULTS AND FADING CHANNELS

Mahmoud Hussein[1], Youmin Zhang[2], Zhaoheng Liu[3]

[1] Departement of Electrical Engineering, École de technologie supérieure,
1100 Notre-Dame Ouest, Montréal, Québec, Canada H3C 1K3
[2] Department of Mechanical, Industrial, and Aerospace Engineering, Concordia University,
1455 De Maisonneuve Blvd. W. Montréal, Québec, Canada H3G 1M8
[3] Département de Génie Mécanique, École de technologie supérieure,
1100 Notre-Dame Ouest, Montréal, Québec, Canada H3C 1K3

Article submitted for publication to IEEE Transactions on Control Systems Technology in March 2023.

Abstract

This article addresses the fault-tolerant cooperative control problem for a team of car-like vehicles subject to multiplicative and additive actuator faults with the presence of faded neighborhood information. The motivation for this study stems from the observation that agents exchange information over wireless networks, which inherently introduce random fading to the transmitted signals. In the cooperative control of networked systems with a restricted communication bandwidth, continuous interaction between neighboring agents would inevitably increase the network transmission load and limit the practical application of the system. Moreover, cooperative control becomes more challenging when there are limitations on communication in the real world. It is thus important to investigate how to ensure the convergence of the team members to the desired trajectory in the presence of actuator faults using contaminated data. To this end, a cooperative controller is proposed to ensure the convergence of the system states to the desired ones in a finite time under fault-free and fault conditions. The rigorous proofs are provided by using the Lyapunov stability theorem. The effectiveness of the proposed controller is validated in a real system using the latest Quanser self-driving car (QCar) platform.

Keywords: Car-like vehicles, actuator faults, fading channel, nonlinear control, fault-tolerant cooperative control.

4.1 Introduction

Cooperative control of unicycle mobile robots has been widely investigated over the past decade (Sun *et al.*, 2009; Kostić *et al.*, 2010; Sadowska *et al.*, 2011). Various control strategies have been developed to address the cooperative control problem for mobile robots, including the leader-follower approach (Tanner *et al.*, 2004; Mesbahi & Hadaegh, 1999), behavior-based control (Balch & Arkin, 1998; Lawton *et al.*, 2003), virtual vehicle approach (Beard *et al.*, 2001; Ren & Beard, 2004b), artificial potentials (Liu & Passino, 2006; Leonard & Fiorelli, 2001) and graph theory strategies (Lafferriere *et al.*, 2005; Fax & Murray, 2004). To our knowledge, however, few studies addressed the cooperation problem for car-like vehicles. Nonetheless, this is an important topic to explore, as it pertains to a broader category of robots than unicycle-type robots, and hence, more investigation is needed towards autonomous and safe driving of future self-driving cars in realistic conditions.

The cooperative control problem is closely related to the consensus problem. When all vehicles in the team reach an agreement on a variable value of interest, they are said to reach a consensus. Information consensus ensures that all vehicles exchanging information across a network topology have a consistent view of the data essential to the cooperation task. Several results on the cooperative control problems for mobile robots have been published in the literature based on the consensus theory. For instance, Olfati-Saber & Murray (2004) and Ren & Beard (2005) investigated the consensus tracking problem for networked systems with switching and fixed topologies. More complicated control strategies have been reported recently as in (Feng & Zheng, 2019); the authors proposed adaptive neural network tuning laws for nonlinear multi-agent systems (MASs) with uncertain dynamics to accomplish robust tracking control. In Zou *et al.* (2019), the distributed predictive control (DPC) problem for MAS subject to disturbances is addressed, and the goal is to reduce the energy consumption and the load of computation. A sliding mode control method was used to solve the second-order MAS's confinement control problem with norm-bounded nonlinear perturbation in (Yu & Ji, 2018). In Meng, Jia & Du (2014), the robustness issues under state shifts, disturbances, and topological switching were solved using a distributed iterative learning control (ILC) approach that used nearby agent information to reach consensus for agents in an undirected communication graph. The researchers also focused on the cooperative control problem for nonhomogeneous MAS, such as the study in (Shen & Xu, 2018), which was conducted on the heterogeneous high-order nonlinear MAS with output limitations. The proposed technique solves the consensus tracking problem by incorporating a barrier Lyapunov function. This work includes both control strategies and performance evaluations.

However, in practice, faults in MAS are more likely to occur in one of the agents' components, i.e., actuators, sensors, etc., and that can not be prevented. However, it can be mitigated by means of fault-tolerant control (FTC) methods (Zhang & Jiang, 2008). Few recent results have been introduced for the cooperative control problem with the actuator faults based on FTC techniques. In Kamel *et al.* (2018), an FTC scheme with the linear MPC is developed to accommodate partial and severe actuator faults in the team of differentially driven mobile robots. The proposed controller has the capability to reconfigure the formation and re-coordinate the motion of each agent in the team formation. Another study investigated the cooperation control problem with actuator faults, external disturbances, and input saturation simultaneously for a team of unmanned aerial vehicles (UAVs) in (Yu, Qu & Zhang, 2018). The disturbance observer (DO) is used to compensate for the uncertainty caused by the actuator faults and disturbances. Moreover, dynamic surface control (DSC) is utilized to reduce the computational complexity presented in the conventional backstepping design. More studies on the FTC for networked systems with actuator faults can be found in (Deng & Yang, 2019; Dehshalie, Menhaj & Karrari, 2019; Zuo, Zhang & Wang, 2014; Wang & Wang, 2018). Nevertheless, when data exchange is incomplete, the proposed control systems may not be practical.

With the rapid growth of computer network technology, an increasing amount of system data is exchanged via communication networks. During the transfer of information over the communication medium, a portion of the energy could be transformed randomly into heat energy or absorbed by the communication medium. In addition, the signal amplitude may fluctuate due to interference from the external environment, resulting in signal distortion. This phenomenon is called fading channel (Shen & Qu, 2019).

In real-world applications, the fading problem is a significant channel-induced phenomenon in wireless networks caused by refraction, reflection, and diffraction during propagation (Elia, 2005). Fading damages the transmitted data, i.e., position, velocity, etc., which is critical for the control design of the networked systems. Thus, it is important to consider the effect of fading channels on the cooperative control of networked control systems (NCSs) (Panagou *et al.*, 2015; Li & Niu, 2019). One of the main challenges in developing a cooperative control system for NCSs is the lack of complete information and the presence of actuator faults in the system. A fault-tolerant cooperative controller is designed not only to compensate for actuator faults but also to achieve cooperative tracking over a communication network. However, this objective can not be accomplished with the lack of complete information that may occur due to some communication issues, i.e., fading channels. Recently, many reported results for NCSs with actuator faults, such as in (Xu *et al.*, 2019; Yazdjerdi & Meskin, 2020; Li *et al.*, 2023) assume that the information exists all the time and there are no fading channels in the network. In practice, the impact of one vehicle's failure can spread to the rest of the vehicles when there is a lack of complete information exchanged between vehicles. This limitation inspires us to study both the actuators and fading channels' problems for NCSs. Compared to the aforementioned recent studies, our proposed controller has the capability to handle the multiplicative and additive actuator faults and ensure the stability of the overall system in the presence of faded neighborhood information. To the best of the authors' knowledge, this is the first attempt to investigate the simultaneous occurrence of such faults issues for a team of car-like vehicles.

Motivated by the aforementioned studies, this article considers the fault-tolerant cooperative control (FTCC) problem for leader-follower networks in the presence of actuator faults and fading channels. First, we design the FTCC under the effect of a fading channel using sliding mode control. The tracking variables cannot be properly calculated with fading channel conditions. To overcome this issue, the information exchanged over the fading channel is utilized to evaluate the error of tracking variables. Using this strategy not only increases the precision of the controller's design but also provides a practical solution to the consistency problem of leader-follower networks with channel fading. Second, we develop an FTCC approach under the influence of fading channels and actuator faults. Specifically, the multiplicative and additive actuator faults are considered in this study. The FTCC is designed based on the integral terminal sliding mode (ITSM) technique. Compared to sophisticated algorithms, ITSM is known for its responsiveness, robustness, and stability in unknown conditions. Furthermore, this controller is simple in structure and easy to implement in practical applications.

The main contributions of this paper can be summarized as follows:

1. This work introduces the first results for a team of car-like vehicles subject to simultaneous actuator faults and faded neighborhood communication information. The fading channel's effect and the vehicle dynamics' nonlinearity are carefully analyzed, providing guidelines for the fault-tolerant control design.

2. Compared to the existing studies in (Ren & Chen, 2015) and (Li *et al.*, 2022), the settling time function in our study relies only on design parameters rather than the initial states, which restricts the practical application since the vehicles' information variables, may not be accurately measured as they are often distorted by noises and disturbances.

3. The proposed methodology is implemented in real vehicles using the latest Quanser self-driving car (QCar) platform to validate the controller's performance in the presence of faults under investigation.

This paper is organized as follows. Graph theory is introduced in Section 4.2. Section 4.3 presents a system description and objectives of the control design. Consensus tracking control design in the presence of fading channels is developed in Section 4.4. Section 4.5 proposes a fault-tolerant consensus tracking control under the influence of fading channels and actuator faults, and rigorous proof of the stability analysis is provided. Section 4.6 discusses the experimental results and analysis of the vehicles' behavior in the fault conditions. Finally, the conclusion and future work are introduced in Section 4.7.

4.2 Preliminaries

Graph theory (West, 2001)

Let $G = (V, E, A)$ be a weighted directed graph that represents a team communication topology with $V = \{v_1, v_2, ..., v_n\}$ and $E = \{e_{ij} = (v_i, v_j)\}$ are set of vertices and edges respectively. $A = [a_{ij}]_{n\times n}$ is a non negative weighted adjacency matrix. The adjacency element $a_{ij} > 0$ is associated with the fact that there exists an edge between node v_i and node v_j; otherwise, $a_{ij} = 0$. A graph G is said to be strongly connected if, for any pair of distinct nodes, there exists a path between v_i and v_j such that $(v_i, v_j) \in E \implies (v_j, v_i) \in E$.

The Laplacian matrix L_m of a weighted graph is defined by:

$$L_m = D - A = [l_{ij}] \in \mathbb{R}^{n\times n}, \tag{4.1}$$

where the degree matrix $D = \text{diag}(d_1, d_2, ...d_n)$, $d_i = \sum_{j=1}^{N} a_{ij}$, $l_{ij} = -a_{ij}$, $\forall j \neq i$ and $\sum_{j=1}^{N} l_{ij} = l_{ii}, \forall i = 1, 2, ..., N$.

In this study, we consider a team of car-like vehicles that consists of one leader denoted by l and N followers denoted by $i = 1, 2, ..., N$. The digraph graph G is used to represent the communication between the leader and followers. To describe communication between the leader and all followers, we introduce the matrix $B = \text{diag}(b_1, b_2, ..., b_N)$ such that $b_i = 1$ when there is a direct connection between i^{th} follower and the leader; otherwise, it is zero.

4.3 Problem Statement

4.3.1 System description

This paper considers a team of car-like vehicles consisting of one virtual leader and multiple followers. The dynamic model of i^{th} follower is given by (Ren & Chen, 2015):

$$\begin{cases} \dot{q}_i &= J_i \bar{\omega}_i \\ \dot{\bar{\omega}}_i &= \bar{M}^{-1} \bar{B}(q_i)\tau_i - h_i(q_i, \dot{q}_i). \end{cases} \tag{4.2}$$

Also, the dynamic of leader l is described by

$$\begin{cases} \dot{q}_l &= J_i \bar{\omega}_l \\ \dot{\bar{\omega}}_l &= \bar{M}^{-1} \bar{B}(q_l)\tau_l - h_l(q_l, \dot{q}_l), \end{cases} \tag{4.3}$$

where

$$h_i(q_i, \dot{q}_i) = \bar{M}^{-1}\bar{V}(q_i, \dot{q}_i)\bar{\omega}_i, \quad h_l(q_l, \dot{q}_l) = \bar{M}^{-1}\bar{V}(q_l, \dot{q}_l)\bar{\omega}_l,$$

$$\bar{\omega}_i = \begin{bmatrix} v_i & w_i \end{bmatrix}^T, \quad \bar{M} = J_i^T M J_i, \quad \bar{V} = J_i^T (M\dot{J}_i + VJ_i),$$

$$\bar{B} = J_i^T B, \quad J_i = \begin{bmatrix} \cos\phi_i & 0 \\ \sin\phi_i & 0 \\ \frac{tan(\psi_i)}{l} & 0 \\ 0 & 1 \end{bmatrix},$$

$$M = \begin{bmatrix} m & 0 & I_c \sin(\phi_i) & 0 \\ 0 & m & -I_c \cos(\phi_i) & 0 \\ I_c \sin(\phi_i) & -I_c \cos(\phi_i) & I_b & I_w \\ 0 & 0 & I_w & I_w \end{bmatrix},$$

$$V = \begin{bmatrix} 0 & 0 & -I_c\dot{\phi}\cos(\phi_i) & 0 \\ 0 & 0 & -I_c\dot{\phi}\sin(\phi_i) & 0 \\ 0 & 0 & 0 & 0 \\ 0 & 0 & 0 & 0 \end{bmatrix}, B = \begin{bmatrix} \cos(\phi_i) & 0 \\ \sin(\phi_i) & 0 \\ L\sin(\psi_i)\cos(\psi_i) & 0 \\ 0 & 1 \end{bmatrix},$$

where $q_i = (x_i, y_i, \phi_i, \psi_i)^T$ and $q_l = (x_l, y_l, \phi_l, \psi_l)^T$ are the state vectors of the i^{th} follower and leader respectively. (x_i, y_i) is the position of i^{th} follower as shown in Figure 2.1. The linear and steering velocities are v_i and ω_i, respectively. ϕ_i and ψ_i are heading and steering angles of i^{th} follower. τ_i is the torque acting on the actuators of the i^{th} follower. $m = m_c + 4m_w$, $I_c = (L - b)m_c + 2Lm_w$, $I_b = m_c(L - b)^2 + 4W^2 m_w + I_{bzz} + 4I_{wzz}$, m_c and m_w are the vehicle and wheel masses, respectively. The moment of inertia of each wheel with a motor about the wheel axis is denoted by I_w. I_{bzz} is the moment of inertia of a vehicle body about the z-axis passing through the car's center of mass. The wheel's moment of inertia about the z-axis passing through the wheel centroid is represented by I_{wzz}. As indicated in Figure 2.1, CoR is the center of the rotation along the axis of the rear wheels. L is the distance between the front and rear axles. b is the distance from the center of mass to the rear axle.

Remark 4. *The friction between the wheel and the surface is modeled in the sense of pure rolling and no slipping, representing a perfect joint between the wheel and the ground. Hence, the wheel's contact point with the ground leads to a simplified resistive friction effect of the ground on the wheels with respect to the steering axis.*

Assumption 2. *(Ren & Chen, 2015) For any q_i, $\bar{\omega}_i$, $i \in [0,1,...]$, there exist positive constants μ_1 and μ_2 such that:*

$$\|H(q, \bar{\omega}, t) - 1 \otimes h(q_l, \bar{\omega}_l, t)\| \leq \mu_1\|q - 1 \otimes q_l\| + \mu_2\|\bar{\omega} - 1 \otimes \bar{\omega}_l\|, \tag{4.4}$$

where $H(q, \bar{\omega}, t) = [h_1(q, \bar{\omega}), ..., h_N(q, \bar{\omega})]^T$ *and $\otimes$ is the Kronecker product.*

Remark 5. *Assumption 2 is important in synthesizing the controller to guarantee the uniqueness of the solution. This assumption is satisfied when the function $h(q, \bar{\omega}, t)$ is continuous and bounded. The function h is Lipschitz and is used due to the fact that there is always some* *limit on how fast a function can change. Hence, when we attempt to determine the function's boundedness, we consider the Lipschitz condition. In practice, the controller can ensure the convergence of the vehicles to the reference trajectories when the condition in Assumption 2 is satisfied.*

Lemma 1. *(Khoo, Xie & Man, 2009) Considering the Laplacian matrix L_m from (4.1) and the matrix B such that $L_m + B$ is invertible if the digraph G has a directed spanning tree.*

Lemma 2. *(Zuo & Tie, 2016) Consider a scalar system*

$$\dot{f} = -\alpha f^{\frac{n}{m}} - \beta f^{\frac{r}{z}}, \tag{4.5}$$

where $\alpha > 0$ and $\beta > 0$, m, n, r, z are all positive odd integers satisfying $m > n$ and $r < z$. Then, Eq. (4.5) is globally stable, and the settling time is bounded by

$$T \leq \frac{m}{\alpha(n-m)} + \frac{z}{\beta(z-r)}. \tag{4.6}$$

4.3.2 Objectives of the control design

The proposed fault-tolerant cooperative control aims to drive all the followers to move along their desired trajectories and achieve a common team behavior. To satisfy this goal, let's first define the consensus tracking errors e_{1i} and e_{2i} for i^{th} follower in the fault-free condition as follows:

$$\begin{cases} e_{1i} &= \sum_{j=1}^{N} a_{ij}(p_i - p_j - \Delta_{ij}) + b_i(p_i - p_L - \Delta_{iL}) \\ e_{2i} &= \sum_{j=1}^{N} a_{ij}(\bar{\omega}_i - \bar{\omega}_j) + b_i(\bar{\omega}_i - \bar{\omega}_l), \end{cases} \tag{4.7}$$

where $p_i = (x_i, y_i, \psi_i)^T$. $\Delta_{ij} \in \mathbb{R}^m$ is the distance between the i^{th} follower and its neighbor j and Δ_{iL} is the distance between the i^{th} follower and the leader. The team members achieve the consensus and track the leader states when the error variables in (4.7) reach zero. For convenience, (4.7) can be transformed into the compact form as follows:

$$\begin{cases} \varepsilon_1 & = (L_m + B) \otimes I_m . \tilde{p} \\ \varepsilon_2 & = (L_m + B) \otimes I_m . \tilde{\bar{\omega}}, \end{cases} \tag{4.8}$$

where $\varepsilon_1 = [\varepsilon_{11}, ..., \varepsilon_{1N}]^T$, $\varepsilon_2 = [\varepsilon_{21}, ..., \varepsilon_{2N}]^T$, $\tilde{p} = p - 1 \otimes (\mathrm{p}_l - \Delta_{iL})$ with $p = [p_i, p_2, ..., p_N]$ that represents the position of followers in the configuration. The tracking error variables of the linear and steering velocities of all followers with respect to the leader's velocities are defined by $\tilde{\bar{\omega}} = \bar{\omega} - 1 \otimes \bar{\omega}_l$, $I_m \in R^{\, m \times m}$.

The time derivative of (4.8) is given by

$$\begin{cases} \dot{\varepsilon}_1 & = (J_{3\times 2})\varepsilon_2 \\ \dot{\varepsilon}_2 & = (L_m + B) \otimes I_m . \Big(H - 1 \otimes h(q_l, \dot{q}_l) + \bar{M}^{-1}\tau - 1 \otimes \bar{M}^{-1}\tau_l \Big), \end{cases} \tag{4.9}$$

where $J_{3\times 2} = [J_1, J_2 ..., J_N]^T, \tau = [\tau_1, \tau_2, ..., \tau_N]^T, \bar{M}^{-1} = \mathrm{diag}[\bar{M}_1^{-1}, ..., \bar{M}_N^{-1}]^T$. It can be demonstrated that the cooperative control problem of the system (4.2) and (4.3) is equivalent to the consensus tracking errors in (4.9) since $L_m + B$ is invertible.

Remark 6. *The graph G represents the communication topology for the entire system in which the interactions among the followers are described by the laplacian matrix L_m in (4.1), and the links from the leader to the followers are denoted by the matrix B as defined in Section 4.2. Therefore, the matrix $L_m + B$ as introduced in (4.8) and (4.9) describes the overall communication network of the system. It is crucial in solving the group consensus problem.*

4.4 Consensus Tracking Control Design in the Presence of Fading Channels

In this study, we assume that the fading signal occurs during the transmission of information among followers, and there is no fading in the transmitted information from the leader to the followers as shown in Figure 4.1. The transmitted information among the followers is the state variables p_i, ψ_i, v_i, and ω_i. This information is essential in the controller design for each follower, enabling each one to move on its desired trajectory and cooperate with the local neighbors to achieve a common team goal. In real systems, many factors will interfere with information transmission between agents, resulting in the agents receiving only faded information rather than accurate information transmitted by neighboring agents. This phenomenon can be expressed using the random weakening amplitude of real state information, which is achieved by multiplying the real information by a random variable δ_{ji} with a value between 0 and 1. It is reported that fading involves damage to the transmitted information and deteriorates the overall system's performance (Qu, Shen & Yu, 2021). Therefore, it is important to investigate this phenomenon's impact on the system's stability and provide a solution to handle this problem. First, we introduce a model that includes the presence of fading channels in the system. Then, we design a fault-tolerant controller to overcome the impact of this phenomenon on the team mission.

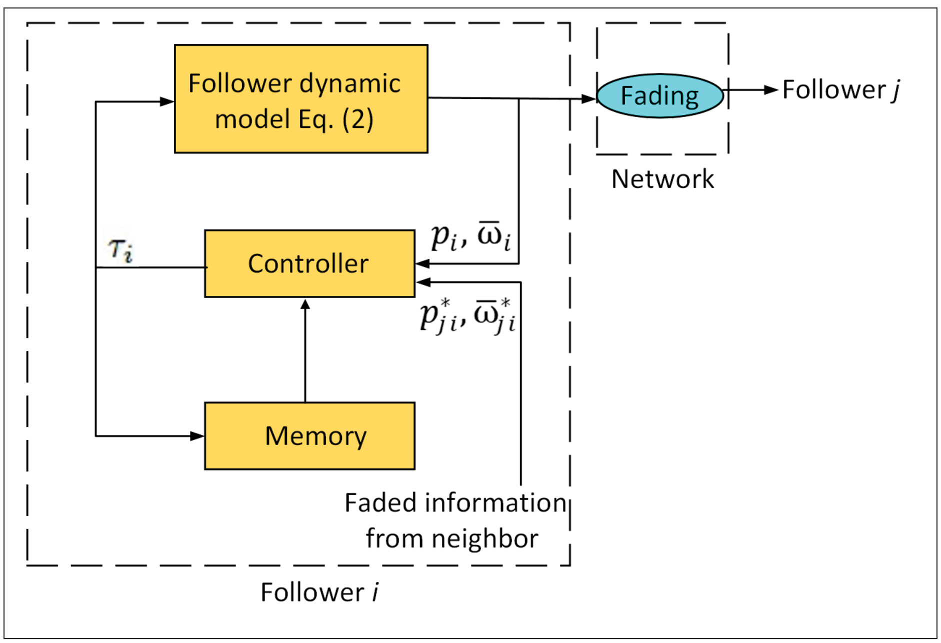

Figure 4.1 Block diagram of communication network with faded neighborhood information

Remark 7. *It is important to note that many factors can lead to fading channels in practice, including time, geographic location, radio frequency, etc. Hence, fading is usually modeled as a random change in the amplitude and phase of the transmitted signal over time.*

In the presence of a fading channel, Eq. (4.7) can be rewritten as:

$$\begin{cases} e^{\star}{}_{1i} &= \sum_{j=1}^{N} a_{ij}(p_i - p_j^{\star} - \Delta_{ij}) + b_i(p_i - p_L - \Delta_{iL}) \\ e^{\star}{}_{2i} &= \sum_{j=1}^{N} a_{ij}(\bar{\omega}_i - \bar{\omega}_j^{\star}) + b_i(\bar{\omega}_i - \bar{\omega}_l), \end{cases} \tag{4.10}$$

where $p_j^{\star}$ and $\bar{\omega}_j^{\star}$ are the signals that i^{th} follower receives from its neighbor j.

$$\begin{cases} p_j^{\star} &= \frac{1}{\delta^{\star}}\delta_{ji}p_j \\ \bar{\omega}_j^{\star} &= \frac{1}{\delta^{\star}}\delta_{ji}\bar{\omega}_j, \end{cases} \tag{4.11}$$

where $\delta^{\star}$ is the mean value, δ_{ji} is not estimated; for this purpose, the expectation of the random coefficient of the fading channel is involved in Eq. (4.11) to compute the error tracking variables between follower i and its neighbor j accurately. When the coefficient of the fading channel follows a normal distribution with a mean value $\delta^{\star}$, this coefficient is more likely to take the value near the mean. Therefore, the mathematical expectation expression is believed to somewhat enhance the calculation accuracy.

For the design of the controller, we assume that all the followers are subject to fading channels. Therefore, we define α_i, whose all elements are set to zero except the i^{th} is 1. Then, the consensus tracking error (4.10) can be transformed to a convenient form as follows:

$$\begin{cases} \varepsilon^{\star}{}_1 &= (L_m + B) \otimes I_m . \sum_{i=1}^{N} \Big(\frac{1}{\delta^{\star}}\Pi_i(p - \alpha_i \otimes (p_i - \Delta_{ij}) + (\alpha_i \otimes p_i) \\ & \quad -1_N \otimes (p_l - \Delta_{iL}) \Big) \\ \varepsilon^{\star}{}_2 &= (L_m + B) \otimes I_m . \sum_{i=1}^{N} \Big(\frac{1}{\delta^{\star}}\Pi_i(\bar{\omega} - \alpha_i \otimes \bar{\omega}_i) + \alpha_i \otimes \bar{\omega}_i - 1_N \otimes \bar{\omega}_l \Big), \end{cases} \tag{4.12}$$

where $\Pi_1 = \text{diag}[0, \delta_{12}, ..., \delta_{1N}]$, $\Pi_2 = \text{diag}[\delta_{21}, 0, ..., \delta_{2N}]$, this term $\Pi_i(q - \alpha_i \otimes q_i)$ refers to the transmitted state information from team members to i^{th} follower.

The time derivative of (4.12) can be given as:

$$\begin{cases} \dot{\varepsilon^{\star}}_1 & = \bar{\varepsilon}_2^{\star} \\ \dot{\varepsilon^{\star}}_2 & = (L_m + B) \otimes I_m.\Big(\bar{H} - 1 \otimes h(q_l, \dot{q}_l) + \bar{M}^{-1}\tau - 1 \otimes \bar{M}^{-1}\tau_l\Big), \end{cases} \tag{4.13}$$

where

$$\bar{\varepsilon}_2^{\star} = (J_{3\times 2})\varepsilon_2^{\star}, \quad \bar{H} = \sum_{j=1}^{N} \frac{1}{\delta^{\star}}\Pi_i(\dot{\bar{\omega}} - \alpha_i \otimes \dot{\bar{\omega}}_i) + \alpha_i \otimes \dot{\bar{\omega}}_i.$$

The objective for (4.13) is to drive the states of the entire system to the desired ones such that:

$$lim_{t\to\infty}\varepsilon^{\star}{}_1 = 0, \qquad \text{and} \qquad lim_{t\to\infty}\varepsilon^{\star}{}_2 = 0. \tag{4.14}$$

4.4.1 Stability analysis

Theorem 2. *Consider the system in (4.2) and (4.3) under the influence of fading channel with the control input designed as follows:*

$$\begin{aligned} \tau \;\; = \;\; & \bar{M}(L_m + B)^{-1}.\Big[b \otimes M^{-1}\tau_l - c\bar{\varepsilon}_2^{\star} - k_1 s - k_2 sign(s) - \zeta sign(s)(\mu_1\|\varepsilon^{\star}{}_1\| \\ & +\mu_2\|\varepsilon^{\star}{}_2\|)\Big], \end{aligned} \tag{4.15}$$

then the tracking error variables in (4.13) will reach the sliding surface $s = 0$ in finite time.

Proof. Consider the sliding surface for i^{th} follower as follows:

$$s = \varepsilon^{\star}{}_2 + c\varepsilon^{\star}{}_1, \tag{4.16}$$

where $s = [s_i^T, s_2^T, ..., s_N^T]$, and c is a positive constant.

Then, the candidate Lyapunov function is chosen as:

$$V_1 = \frac{1}{2} s^T s. \tag{4.17}$$

Taking the time derivative of (4.17), we get that

$$\dot{V}_1 = s^T (\dot{\varepsilon^{\star}}_2 + c\dot{\varepsilon^{\star}}_1). \tag{4.18}$$

By substituting (4.13) into (4.18), we get that

$$\dot{V}_1 \;\; = \;\; s^T \Big[(L_m + B) \otimes I_m . \Big(\bar{H} - 1 \otimes h(q_l, \dot{q}_l) + \bar{M}^{-1} \tau - 1 \otimes \bar{M}^{-1} \tau_l \Big) + c \bar{\varepsilon}_2^{\star} \Big]. \tag{4.19}$$

According to Assumption 2 and the properties of the norm, we have

$$\begin{aligned}
\|\bar{H} - 1 \otimes h_l\| &= \|(\bar{h}_1(q_1, \bar{\omega}_1, t) - h_l(q_l, \bar{\omega}_l, t))^T, ..., (\bar{h}_n(q_n, \bar{\omega}_n, t) - h_l(q_l, \bar{\omega}_l, t))^T\| \\
&\leq \|(\|\bar{h}_1(q_1, \bar{\omega}_1, t) - h_l(q_l, \bar{\omega}_l, t)\|, ..., \|(\bar{h}_n(q_n, \bar{\omega}_n, t) - h_l(q_l, \bar{\omega}_l, t)\|)\| \\
&\leq \|(\mu_1\|q_1 - q_l\| + \mu_2\|\bar{\omega}_1 - \bar{\omega}_2\|, ..., \mu_1\|q_n - q_l\| + \mu_2\|\bar{\omega}_n - \bar{\omega}_l\|)\| \\
&\leq \|(\mu_1\|q_1 - q_l\|, ..., +\|q_n - q_l\|)\| + \mu_2\|(\|\bar{\omega}_1 - \bar{\omega}_2\|, ..., \|\bar{\omega}_n - \bar{\omega}_2\|)\| \\
&\leq \mu_1\|\varepsilon_1^{\star}\| + \mu_2\|\varepsilon_2^{\star}\|.
\end{aligned} \tag{4.20}$$

Using the Kronecker product property, we obtain the following:

$$\begin{aligned}
\|(L + B) \otimes I_m\| &= \Big[\lambda_m \Big([(L_m + B) \otimes I_m]^T \times [(L_m + B) \otimes I_m] \Big) \Big]^{\frac{1}{2}} \\
&= [\lambda_m (L_m + B)^T (L_m + B)]^{\frac{1}{2}} \\
&= \|(L_m + B)\|.
\end{aligned} \tag{4.21}$$

From Lemma 1, Eq. (4.20) and Eq. (4.21), we have

$$\begin{aligned}
\|(L_m + B) \otimes I_m(\bar{H} - 1 \otimes h_l)\| &\leq \|L_m + B\|(\mu_1\|\varepsilon_1^\star\| + \mu_2\|\varepsilon_2^\star\|) \\
&\leq \|L_m + B\|\|L_m + B\|^{-1}(\mu_1\|\varepsilon_1^\star\| + \mu_2\|\varepsilon_2^\star\|) \\
&\leq \zeta\mu_1\|\varepsilon_1^\star\| + \zeta\mu_2\|\varepsilon_2^\star\|. \qquad (4.22)
\end{aligned}$$

Replacing Eq. (4.22) into Eq. (4.19), we obtain the following:

$$\dot{V}_1 = s^T\left[(L_m + B) \otimes I_m.\bar{M}^{-1}\tau - b \otimes \bar{M}^{-1}\tau_l + c\bar{\varepsilon}_2^\star\right] + \zeta\|s\|(\mu_1\|\varepsilon_1^\star\| + \mu_2\|\varepsilon_2^\star\|). \qquad (4.23)$$

Substituting the control law τ in (4.15) into (4.23), we get

$$\begin{aligned}
\dot{V}_1 &= s^T[-k_1 s - k_2 sign(s)] \\
&= -k_1 s^T s - k_2|s| \\
&\leq -2k_1 V(s). \qquad (4.24)
\end{aligned}$$

From (4.24), it follows from the Lemma 2 that the tracking error variables in (4.17) converge to the sliding surface $s = 0$ in finite time. When the sliding surface $s = 0$, from (4.16) we have:

$$\varepsilon^\star{}_2 = -c\varepsilon^\star{}_1 \qquad (4.25)$$

Selecting the Lyapunov function as:

$$V_2 = \frac{1}{2}\varepsilon^{\star T}_2\varepsilon^\star{}_2. \qquad (4.26)$$

Taking the time derivative of (4.26), one can obtain

$$\begin{aligned}
\dot{V}_2 &= \varepsilon^{\star T}_2\dot{\varepsilon}^\star{}_2 \\
&= -c\varepsilon^{\star T}_2\dot{\varepsilon}_1^\star \\
&\leq -c\varepsilon_2^\star\bar{\varepsilon}_2^\star. \qquad (4.27)
\end{aligned}$$

It is obvious from (4.27) that $\dot{V}_2$ is negative semi-definite and according to Barbalat's lemma (Nguyen & Nguyen, 2018), it is clear to conclude that $\varepsilon^{\star}{}_1 \to 0$, $\varepsilon^{\star}{}_2 \to 0$, and $\bar{\varepsilon}^{\star}_2 \to 0$ as $t \to 0$. As a result, the overall system (4.2) and (4.3) become asymptotically stable. □

4.5 Fault-Tolerant Consensus Tracking Control Design Under the Influence of Fading Channels and Actuator Faults

This section proposes a novel leader-follower consensus algorithm for a team of car-like vehicles with actuator faults and faded neighborhood information. The consensus algorithm is developed based on the integral terminal sliding mode control and Lyapunov theory under the following assumption:

Assumption 3. *(Chen, Song & Lewis, 2016; Xiao, Yin & Gao, 2017) The multiplicative and additive actuator faults $\boldsymbol{\gamma}_i(t), \vartheta_i(t)$ are bounded, and their derivatives exist and are also bounded. Furthermore, we have $\|\vartheta_i\| \leq \bar{\vartheta}_i$ where $\bar{\vartheta}_i$ is a known bound.*

In the light of Assumption 3, the actuator fault acting on i^{th} follower can be described as:

$$\tau_i = (1 - \gamma_i(t))\tau_N + \vartheta_i(t), \tag{4.28}$$

where τ_N denotes the nominal control signal, $\gamma_i(t) \in \mathbb{R}^{2\times 2}$ and $\vartheta_i(t) \in \mathbb{R}^2$ are the multiplicative and additive actuator faults, respectively, with $\gamma_i(t) = \text{diag}[\gamma_{i1}(t), \gamma_{i2}(t)]$, with $0 < \gamma_i(t) \leq \gamma_{max} < 1$. In the fault-free condition, all the elements of $\gamma_i(t)$ and $\vartheta_i(t)$ are assumed to equal zero.

Considering the case of faded neighborhood information and actuator faults, the described system in (4.2) can be re-defined as follows:

$$\begin{cases} \dot{q}_i &= J_i\bar{\omega}_i \\ \dot{\bar{\omega}}_i &= \bar{M}^{-1}\bar{B}(q_i)(1 - \gamma_i(t))\tau_N + \vartheta_i(t) - \bar{M}^{-1}\bar{V}(q_i, \dot{q}_i)\bar{\omega}_i. \end{cases} \tag{4.29}$$

The tracking error in (4.13) becomes:

$$\begin{cases} \dot{\varepsilon^{\star}}_1 & = \bar{\varepsilon}^{\star}_2 \\ \dot{\varepsilon^{\star}}_2 & = (L_m + B) \otimes I_m . \Big(\bar{H} - 1 \otimes h(q_l, \bar{\omega}_l, t) + \bar{M}^{-1}(1 - \gamma(t))\tau_N \\ & +\vartheta(t) - 1 \otimes \bar{M}^{-1}\tau_l \Big), \end{cases} \tag{4.30}$$

where the fault parameters $\gamma(t) = \text{diag}[\gamma_1, \gamma_2, ..., \gamma_N]$ and $\vartheta(t) = [\vartheta_1, \vartheta_2, ..., \vartheta_N]^T$.

Theorem 3. *Consider the system with the followers and leader given in (4.2) and (4.3) with the Assumption 3. The control input is designed as follows:*

$$\begin{aligned} \tau_N \;=\; & -\frac{1}{(I - \gamma_{max})}\bar{M}(L + B)^{-1}\Big[\zeta(\mu_1\|\varepsilon^{\star}{}_1\| + \mu_2\|\varepsilon^{\star}{}_2\|) + \|L_m + B\|\sqrt{N}\bar{\vartheta}(t) + k_1(\varepsilon^{\star}{}_2)^{\frac{n_1}{m_1}} \\ & +k_2(\varepsilon^{\star}{}_1)^{\frac{n_2}{m_2}} + k_3 sign(s)^{\frac{n3}{m3}} + k_4 sign(s)^{\frac{p3}{q3}} - b \otimes \bar{M}^{-1}\tau_l\Big]. \end{aligned} \tag{4.31}$$

By Lemma 2, the control law (4.31) can guarantee the convergence of the consensus tracking error variables in (4.30) to the sliding surface $s = 0$ with the settling time T bounded by:

$$T < \Big(\frac{1}{k_3}\frac{m_3}{m_3 - n_3} + \frac{1}{k_4}\frac{z}{z - r}\Big), \tag{4.32}$$

where k_1, k_2, k_3, k_4, n_1, n_2, n_3, m_1, m_2, m_3, r and z are all positive gains.

Proof. Consider the sliding surface as follows:

$$s = \varepsilon^{\star}{}_2 + k_1 \int_0^t (\varepsilon^{\star}{}_2)^{\frac{n_1}{m_1}} + k_2 \int_0^t (\varepsilon^{\star}{}_1)^{\frac{n_2}{m_2}}, \tag{4.33}$$

where n_1, n_2, m_1, m_2 are positive odd integers satisfy that $n_1 > m_1, n_2 > m_2$.

It is observed that the integral terminal sliding mode control can increase the system's convergence rate. With the aid of the Lyapunov theorem, the sliding surface in (4.33) is selected such that the system (4.2) and (4.3) with the control law in (4.31) can reach the sliding surface and achieve the convergence to the desired trajectory in finite time. To satisfy this control goal, let's define the Lyapunov candidate function as follows:

$$V_3 = \frac{1}{2}s^T s. \tag{4.34}$$

The time derivative of (4.34) is given by

$$\dot{V}_3 = s^T\Big[\dot{\varepsilon^{\star}}_2 + k_1(\varepsilon^{\star}{}_2)^{\frac{n_1}{m_1}} + k_2(\varepsilon^{\star}{}_1)^{\frac{n_2}{m_2}}\Big]. \tag{4.35}$$

Replacing (4.30) into (4.35), one can obtain

$$\begin{aligned}\dot{V}_3 \;&=\; s^T\Big[(L_m + B)\otimes I_m.\Big(\bar{H} - 1\otimes h(q_l, \bar{\omega}_l, t) + \bar{M}^{-1}(1-\gamma(t))\tau_N + \vartheta(t) - 1\otimes \bar{M}^{-1}\tau_l\Big)\\ &\quad + k_1(\varepsilon^{\star}{}_2)^{\frac{n_1}{m_1}} + k_2(\varepsilon^{\star}{}_1)^{\frac{n_2}{m_2}}\Big].\end{aligned} \tag{4.36}$$

By using the relation in (4.22), (4.36) can be rewritten as follows:

$$\begin{aligned}\dot{V}_3 \;&=\; s^T\Big[(L + B)\otimes I_m.\Big(\bar{M}^{-1}(1-\gamma(t))\tau_N + \vartheta(t)\Big) - b\otimes \bar{M}^{-1}\tau_l + k_1(\varepsilon^{\star}{}_2)^{\frac{n_1}{m_1}} + k_2(\varepsilon^{\star}{}_1)^{\frac{n_2}{m_2}}\Big]\\ &\quad + \zeta\|s\|(\mu_1\|\varepsilon_1^{\star}\| + \mu_2\|\varepsilon_2^{\star}\|).\end{aligned} \tag{4.37}$$

Substituting the control law τ_N in (4.31) into (4.37) one has

$$\begin{aligned}\dot{V}_3 \;&=\; s^T\Big[(L_m + B)\otimes I_m.\Big((1-\gamma(t))\frac{-1}{(I-\gamma_{max})}(L_m+B)^{-1}\otimes I_m.\Upsilon\Big) - b\otimes \bar{M}^{-1}\tau_l\\ &\quad + k_1(\varepsilon^{\star}{}_2)^{\frac{n_1}{m_1}} + k_2(\varepsilon^{\star}{}_1)^{\frac{n_2}{m_2}}\Big] + \zeta\|s\|\Big(\mu_1\|\varepsilon_1^{\star}\| + \mu_2\|\varepsilon_2^{\star}\|\Big) + \|L_m + B\|.\|s\|\\ &\quad .\sqrt{N}\bar{\vartheta}(t),\end{aligned} \tag{4.38}$$

where

$$\begin{aligned}\Upsilon \;&=\; \zeta(\mu_1\|\varepsilon^{\star}{}_1\| + \mu_2\|\varepsilon^{\star}{}_2\|) + \|L_m + B\|\sqrt{N}\bar{\vartheta}(t) + k_1(\varepsilon^{\star}{}_2)^{\frac{n_1}{m_1}} + k_2(\varepsilon^{\star}{}_1)^{\frac{n_2}{m_2}} + k_3 sign(s)^{\frac{n3}{m3}}\\ &\quad + k_4 sign(s)^{\frac{p3}{q3}} - b\otimes \bar{M}^{-1}\tau_l.\end{aligned} \tag{4.39}$$

Eq. (4.38) can be rearranged as follows:

$$\begin{aligned}
\dot{V}_3 &= -\frac{1}{I-\gamma_{max}} s^T(L_m+B)\otimes I_m.(1-\gamma(t))\times(L_m+B)^{-1}\otimes I_m.\Upsilon - \|s\|\Big[b\otimes\bar{M}^{-1}\tau_l \\
&\quad -k_1(\varepsilon^\star{}_2)^{\frac{n_1}{m_1}} - k_2(\varepsilon^\star{}_1)^{\frac{n_2}{m_2}}\Big] + \zeta\|s\|\Big[(\mu_1\|\varepsilon_1^\star\| + \mu_2\|\varepsilon_2^\star\|\Big] + \|L_m+B\|.\|s\|\sqrt{N}\bar{\vartheta}(t) \\
&\leq -\frac{1}{I-\gamma_{max}}\Upsilon\|s\|\lambda_{min}\Big[(L_m+B)\otimes I_m.(1-\gamma(t))(L_m+B)^{-1}\otimes I_m\Big] - \|s\|\Big[b\otimes\bar{M}^{-1}\tau_l \\
&\quad -k_1(\varepsilon^\star{}_2)^{\frac{n_1}{m_1}} - k_2(\varepsilon^\star{}_1)^{\frac{n_2}{m_2}}\Big] + \zeta\|s\|\Big[(\mu_1\|\varepsilon_1^\star\| + \mu_2\|\varepsilon_2^\star\|\Big] + \|L_m+B\|.\|s\|\sqrt{N}\bar{\vartheta}(t) \\
&\leq -\frac{1}{I-\gamma_{max}}\Upsilon\|s\|\Big[1-\lambda_{max}(L_m+B)\otimes I_m.\gamma(t)(L_m+B)^{-1}\otimes I_m\Big] - \|s\|\Big[b\otimes\bar{M}^{-1}\tau_l \\
&\quad -k_1(\varepsilon^\star{}_2)^{\frac{n_1}{m_1}} - k_2(\varepsilon^\star{}_1)^{\frac{n_2}{m_2}}\Big] + \zeta\|s\|\Big[(\mu_1\|\varepsilon_1^\star\| + \mu_2\|\varepsilon_2^\star\|\Big] + \|L_m+B\|.\|s\|\sqrt{N}\bar{\vartheta}(t) \\
&\leq -\frac{1}{I-\gamma_{max}}\Upsilon[1-\gamma_{max}]\|s\| - \|s\|\Big[b\otimes\bar{M}^{-1}\tau_l - k_1(\varepsilon^\star{}_2)^{\frac{n_1}{m_1}} - k_2(\varepsilon^\star{}_1)^{\frac{n_2}{m_2}}\Big] \\
&\quad +\zeta\|s\|\Big[(\mu_1\|\varepsilon_1^\star\| + \mu_2\|\varepsilon_2^\star\|\Big] + \|L_m+B\|.\|s\|\sqrt{N}\bar{\vartheta}(t) \\
&\leq -[k_3 sig(s)^{\frac{n3}{m3}} + k_4 sig(s)^{\frac{p3}{q3}}]\|s\|. \qquad (4.40)
\end{aligned}$$

From (4.40), it is clear that $\dot{V}_3 \leq 0$. It follows from Lemma 2 that the error variables in (4.30) reach the siding surface $s = 0$ and maintain sliding on it.

Theorem 4. *Consider the sliding surface (4.33). Choose positive odd integers n_1, m_1, n_2, m_2 such that $n_1 > m_1, n_2 > m_2$ then $\varepsilon_1^\star$ and $\varepsilon_2^\star$ reach the sliding manifold in finite time.*

Proof. Let's consider the Lyapunov candidate function as follows:

$$V_4 = k_2(1+\frac{n_2}{m_2})^{-1}\|\varepsilon_1^\star\|^{1+\frac{n_2}{m_2}} + \frac{1}{2}\varepsilon_2^{\star 2}. \qquad (4.41)$$

Taking the time derivative of (4.41), we get

$$\dot{V}_4 = k_2(\varepsilon_1^\star)^{\frac{n_2}{m_2}}\varepsilon_2^\star + \varepsilon_2^\star\dot{\varepsilon}_2^\star. \qquad (4.42)$$

When $s = 0$, from (4.33) we have

$$\dot{\varepsilon^\star}_2 = -k_1(\varepsilon^\star{}_2)^{\frac{n_1}{m_1}} - k_2(\varepsilon^\star{}_1)^{\frac{n_2}{m_2}}. \qquad (4.43)$$

Substitute (4.43) into (4.42), we get that

$$\dot{V}_4 = -k_1(\varepsilon^{\star}{}_2)^{\frac{n_1+m_1}{m_1}}. \tag{4.44}$$

From (4.44), we can guarantee that the cooperative control law (4.31) can drive the states of the overall system to the desired ones in finite time. This completes the proof. □

4.6 Experimental Results and Analysis

In this section, we demonstrate the effectiveness of our proposed control scheme on the latest Quanser self-driving car (QCar) platform. The experiments have been conducted in the Networked Autonomous Vehicles Laboratory (NAV Lab) at Concordia University. The experimental tests of the QCar carried out in this study can be viewed on the NAV lab YouTube Channel (NAV Lab YouTube Channel, 2022).

4.6.1 Experimental setup

As shown in Figure 3.2, the experimental testbed includes two QCars, each with a 9-axis inertial measurement unit (IMU), servo motors, and a Jetson TX2 processor. The vehicles receive the commands from the PC and map them into the pulse width modulation (PWM) to power the motors. Once the motors respond to the control signals, the onboard processor receives the IMU measurements and sends data through wireless communication Wi-Fi to the PC to generate the appropriate PWM signals for the desired motion along the pre-defined trajectory. In the experiments, the two vehicles are required to track the coordinates of the virtual leader and converge to their desired S-shaped path during the mission. The reference trajectory of the leader is defined as:

$$\begin{aligned} x_d(t) &= rsin(-2t), \\ y_d(t) &= rcos(t), \end{aligned} \tag{4.45}$$

where r is the radius of the trajectory. The initial position of vehicle 1 is $p_1 = [0.195, 0.24, 10^o]$ and vehicle 2 is $p_2 = [-0.15, 0, 10^o]$.

Remark 8. *The dynamic model parameters of mechanical systems can not be precisely obtained in real applications. However, there are several methods for identifying the dynamic parameters, which can be classified as online or offline techniques. Offline methods allow the evaluation of vehicle parameters prior to the analysis and do not impose any time restrictions on the computation process. On the other hand, the online methods involve real-time updates to the parameters during vehicle operations. In this study, we used the offline identification method to evaluate the parameters of the two vehicles.*

4.6.2 Analysis of experimental results

To verify the performance of the proposed methodology under fault conditions, the right and left actuators of Vehicle 1 are subjected to multiplicative faults $\gamma_i(t)$ of $0.4 + 0.1e^{-0.2t}$ $(N.m)$ and $0.35 + 0.1e^{-0.2t}$ $(N.m)$ respectively and additive faults $\vartheta_i(t)$ of $(0.1sin(t))eye(2)$ $(N.m)$ at time 8 s. As introduced in (Xu, Zheng, Xiao & Xie, 2018), the multiplicative faults are modeled as parameter changes, whereas the additive faults appear as time-varying signals acting on the actuators. In addition, it is assumed that the information received from Vehicle 2 by Vehicle 1 is transmitted over a fading channel that occurs simultaneously with the actuators' faults at time 8 s. In this work, the random variable δ_{ji} introduced in (4.11) is acting on the communication channel of Vehicle 2 as defined in Section 4.4. This study assumes that the fading channel coefficient follows a normal distribution with a mean value $\delta^\star$ selected in the experiment as 0.45. The random fading channel variable δ_{ji} in (4.11) obeys the Gaussian distribution. In this experiment, δ_{ji} is selected as 0.45, acting on the communication channel of Vehicle 2. Before the occurrence of faults, the vehicles operated in normal conditions. As can be observed from Figure 4.2, the proposed controller provided good tracking performance for the two vehicles during the mission. In particular, after time 8 s, Vehicle 1 deviated from the reference trajectory for a few seconds, then the controller accommodated the faults and enabled Vehicle 1 to move along the desired path. Figure 4.3 shows the velocity profiles of the two vehicles as they are

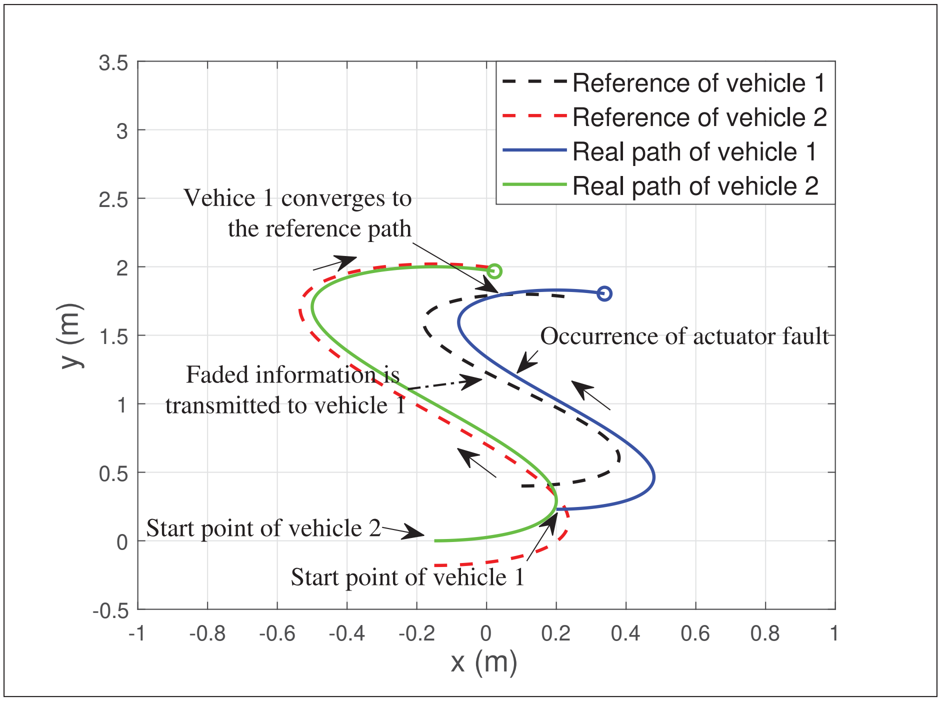

Figure 4.2 Reference and actual trajectories of car-like vehicles subject to actuators' faults in vehicle 1 and fading channel in vehicle 2 at $t = 8$ s

tracking the S-shaped trajectory. As can be seen, the vehicles are moving at approximately the same velocity, which is important for the cooperative motion mission. Also, it can be noticed that the two vehicles adjusted their speeds after the occurrence of faults and kept moving together to the end of the mission. In addition, the heading and steering angles of the two vehicles in Figure 4.4 and Figure 4.5 are in the same direction. Hence, the results demonstrate the effectiveness of the proposed controller in providing a good tracking performance and satisfying the control objectives under fault conditions.

4.7 Conclusion and Future Work

This article has proposed a fault-tolerant cooperative control scheme against simultaneous actuator faults and faded neighborhood information. The developed controller is based on the integral terminal sliding mode technique due to its responsiveness, robustness, and stability

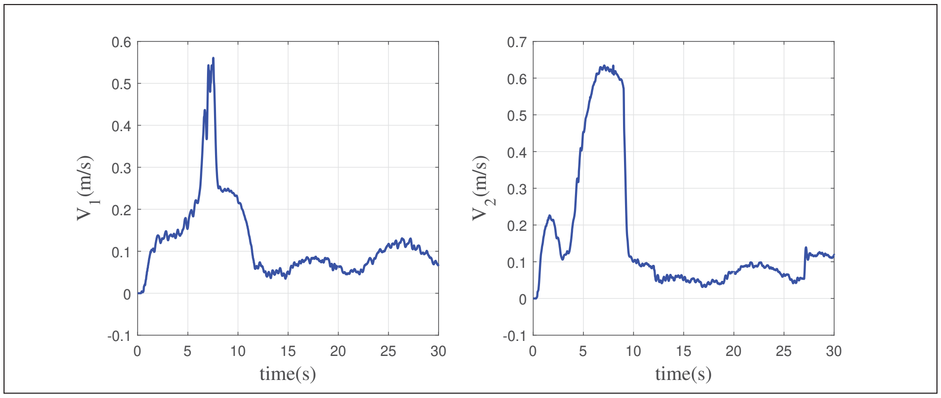

Figure 4.3 Velocity profiles of vehicle 1 (V_1) and vehicle 2 (V_2) with the actuators' faults and fading channel conditions at $t = 8$ s

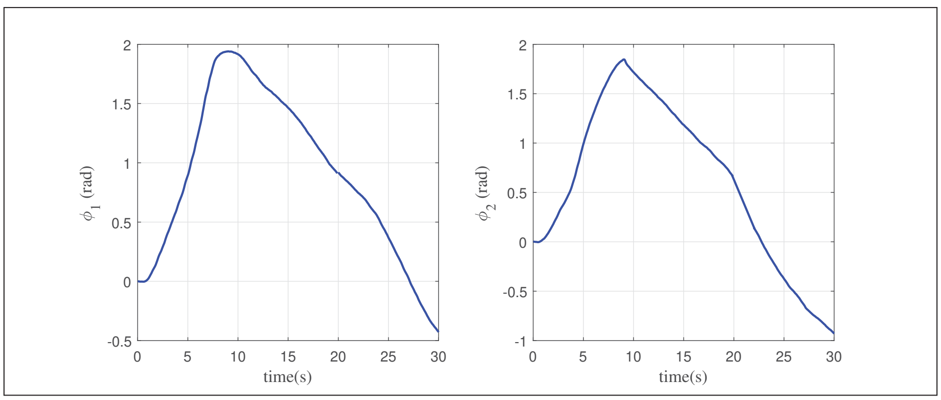

Figure 4.4 Heading angles of vehicle 1(ϕ_1) and vehicle 2 (ϕ_2) with the actuators' faults and fading channel conditions at $t = 8$ s

in unknown conditions. The multiplicative and additive actuator faults are considered with the problem of the fading communication channels. The rigorous proofs are provided with the means of the Lyapunov stability theorem. The performance of the proposed controller is validated on a real system that uses the latest Quanser self-driving car (QCar) platform. For future work, investigating the cooperative control problem with the actuator and communication faults in the presence of stochastic disturbances is of great interest.

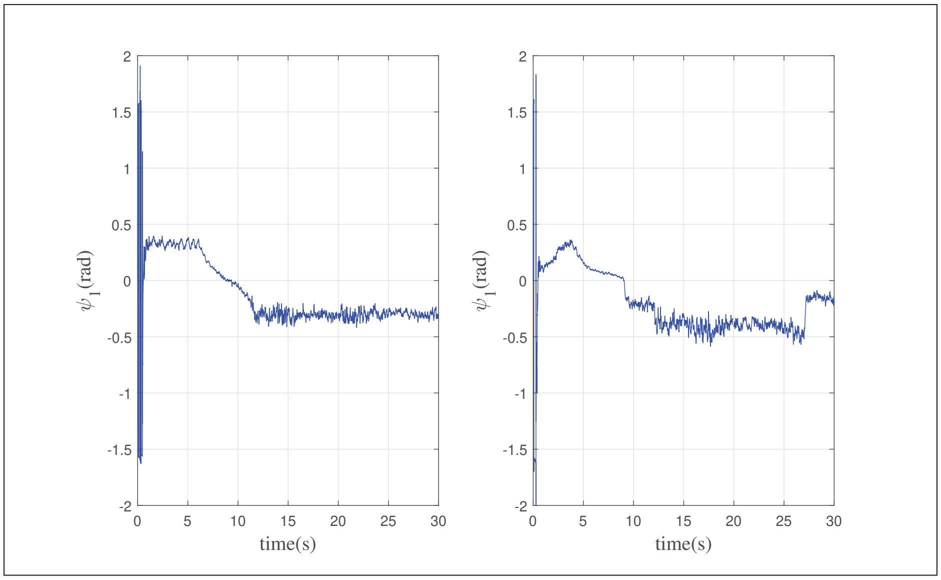

Figure 4.5 Steering angles of vehicle $1(\psi_1)$ and vehicle 2 (ψ_2) with the actuators' faults and fading channel conditions at $t = 8$ s

CHAPTER 5

ADAPTIVE NON-SINGULAR FAST TERMINAL SLIDING MODE CONTROL FOR CAR-LIKE VEHICLES WITH FADED NEIGHBORHOOD INFORMATION AND ACTUATOR FAULTS

Mahmoud Hussein[1], Youmin Zhang[2], Zhaoheng Liu[3]

[1] Departement of Electrical Engineering, École de technologie supérieure,
1100 Notre-Dame Ouest, Montréal, Québec, Canada H3C 1K3
[2] Department of Mechanical, Industrial, and Aerospace Engineering, Concordia University,
1455 De Maisonneuve Blvd. W. Montréal, Québec, Canada H3G 1M8
[3] Département de Génie Mécanique, École de technologie supérieure,
1100 Notre-Dame Ouest, Montréal, Québec, Canada H3C 1K3

Article submitted for publication to the Journal of Intelligent & Robotics Systems in May 2023.

Abstract

This paper discusses the cooperative control problem for a team of car-like vehicles with actuator faults, fading channels, and external disturbances. It is assumed that some followers can't access the leader's states directly over the directed graph. In order to accelerate the consensus tracking and the convergence of the entire system in finite time, the proposed control uses a non-singular fast terminal sliding mode control. This controller is developed to handle both the multiplicative and additive actuator faults as well as the multiplicative randomness of the fading channel. The impact of faded neighborhood information and actuator faults with external disturbance on team performance is carefully analyzed. It is demonstrated by the Lyapunov stability theory that the controller can guarantee good performance of the overall system regardless of these issues. Furthermore, the synchronization of vehicles can be ensured. Simulations are provided to validate the theoretical results.

Keywords: Actuator faults, fading channel, fault-tolerant control, non-singular fast terminal sliding mode, car-like vehicle, mobile robots.

5.1 Introduction

The cooperative control problem of networked control systems (NCSs) has received considerable attention during the past decade from the control community to perform complex tasks such as cooperative control of space formations, unmanned aerial vehicles, mobile robots, and so on (Aldana, Munguía, Cruz-Zavala & Nuño, 2019; Hadi, Khosravi & Sarhadi, 2021; Kamel *et al.*, 2020). Cooperative control is primarily concerned with the consensus problem, which involves formulating a control law that forces all agents to agree on a common value of interest. There have been several interesting results reported on consensus problems of first-order (Yu, Chen, Chen & Hao, 2019a; Wei, Chen, Luo & Huang, 2022), second-order (Zhang, Chen & Zheng, 2019; Lu, Wu, Zhan, Han & Yan, 2022), and high-order systems (Wu, Xu, Lu, Wu & Huang, 2017). Consensus problems were mainly studied with linear systems (Cai, Zhang, Zhang & He, 2020; Ren, Wang & Duan, 2021). The research of consensus for nonlinear systems is more difficult than that for linear systems. Nevertheless, nonlinearity is pervasive in practice, and several studies have been carried out to investigate nonlinear dynamic systems (Cai, Wen, Su & Liu, 2013; Wang, Wang, Cai & Ji, 2018; Liu, Zhang, Yuan, Ciarletta & Theilliol, 2019; Yaghoubi & Talebi, 2020). For instance, the study in (Cai *et al.*, 2013) presented a control scheme for nonlinear systems based on a backstepping approach to compensate for hysteretic actuator faults. However, the unknown nonlinear system components were considered to be linearly parameterized. The impact of stochastic disturbances on nonlinear systems has been studied in (Wang, Zhang, Zhang, Zhang & Huang, 2020) and (Yu & Zhang, 2023). The stability problems in stochastic nonlinear systems are more challenging to solve than in deterministic systems. Physical systems are inherently nonlinear. Therefore, it is more important to consider the nonlinearity in the study of NCSs. Thus, the significance of consensus research for the NCSs that take non-linearity into account increases (Ren, Peng, Deng & Zhang, 2018; Niu, Liu & Man, 2019). Preliminary researchers in Ren *et al.* (2018) proposed two distinct delay-free impulsive pinning control methods to overcome the consensus problem for stochastic disturbances. However, the proposed impulsive pining controller cannot guarantee the synchronization of team members. Sliding mode control (SMC) is a reliable approach that can provide robustness to nonlinear systems against uncertainties and external disturbances. In Niu *et al.* (2019), a finite time consensus tracking for NCSs with uncertainty and perturbation is successfully accomplished utilizing the SMC technique and a time-varying method that can adjust for uncertainties and temporal fluctuations.

In practice, the convergence rate becomes an essential criterion for evaluating the error-tracking mechanism. The finite-time consensus is capable of achieving a faster convergence rate than asymptotic convergence. Therefore, NCSs must be further investigated in the context of finite-time consensus. Meanwhile, the terminal sliding mode control (TSMC) approach has the ability to drive state errors to zero within a finite period of time. The TSMC provides rapid responsiveness, resilience, and finite-time convergence. Nevertheless, TSMCs may experience singularity when errors reach zero, resulting in unbounded parameters. This limitation has been mitigated by the non-singular terminal sliding mode control (NTSMC) approach (Muñoz, Espinoza, González-Hernández, Salazar & Lozano, 2019; Wu & Huang, 2022). In addition, some researchers have developed a new form of NTSMC called the non-singular fast terminal sliding mode control. The NFTSMC affords a better state convergence than the NTSMC while still maintaining the benefits of the NTSMC (Zhang, Yang, Wei & Liu, 2020; Zhang & Quan, 2022). Nevertheless, several practical issues, such as sensor faults, actuator faults, communication network faults, and state limitations, to mention a few, continue to be challenging to maintain the required system performance. One of the most prevalent faults in real-world applications is an actuator fault, which significantly affects the control performance of NCSs and causes instability in the behavior of subsystems and, eventually, the entire system (Jin, Zhao & He, 2018). None of the aforementioned studies addressed the components' fault problems and their effect on the stability of NCSs, which motivates this study.

Actuator faults may arise in physical systems due to power issues, component malfunctions, external disturbances, or uncontrolled crashing. Several types of actuator faults, including loss of effectiveness and bias faults, have been discussed in (Kamel, Ghamry & Zhang, 2017; Yu, Qu & Zhang, 2019b; Kheirandish, Yazdi, Mohammadi & Mohammadi, 2023). Apart from certain common approaches such as fault detection and isolation (FDI)-based methods (Ju, Tian, Liu & Ma, 2021; Yu, Zhang, Jiang & Yu, 2021) and linear matrix inequality (LMI) (Naseri, Vu, Mobayen, Najafi & Fekih, 2022), an adaptive control method was identified as an effective technique for compensating all sorts of actuator faults (Xu, Sun, Wu & Wang, 2021; Xu, Wang, Wang & Peng, 2022). However, the proposed control methodologies could be inapplicable when agents can not exchange information due to some issues in the communication networks, i.e., fading channel, time delay, packet loss, etc.

With the widespread use of wireless communication technologies in real-world systems, we consider a common problem called fading channels. In wireless networks, fading is a significant phenomenon induced by diffraction, reflection, and refraction upon propagation (Qu *et al.*, 2021). In other words, fading is caused by the attenuation of transmitted data across certain propagation mediums. This damages the shared state information between agents, i.e., position, velocity, etc., which is critical for the control design and stability of the NCSs. This fact encourages a significant control direction over random and uncertain networks (Shen, 2017; Zhang & Li, 2017; Hu, 2021). The tracking problem of NCSs with fading channels has been addressed in several studies (Shen & Qu, 2019; Qu & Shen, 2019; Shen & Yu, 2020). The authors (Shen & Qu, 2019) used a learning control technique to improve the tracking performance of linear systems with fading channels without imposing restrictive constraints on the fading channel. A Kalman filtering-based framework is used in (Qu & Shen, 2019) in order to optimize the learning gain matrix based on the input error covariance matrices. A stochastic algorithm based on approximations is employed in (Shen & Yu, 2020) in order to solve the tracking problem for unknown systems with unknown fading channels. Random fading channels are modeled as a combination of additive and multiplicative randomness in the framework proposed. More relative studies can be found in (Bu, Yu, Yu, Hou & Yang, 2021; Cao, Yan, Yang, Luo & Guan, 2023). However, up to now, the control tracking problem for the NCSs with actuator faults, fading channels, and external disturbances, which are common problems in such large-scale systems, have not been studied.

This paper investigates the cooperative control problem for NCSs with fading channels, actuator faults, and external disturbances in light of the above discussions. We develop an adaptive fault-tolerant cooperative control scheme based on NFTSMC for a team of car-like vehicles that allows each vehicle to compensate for the impact of faults if they exist and continue the mission with the rest of the team members. First, we develop adaptive fault-tolerant cooperative control to cope with fading channels and external disturbances. Second, we develop an adaptive fault-tolerant cooperative control design under the influence of fading channels, actuator faults, and external disturbances. The proposed controller is based on NFTSMC as it can overcome the singularity in the consensus tracking problem and provide fast convergence rates.

The main contributions of this study are as follows:

1. To the best of the authors' knowledge, the problem of the simultaneous occurrence of the fading channel and actuator faults for networked systems has not been reported. This study introduces the first result of the cooperative control problem, considering the effect of fading channel and actuator fault with the presence of external disturbances.

2. In contrast to the existing adaptive fault-tolerant control strategies, in our developed adaptive control, the adaptive mechanism is able to modify the gain of sliding mode control automatically. This provides an advantage over a constant control gain in that the sliding mode control can function properly without prior knowledge of uncertainties and disturbances in the system.

3. As compared to existing fault-tolerant control methods, our developed control has a simple structure and can be readily implemented in practice.

The remainder of this paper is organized as follows. Preliminaries and problem formulation are presented in Section 5.2. Section 5.3 proposes a controller for leader–follower systems under the effect of fading channels, actuator faults, and external disturbances with the corresponding stability analysis. In Section 5.4, numerical simulations are presented to verify the effectiveness of the proposed approach. Finally, the conclusion and future work are given in Section 5.5

5.2 Preliminaries and Problem Formulation

5.2.1 Communication topology (West, 2001)

The graph $G = (V, E, A)$ represents a team communication topology with $V = \{v_1, v_2, ..., v_n\}$ and $E = \{e_{ij} = (v_i, v_j)\}$ respectively. An adjacency matrix A is defined as $A = [a_{ij}]_{n\times n}$. Adjacency element $a_[ij] > 0$ indicating that there is an edge between node v_i and node v_j; otherwise, $a_{ij} = 0$. A graph G is said to be strongly connected if there is a path between v_i and v_j for every pair of distinct nodes. $(v_i, v_j) \in E \implies (v_j, v_i) \in E$.

The Laplacian matrix L_m of a weighted graph is defined by:

$$L_m = D - A = [l_{ij}] \in \mathbb{R}^{n\times n}, \tag{5.1}$$

where the degree matrix $D = \mathrm{diag}(d_1, d_2, ...d_n)$, $d_i = \sum_{j=1}^{N} a_{ij}$, $l_{ij} = -a_{ij}$, $\forall j \neq i$ and $\sum_{j=1}^{N} l_{ij} = l_{ii}, \forall i = 1, 2, ..., N$.

This study considers a team of car-like vehicles with l as the leader and $i = 1, 2, ..., N$ as followers. Digraphs G are used to represent communication between leaders and followers. A matrix $B = \mathrm{diag}(b_1, b_2, ..., b_N)$ describes communication between the leader and all followers when $b_i = 1$, otherwise, it is zero.

5.2.2 System description

This paper considers a team of car-like vehicles to consist of one virtual leader and multiple followers. The dynamics of i^{th} follower is given by (Ren & Chen, 2015) as:

$$\begin{cases} \dot{q}_i &= J_i \bar{\omega}_i \\ \dot{\bar{\omega}}_i &= \bar{M}^{-1}\bar{B}(q_i)\tau_i - h_i(q_i, \dot{q}_i) + d_i, \end{cases} \tag{5.2}$$

and the dynamic of leader l is introduced as follows:

$$\begin{cases} \dot{q}_l &= J_i \bar{\omega}_l \\ \dot{\bar{\omega}}_l &= \bar{M}^{-1}\bar{B}(q_l)\tau_l - h_l(q_l, \dot{q}_l), \end{cases} \tag{5.3}$$

where

$$h_i(q_i, \dot{q}_i) = \bar{M}^{-1}\bar{V}(q_i, \dot{q}_i)\bar{\omega}_i, \quad h_l(q_l, \dot{q}_l) = \bar{M}^{-1}\bar{V}(q_l, \dot{q}_l)\bar{\omega}_l,$$

$$\bar{\omega}_i = \begin{bmatrix} v_i & w_i \end{bmatrix}^T, \quad \bar{M} = J_i^T M S_i, \quad \bar{V} = J_i^T(M\dot{J}_i + VJ_i),$$

$$\bar{B} = J_i^T B, \quad J_i = \begin{bmatrix} \cos\phi_i & 0 \\ \sin\phi_i & 0 \\ \frac{tan(\psi_i)}{l} & 0 \\ 0 & 1 \end{bmatrix},$$

$$M = \begin{bmatrix} m & 0 & I_c \sin(\phi_i) & 0 \\ 0 & m & -I_c\cos(\phi_i) & 0 \\ I_c\sin(\phi_i) & -I_c\cos(\phi_i) & I_b & I_w \\ 0 & 0 & I_w & I_w \end{bmatrix},$$

$$V = \begin{bmatrix} 0 & 0 & -I_c\dot{\phi}\cos(\phi_i) & 0 \\ 0 & 0 & -I_c\dot{\phi}\sin(\phi_i) & 0 \\ 0 & 0 & 0 & 0 \\ 0 & 0 & 0 & 0 \end{bmatrix}, B = \begin{bmatrix} \cos(\phi_i) & 0 \\ \sin(\phi_i) & 0 \\ L\sin(\psi_i)\cos(\psi_i) & 0 \\ 0 & 1 \end{bmatrix},$$

where $q_i = (x_i, y_i, \phi_i, \psi_i)^T$ and $q_l = (x_l, y_l, \phi_l, \psi_l)^T$ are the state vectors of the i^{th} follower and leader respectively. (x_i, y_i) is the position of i^{th} follower as shown in Figure 2.1. The linear and steering velocities are v_i and ω_i, respectively. ϕ_i and ψ_i are heading and steering angles of i^{th} follower. τ_i is the torque acting on the actuators of the i^{th} follower. d_i is the external disturbance. $m = m_c + 4m_w$, $I_c = (L-b)m_c + 2Lm_w$, $I_b = m_c(L-b)^2 + 4W^2 m_w + I_{bzz} + 4I_{wzz}$, m_c and m_w are the vehicle and wheel masses, respectively. The moment of inertia of each wheel with a motor about the wheel axis is denoted by I_w. I_{bzz} is the moment of inertia of a vehicle body about the z-axis passes into the car's center of mass. The wheel's moment of inertia about the z-axis passes into the wheel centroid is represented by I_{wzz}. As indicated in Figure 2.1, CoR is the center of the rotation along the axis of the rear wheels. L is the distance between the front and rear axles. b is the distance from the center of mass to the rear axle.

Assumption 4. *There exists an upper bound for the external disturbances such that* $||d_i|| < \bar{d}$, *where* $\bar{d}$ *is a positive constant.*

Assumption 5. *(Ren & Chen, 2015) For any* q_i, $\bar{\omega}_i$, $i \in [0,1,...]$, *there exist positive constants* μ_1 *and* μ_2 *such that:*

$$\|H(q,\bar{\omega},t) - 1 \otimes h(q_l,\bar{\omega}_l,t)\| \leq \mu_1\|q - 1 \otimes q_l\| + \mu_2\|\bar{\omega} - 1 \otimes \bar{\omega}_l\|, \tag{5.4}$$

where $H(q,\bar{\omega},t) = [h_1(q,\bar{\omega}),...,h_N(q,\bar{\omega})]^T$ *and* $\otimes$ *is the Kronecker product.*

Lemma 3. *(Khoo* et al.*, 2009) The matrix* $L_m + B$ *is invertible if the digraph G has a directed spanning tree.*

Definition 5.1. *(Zhang & Lewis, 2012) The tracking error for any networked system is said to be cooperatively uniformly ultimately bounded if there exists a compact set* $\bar{\theta}^{\varepsilon_1} \subset \mathbb{R}^N$ *and* $\bar{\theta}^{\varepsilon_2} \subset \mathbb{R}^N$ *with the property that* $\{0\} \subset \bar{\theta}^{\varepsilon_1}$ *and* $\{0\} \subset \bar{\theta}^{\varepsilon_2}$, $\forall\, \varepsilon_1 \in \bar{\theta}^{\varepsilon_1}$ *and* $\varepsilon_2 \in \bar{\theta}^{\varepsilon_2}$ *there exist bounds* $\bar{B}^{\varepsilon_1}$ *and* $\bar{B}^{\varepsilon_2}$ *and time* $T(\bar{B}^{\varepsilon_1}, \bar{B}^{\varepsilon_2}, \varepsilon_1, \varepsilon_2)$ *such that* $\|\varepsilon_1\| \leq \bar{B}^{\varepsilon_1}$, $\|\varepsilon_2\| \leq \bar{B}^{\varepsilon_2}$, $\forall t \geq t_o + T_a$, *where* ε_1 *and* ε_2 *are the system's tracking errors of position and velocity, respectively.*

Remark 1. *The goal of the cooperative control problem for systems based on the leader-follower approach is to have each follower's position and velocity converge to those of the leader. However, in practice, precise control tracking is not possible due to unknown dynamics, external disturbances, component faults, etc. Therefore, the cooperative uniform ultimate boundedness (CUUB) is developed to handle unexpected changes in practical applications.*

In the fault-free conditions, the control tracking problem for i^{th} follower can be solved by defining the tracking error as follows (Khoo *et al.*, 2009):

$$\begin{cases} e_{1i} &= \sum_{j=1}^{N} a_{ij}(p_i - p_j - \Delta_{ij}) + b_i(p_i - p_L - \Delta_{iL}) \\ e_{2i} &= \sum_{j=1}^{N} a_{ij}(\bar{\omega}_i - \bar{\omega}_j) + b_i(\bar{\omega}_i - \bar{\omega}_l), \end{cases} \tag{5.5}$$

where e_{1i} and e_{2i} are the position and velocity tracking error variables respectively. $a_{ij} = 1$ when there is interaction between i^{th} follower and its neighbor j; otherwise it is zero. $b_i = 1$ when there is interaction between i^{th} follower and the leader; otherwise it is zero $p_i = (x_i, y_i, \psi_i)^T$, $\Delta_{ij} = (\Delta_j - \Delta_i)$ is the distance between the i^{th} follower and its neighbor j and Δ_{iL} is the distance between the i^{th} follower and the leader. The team members achieve the consensus and track the leader states when the error variables in (5.5) reach zero. For convenience, Eq. (5.5) can be transformed into the compact form as follows:

$$\begin{cases} \varepsilon_1 &= (L_m + B) \otimes I_m.\tilde{p} \\ \varepsilon_2 &= (L_m + B) \otimes I_m.\tilde{\bar{\omega}}, \end{cases} \tag{5.6}$$

where $\varepsilon_1 = [\varepsilon_{11}, ..., \varepsilon_{1N}]^T$, $\varepsilon_2 = [\varepsilon_{21}, ..., \varepsilon_{2N}]^T$, $\tilde{p} = p - 1 \otimes (p_l - \Delta_{iL})$, $\tilde{\bar{\omega}} = \tilde{\bar{\omega}} - 1 \otimes \tilde{\bar{\omega}}_l$, $I_m \in R^{\ m\times m}$.

The time derivative of (5.6) is given by

$$\begin{cases} \dot{\varepsilon}_1 &= \bar{\varepsilon}_2^{\star} \\ \dot{\varepsilon}_2 &= (L_m + B) \otimes I_m.\Big(H - 1 \otimes h(q_l, \dot{q}_l) + \bar{M}^{-1}\tau - 1 \otimes \bar{M}^{-1}\tau_l\Big), \end{cases} \tag{5.7}$$

where $\bar{\varepsilon}_2^{\star} = J_{3\times 2}\varepsilon_2$, $\tau = [\tau_1, ..., \tau_N]^T$, $M^{-1} = diag[M_1^{-1}, ..., M_N^{-1}]^T$. The goal of (5.7) is to achieve that $\lim_{t\to\infty} \varepsilon_1 = 0$ and $\lim_{t\to\infty} \varepsilon_2 = 0$. However, in the presence of faded neighborhood information and actuator fault conditions, this goal can not be satisfied without considering the effects of these types of faults in the system design.

5.2.3 Faded neighborhood information problem

In real systems, many factors will interfere with information transmission between agents, resulting in the agents receiving only faded information rather than accurate information transmitted by neighboring agents. In this study, we assume that the fading signal occurs during the transmission of information among followers, and there is no fading in the transmitted information from the leader to the followers. The faded information can be modeled as follows:

$$\begin{cases} p_j^\star &= \frac{1}{\delta^\star}\delta_{ji}p_j \\ \bar{\omega}_j^\star &= \frac{1}{\delta^\star}\delta_{ji}\bar{\omega}_j, \end{cases} \tag{5.8}$$

where δ_{ij} is the random fading variable and $\delta^\star$ is the mean value. $p_j^\star$ and $\bar{\omega}_j^\star$ represent the state information in which i^{th} follower receives from neighbor j. Hence, the tracking error variables in (5.5) under the impact of the fading channel can be rewritten as:

$$\begin{cases} e^\star{}_{1i} &= \sum_{j=1}^N a_{ij}(p_i - p_j^\star - \Delta_{ij}) + b_i(p_i - p_L - \Delta_{iL}) \\ e^\star{}_{2i} &= \sum_{j=1}^N a_{ij}(\bar{\omega}_i - \bar{\omega}_j^\star) + b_i(\bar{\omega}_i - \bar{\omega}_l). \end{cases} \tag{5.9}$$

For the simplicity of the analysis, we introduce α_i, which has 1 in its i^{th} element and the rest are zeros. Then (5.9) can be converted to a compact form as follows:

$$\begin{cases} \varepsilon^\star{}_1 &= (L_m + B) \otimes I_m . \sum_{i=1}^N \Big(\frac{1}{\delta^\star}\Pi_i(p - \alpha_i \otimes (p_i - \Delta_{ij}) + (\alpha_i \otimes p_i) \\ & -1_N \otimes (p_l - \Delta_{iL})\Big) \\ \varepsilon^\star{}_2 &= (L_m + B) \otimes I_m . \sum_{i=1}^N \Big(\frac{1}{\delta^\star}\Pi_i(\bar{\omega} - \alpha_i \otimes \bar{\omega}_i)\alpha_i \otimes \bar{\omega}_i - 1_N \otimes \bar{\omega}_l\Big), \end{cases} \tag{5.10}$$

where $\Pi_1 = \text{diag}[0, \delta_{12}, ..., \delta_{1N}]$, $\Pi_2 = \text{diag}[\delta_{21}, 0, ..., \delta_{2N}]$, ..., $\Pi_N = \text{diag}[\delta_{N1}, \delta_{N2}, ..., 0]$ and $\Pi_i(p - \alpha_i \otimes p_i)$ refers to the transmitted state information from team members to i^{th} follower.

Taking the time derivative of (5.10), one can get

$$\begin{cases} \dot{\varepsilon^{\star}}_1 & = \bar{\varepsilon}_2^{\star} \\ \dot{\varepsilon^{\star}}_2 & = (L_m + B) \otimes I_m . \Big(\bar{H} - 1 \otimes h(q_l, \dot{q}_l) + \bar{M}^{-1}\tau - 1 \otimes \bar{M}^{-1}\tau_l \Big), \end{cases} \tag{5.11}$$

where $\bar{\varepsilon}_2^{\star} = J_{3\times2}\varepsilon_2^{\star}$, $\quad \bar{H} = \sum_{j=1}^{N} \frac{1}{\delta^{\star}} \Pi_i(\dot{\bar{\omega}} - \alpha_i \otimes \dot{\bar{\omega}}_i) + \alpha_i \otimes \dot{\bar{\omega}}_i$. Then, the goal of (5.11) is to achieve that $lim_{t\to\infty}\varepsilon^{\star}{}_1 = 0$ and $lim_{t\to\infty}\varepsilon^{\star}{}_2 = 0$.

5.2.4 Actuator fault problem

Within all classes of potential faults, actuator faults are considered one of the most challenging problems to resolve. Faulty actuators can substantially degrade the system's performance and lead to catastrophic accidents. In this study, we investigate the impact of the multiplicative and additive actuator faults on the performance of the follower agents under the following assumption:

Assumption 6. *(Xiao* et al.*, 2017) The multiplicative and additive actuator faults $\gamma_i(t), \vartheta_i(t)$ are bounded, and their derivatives exist and are also bounded. Furthermore, we have $\|\vartheta_i\| \leq \bar{\vartheta}_i$ where $\bar{\vartheta}_i$ is a known bound.*

In the light of Assumptions 6, the actuator faults in (5.2) can be modeled as follows:

$$\tau_i = (1 - \gamma_i(t))\tau_N + \vartheta_1(t), \tag{5.12}$$

where τ_N denotes the nominal torque inputs, $\gamma_i(t) \in \mathbb{R}^{2\times2}$ and $\vartheta_1(t) \in \mathbb{R}^2$ are the multiplicative and additive actuator faults, respectively, with $\gamma_i(t) = \text{diag}([\gamma_1(t), \gamma_2(t)])$, with $0 < \gamma_i(t) \leq 1$. In the fault-free condition, all the elements of $\gamma_i(t)$ and $\vartheta_i(t)$ are assumed to equal zero.

5.3 Main Results

5.3.1 Adaptive fault-tolerant cooperative control design in the presence of fading channels and external disturbances

This section aims to design an adaptive FTC that ensures the stability of the team subjected to faded neighborhood information. We choose a non-singular fast sliding mode surface that avoids singularities and has a rapid convergence speed. A sliding mode surface for i^{th} follower is selected in accordance with the error of position and the linear and steering velocities error as follows:

$$s_i = {\varepsilon^{\star}}_{1i} + K_{1i}(\varepsilon^{\star}_{1i})^{\eta_1} + K_{2i}(\varepsilon^{\star}_{2i})^{\eta_2}, \tag{5.13}$$

where $K_{1i} > 0$ and $K_{2i} > 0$, hence, the compact form of (5.13) can be written as follows:

$$s = {\varepsilon^{\star}}_1 + K_1(\varepsilon^{\star}_1)^{\eta_1} + K_2(\varepsilon^{\star}_2)^{\eta_2}, \tag{5.14}$$

where

$$s = [s_i^T, s_2^T, ..., s_N^T],$$

Taking the time derivative of (5.14), one can get that

$$\begin{aligned} \dot{s} &= \dot{\varepsilon}^{\star}_1 + K_1\Lambda_1 \operatorname{diag}(|\varepsilon^{\star}_1|^{\eta_1 - 1})\dot{\varepsilon}^{\star}_1 + K_2\Lambda_2 \operatorname{diag}(|\varepsilon^{\star}_2|^{\eta_2 - 1})\dot{\varepsilon}^{\star}_2 \\ &= J_{3\times 2}\varepsilon^{\star}_2 + K_1\Lambda_1 \operatorname{diag}(|\varepsilon^{\star}_1|^{\eta_1 - 1})J_{3\times 2}\varepsilon^{\star}_2 + K_2\Lambda_2 \operatorname{diag}(|\varepsilon^{\star}_2|^{\eta_2 - 1})\dot{\varepsilon}^{\star} \\ &= (I + K_1\Lambda_1 \operatorname{diag}(|\varepsilon^{\star}_1|^{\eta_1 - 1}))\bar{\varepsilon}^{\star}_2 + K_2\Lambda_2 \operatorname{diag}(|\varepsilon^{\star}_2|^{\eta_2 - 1})\dot{\varepsilon}^{\star}, \end{aligned} \tag{5.15}$$

where $\Lambda_1 = \operatorname{diag}(\eta_1)$ and $\Lambda_2 = \operatorname{diag}(\eta_2)$ and $|\varepsilon^{\star}_1|^{\eta_1 - 1} = (|\varepsilon^{\star}_{11}|^{\eta_{11} - 1^T}, |\varepsilon^{\star}_{12}|^{\eta_{12} - 1^T}, ..., |\varepsilon^{\star}_{1N}|^{\eta_{1N} - 1^T})^T$ and $|\varepsilon^{\star}_2|^{\eta_2 - 1} = (|\varepsilon^{\star}_{21}|^{\eta_{21} - 1^T}, |\varepsilon^{\star}_{22}|^{\eta_{22} - 1^T}, ..., |\varepsilon^{\star}_{2N}|^{\eta_{2N} - 1^T})^T$.

The adaptive NFTSMC for a team of car-like vehicles with faded neighborhood information is designed as follows:

$$\begin{aligned}\tau \;\; = \;\; & \bar{M}(L_m + B)^{-1} \otimes I_m.\,\mathrm{diag}(|\varepsilon_2^\star|^{1-\eta_2})(K_2\Lambda_2)^{-1}\Big(- (I + K_1\Lambda_1\,\mathrm{diag}(|\varepsilon_1^\star|^{\eta_1-1}))\bar{\varepsilon}_2^\star + \Upsilon(s) \\ & -K_3 s^{\gamma_1} - K_4 s^{\gamma_2}\Big) + 1_N \otimes \tau_l, \qquad (5.16)\end{aligned}$$

where $\Upsilon(s) = [\upsilon(s_1), \upsilon(s_2), ..., \upsilon(s_N)]$ and $\upsilon(s_i)$ is the smoothing function defined in (5.18). By selecting a large switching gain, the cooperative tracking can be achieved in (5.17); however, it may result in extreme actuator chattering and high energy consumption in real physical systems. Therefore, a switching gain σ_i is designed based on the following adaptive mechanism:

$$\dot{\sigma}_i = \mu(\|s_i\| - \kappa\sigma_i), \qquad (5.17)$$

where $\mu > 0$ and $\kappa > 0$. The term $-\kappa\sigma_i$ is introduced to limit the growth of $\dot{\sigma}_i$.

From (5.17), we can write the smoothing function that reduces the chattering as follows:

$$\upsilon(s_i) = \begin{cases} -2\sigma_i \frac{si}{\|s_i\|} & \text{if} \quad \sigma_i\|s_i\| \geq \chi \\ -2\sigma_i \frac{si}{\chi} & \text{if} \quad \sigma_i\|s_i\| < \chi, \end{cases} \qquad (5.18)$$

where $\chi > 0$, and σ_i is computed by the adaptive law in (5.17).

Theorem 5. *Consider the system in (5.2) and (5.3) under the influence of a fading channel, and by applying the control law in (5.16), the tracking error variables in (5.11) can converge to zero in finite time.*

Proof. Consider the candidate Lyapunov function is selected as:

$$V_1 = \frac{1}{2}s^T s + \frac{1}{2\mu}\sum_{i=1}^{N}(\sigma_i - \bar{\sigma})^2 + \frac{1}{2\mu}\sum_{i=1}^{N}\sigma_i^2, \qquad (5.19)$$

where $\bar{\sigma}_i$ is the upper bound of σ_i. A $\bar{\sigma}_i$ is designed to be $\bar{\sigma}_i > \varphi + \sigma_0$, and $\sigma_0 > 0$.

Taking the time derivative of (5.19), we get that

$$\begin{aligned}\dot{V}_1 &= s^T\Big((I + K_1\Lambda_1 \operatorname{diag}(|\varepsilon_1^\star|^{\eta_1-1}))\bar{\varepsilon}_2^\star + K_2\Lambda_2 \operatorname{diag}(|\varepsilon_2^\star|^{\eta_2-1})\dot{\varepsilon}_2^\star\Big) + \sum_{i=1}^{N}(\sigma_i - \bar{\sigma})(\|s_i\| - \kappa\sigma_i) \\ &\quad + \sum_{i=1}^{N}\sigma_i(\|s_i\| - \kappa\sigma_i). \qquad (5.20)\end{aligned}$$

Substituting (5.11) into (5.20) one has

$$\begin{aligned}\dot{V}_1 &= s^T\Big((I + K_1\Lambda_1 \operatorname{diag}(|\varepsilon_1^\star|^{\eta_1-1}))\bar{\varepsilon}_2^\star + K_2\Lambda_2 \operatorname{diag}(|\varepsilon_2^\star|^{\eta_2-1})(L_m + B)\otimes I_m.(\bar{H} - 1 \\ &\quad \otimes h(q_l, \bar{\omega}_l, t) + d + \bar{M}^{-1}\tau - 1\otimes \bar{M}^{-1}\tau_l)\Big) + \Xi(s_i, \sigma), \qquad (5.21)\end{aligned}$$

where

$$\Xi(s_i, \sigma) = \sum_{i=1}^{N}(\sigma_i - \bar{\sigma})(\|s_i\| - \kappa\sigma_i) + \sum_{i=1}^{N}\sigma_i(\|s_i\| - \kappa\sigma_i). \qquad (5.22)$$

According to Assumption 5 and the properties of the norm, we have

$$\begin{aligned}\|\bar{H} - 1\otimes h_l\| &= \|(\bar{h}_1(q_1, \bar{\omega}_1, t) - h_l(q_l, \bar{\omega}_l, t))^T, ..., (\bar{h}_n(q_n, \bar{\omega}_n, t) - h_l(q_l, \bar{\omega}_l, t))^T\| \\ &\leq \|(\|\bar{h}_1(q_1, \bar{\omega}_1, t) - h_l(q_l, \bar{\omega}_l, t)\|, ..., \|(\bar{h}_n(q_n, \bar{\omega}_n, t) - h_l(q_l, \bar{\omega}_l, t)\|)\| \\ &\leq \|(\mu_1\|q_1 - q_l\| + \mu_2\|\bar{\omega}_1 - \bar{\omega}_2\|, ..., \mu_1\|q_n - q_l\| + \mu_2\|\bar{\omega}_n - \bar{\omega}_l\|)\| \\ &\leq \|(\mu_1\|q_1 - q_l\|, ..., +\|q_n - q_l\|)\| + \mu_2\|(\|\bar{\omega}_1 - \bar{\omega}_2\|, ..., \|\bar{\omega}_n - \bar{\omega}_2\|)\| \\ &\leq \mu_1\|\varepsilon_1^\star\| + \mu_2\|\varepsilon_2^\star\|. \qquad (5.23)\end{aligned}$$

Using the Kronecker product property, we obtain the following:

$$\begin{aligned}\|(L + B)\otimes I_m\| &= \Big[\lambda_m\Big([(L_m + B)\otimes I_m]^T[(L_m + B)\otimes I_m]\Big)\Big]^{\frac{1}{2}} \\ &= [\lambda_m(L_m + B)^T(L_m + B)]^{\frac{1}{2}} \\ &= \|(L_m + B)\| \qquad (5.24)\end{aligned}$$

From Lemma 3, (5.23) and (5.24), we have

$$\begin{aligned}
\|(L_m + B) \otimes I_m(\bar{H} - 1 \otimes h_l)\| &\leq \|L_m + B\|(\mu_1\|\varepsilon_1^\star\| + \mu_2\|\varepsilon_2^\star\|) \\
&\leq \|L_m + B\|\|L_m + B\|^{-1}(\mu_1\|\varepsilon_1^\star\| + \mu_2\|\varepsilon_2^\star\|) \\
&\leq \zeta\mu_1\|\varepsilon_1^\star\| + \zeta\mu_2\|\varepsilon_2^\star\|. \qquad (5.25)
\end{aligned}$$

By means of (5.24) and (5.25) one has

$$\begin{aligned}
\dot{V}_1 = \; & s^T\Big((I + K_1\Lambda_1 \operatorname{diag}(|\varepsilon_1^\star|^{\eta_1-1}))\bar{\varepsilon}_2^\star + K_2\Lambda_2 \operatorname{diag}(|\varepsilon_2^\star|^{\eta_2-1})(\zeta\mu_1\|\varepsilon_1^\star\| + \zeta\mu_2\|\varepsilon_2^\star\|) \\
& + K_2\Lambda_2 \operatorname{diag}(|\varepsilon_2^\star|^{\eta_2-1})(L_m + B) \otimes I_m(\bar{M}^{-1}\tau - 1 \otimes \bar{M}^{-1}\tau_l + \sqrt{N}\bar{d})\Big) \\
& + \Xi(s_i, \sigma). \qquad (5.26)
\end{aligned}$$

By replacing (5.16) into (5.26), the following inequality holds:

$$\begin{aligned}
\dot{V}_1 \leq \; & K_2\Lambda_2 \operatorname{diag}(|\varepsilon_2^\star|^{\eta_2-1})\Big[(\zeta(\mu_1\|\varepsilon_1^\star\| + \mu_2\|\varepsilon_2^\star\|) + \|L_m + B\|\sqrt{N}\bar{d}\Big]\|s\| \\
& - (K_3 s^{\nu_1} + K_4 s^{\nu_2})\|s\| + s^T\Upsilon(s) + \Xi(s_i, \sigma). \qquad (5.27)
\end{aligned}$$

To proceed with the theoretical analysis, there are two cases we need to consider:

First, when $\sigma_i\|s_i\| \geq \chi$, $\forall i = 1,...,N$, $s^T\Upsilon(s) = -\sum_{i=1}^N \sigma_i\|s_i\|$. Then, (5.27) can be rewritten as follows:

$$\dot{V}_1 \leq \varphi\|s\| + \Xi(s_i, \sigma) - 2\sum_{i=1}^N \sigma_i\|s_i\| - K_3\sum_{i=1}^N \|s_i\|^{\nu_{1i}+1} - K_4\sum_{i=1}^N \|s_i\|^{\nu_{2i}+1}, \qquad (5.28)$$

where $\varphi = K_2\Lambda_2 \operatorname{diag}(|\varepsilon_2^\star|^{\eta_2-1})\Big(\zeta(\mu_1\|\varepsilon_1^\star\| + \mu_2\|\varepsilon_2^\star\|) + \|(L_m + B)\|\sqrt{N}\bar{d}\Big)$.
From (5.22), one can write

$$\begin{aligned}\Xi(s_i,\sigma_i) &= 2\sum_{i=1}^{N}\sigma_i\|s_i\| - \kappa\sum_{i=1}^{N}(\sigma_i-\bar{\sigma})\sigma_i - \kappa\sum_{i=1}^{N}(\sigma_i)^2 - \bar{\sigma}\sum_{i=1}^{N}\|s_i\| \\ &= 2\sum_{i=1}^{N}\sigma_i\|s_i\| + \kappa\bar{\sigma}\sum_{i=1}^{N}\sigma_i - 2\kappa\sum_{i=1}^{N}(\sigma_i)^2 - \bar{\sigma}\sum_{i=1}^{N}\|s_i\|. \end{aligned} \tag{5.29}$$

Replacing (5.29) into (5.28), we get that

$$\dot{V}_1 \leq -(\bar{\sigma}-\varphi)\|s\| + \kappa\bar{\sigma}\sum_{i=1}^{N}\sigma_i - 2\kappa\sum_{i=1}^{N}(\sigma_i)^2 - (K_3+K_4)\sum_{i=1}^{N}\|s_i\|^{\bar{\gamma}+1}. \tag{5.30}$$

Since σ_i reaches its maximum value when $\sigma_i = \bar{\sigma}$, one has

$$\dot{V}_1 \leq -(\sigma_o)\|s\| + \rho_1 \tag{5.31}$$

with $\rho_1 = -\kappa N\bar{\sigma}^2 - (K_3+K_4)\sum_{i=1}^{N}\|s_i\|^{\bar{\gamma}+1}$.

Second, when $\sigma_i\|s_i\| < \chi$, $\forall\, i = 1,...,N$, $s^T\Upsilon(s) = \sum_{i=1}^{N}\frac{\sigma}{\chi}\|s_i\|$. It follows from (5.27) that

$$\begin{aligned}\dot{V}_1 &\leq \varphi\|s\| + \sum_{i=1}^{N}(\sigma_i-\bar{\sigma})(\|s_i\| - \kappa\sigma_i) - \sum_{i=1}^{N}\frac{\sigma_i}{\chi}\|s_i\| \\ &\leq -(\sigma_o)\|s\| - \rho_1 - \sigma_i\sum_{i=1}^{N}(\frac{1}{\chi} - \sigma_i)\|s_i\| \\ &\leq -(\sigma_o)\|s\| - \rho_2, \end{aligned} \tag{5.32}$$

with $\rho_2 = \rho_1 + \sigma_i\sum_{i=1}^{N}(\frac{1}{\chi} + \sigma_i)\|s_i\|$.

By combining Case I and Case II, the following inequality holds:

$$\begin{aligned}\dot{V}_1 &\leq -(\sigma_o)\|s\| + \rho \\ &\leq -(1-\Omega)\sigma_0\|s\|, \end{aligned} \tag{5.33}$$

where $\rho = max\{\rho_1, \rho_2\}$, $0 < \Omega < 1$. Thus, the boundary layer $\bar{\theta}$ will be reached by the sliding manifold s in finite time.

$$\bar{\theta} = \left\{ \|s\| \leq \frac{\sigma}{\Omega \sigma_0} \right\}. \tag{5.34}$$

The ultimate boundedness of s indicates that $\varepsilon_1^\star$ and $\varepsilon_2^\star$ are ultimately bounded. Then, it follows from Definition 5.1 that the CUUB is achieved. This completes the proof. □

5.3.2 Adaptive fault-tolerant cooperative control design under the influence of fading channels, actuator faults, and external disturbances

This section proposes a novel leader-follower consensus algorithm for a team of car-like vehicles with actuator faults, faded neighborhood information, and external disturbances.

Theorem 6. *The tacking of the CUUB for a team of car-like vehicles subject to actuator faults, fading channels, and external disturbances can be achieved with the control law (5.16) and the adaptive mechanism (5.17) if*

$$\epsilon = (L_m + B)\bar{\gamma}(L_m + B)^{-1}, \tag{5.35}$$

where $\epsilon > 0$ *and* $\bar{\gamma} = diag\{\gamma_1(t), ..., \gamma_N(t)\}$.

Proof. Consider the following candidate Lyapunov function:

$$V_1 \;=\; \frac{1}{2} s^T s + \frac{\epsilon}{2\psi} \sum_{i=1}^{N} ((\sigma_i - \bar{\sigma})^2 + \sigma_i^2), \tag{5.36}$$

we assume that $\bar{\sigma}_i > \varphi' + \sigma_o'$, where φ' will be defined later and $\sigma_o' > 0$.

Taking the time derivative of (5.36) and by means of (5.11), (5.12) and (5.25), one has

$$\begin{aligned}\dot{V}_1 \;&=\; s^T\Big((I + K_1\Lambda_1 \operatorname{diag}(|\varepsilon_1^\star|^{\eta_1-1}))\bar{\varepsilon}_2^\star + K_2\Lambda_2 .\operatorname{diag}(|\varepsilon_2^\star|^{\eta_2-1})(\zeta\mu_1\|\varepsilon_1^\star\| + \zeta\mu_2\|\varepsilon_2^\star\|) + K_2\Lambda_2 \\ &\quad .\operatorname{diag}(|\varepsilon_2^\star|^{\eta_2-1})(L_m + B)I_m.(\bar{M}^{-1}.(I - \gamma_i(t))\tau_N + \vartheta_i(t) - 1 \otimes \bar{M}^{-1}\tau_l + \sqrt{N}\bar{d})\Big) \\ &\quad +\epsilon\Xi(s_i, \sigma). \qquad (5.37)\end{aligned}$$

By replacing (5.16) and (5.35) into (5.37) we obtain the following:

$$\begin{aligned}\dot{V}_1 \;&=\; s^T\Big(K_2\Lambda_2 \operatorname{diag}(|\varepsilon_2^\star|^{\eta_2-1}\Big[(\zeta(\mu_1\|\varepsilon_1^\star\| + \mu_2\|\varepsilon_2^\star\|) + \|L_m + B\|.\sqrt{N}\bar{d} + \|L_m + B\|.\sqrt{N}\bar{\vartheta}_i\Big] \\ &\quad -(K_3 s^{\nu_1} + K_4 s^{\nu_2}) + \Upsilon(s) - \|L_m + B\|\bar{\gamma}\|L_m + B\|^{-1} \otimes I_n.\Big[b \otimes \bar{M}^{-1}\tau_l - (I + K_1\Lambda_1 \\ &\quad \operatorname{diag}(|\varepsilon_1^\star|^{\eta_1-1}))\bar{\varepsilon}_2^\star\Upsilon(s) - K_3 s^{\nu_1} - K_4 s^{\nu_2}\Big]\Big) + \epsilon\Xi(s_i, \sigma) \\ &\leq\; K_2\Lambda_2 \operatorname{diag}(|\varepsilon_2^\star|^{\eta_2-1}\Big[(\zeta(\mu_1\|\varepsilon_1^\star\| + \mu_2\|\varepsilon_2^\star\|) + |L_m + B\|.\sqrt{N}\bar{d}\Big]\|s\| - \|L_m + B\|\bar{\gamma} \\ &\quad \times\|L_m + B\|^{-1} \otimes I_n.\Big[b \otimes \bar{M}^{-1}\tau_l - (I + K_1\Lambda_1 \operatorname{diag}(|\varepsilon_1^\star|^{\eta_1-1}))\bar{\varepsilon}_2^\star\Big]\|s\| \; - \epsilon s^T(K_3 s^{\nu_1} \\ &\quad +K_4 s^{\nu_2}) + \epsilon s^T\Upsilon(s) + \|L_m + B\|.\sqrt{N}\bar{\vartheta}\|s\| + \epsilon\Xi(s_i, \sigma) \\ &\leq\; \varphi'\|s\| + \epsilon s^T\Upsilon(s) - \epsilon s^T(K_3 s^{\nu_1} + K_4 s^{\nu_2}) + \epsilon\Xi(s_i, \sigma), \qquad (5.38)\end{aligned}$$

where $\varphi'{=}\varphi - \|L_m + B\|\bar{\gamma}\|L_m + B\|^{-1} \otimes I_n.\Big[b \otimes \bar{M}^{-1}\tau_l - (I + K_1\Lambda_1 \operatorname{diag}(|\varepsilon_1^\star|^{\eta_1-1}))\bar{\varepsilon}_2^\star\Big] + \|L_m + B\|\sqrt{N}\bar{\vartheta}$.

Now, lets consider that when $\sigma_i\|s_i\| \geq \chi$, $\forall_i = 1,..., N$, $s^T\Upsilon(s) = \sum_{i=1}^N \sigma\|s_i\|$.

$$\begin{aligned}\dot{V}_1 \;&\leq\; \varphi'\|s\| - \epsilon\bar{\sigma}\sum_{i=1}^N \|s_i\| + \epsilon\Big[\kappa\bar{\sigma}\sum_{i=1}^N \sigma_i - 2\kappa\sum_{i=1}^N(\sigma_i)^2 - (K_3 + K_4)\sum_{i=1}^N \|s_i\|^{\bar{\nu}+1}\Big] \\ &\leq\; -(\sigma_o')\|s\| + \epsilon\rho_1. \qquad (5.39)\end{aligned}$$

Second, when $\sigma_i\|s_i\| < \chi$, $\forall_i = 1,...,N$, $s^T\Upsilon(s) = \sum_{i=1}^{N} \frac{\sigma}{\chi}\|s_i\|$.

$$\begin{aligned} \dot{V}_1 &\leq \varphi'\|s\| + \sum_{i=1}^{N}(\sigma_i - \bar{\sigma})(\|s_i\| - \kappa\sigma_i) - \sum_{i=1}^{N}\frac{\sigma_i}{\chi}\|s_i\| \\ &\leq -(\sigma_o')\|s\| - \rho_1' - \sigma_i\sum_{i=1}^{N}(\frac{1}{\chi} - \sigma_i)\|s_i\| \\ &\leq -(\sigma_o')\|s\| - \rho_2', \end{aligned} \tag{5.40}$$

with $\rho_2' = \rho_1' + \sigma_i\sum_{i=1}^{N}(\frac{1}{\chi} + \sigma_i)\|s_i\|$.

By combining Case I and Case II, the following inequality holds:

$$\begin{aligned} \dot{V}_1 &\leq -(\boldsymbol{\sigma_o'})\|\boldsymbol{s}\| + \boldsymbol{\rho'} \\ &\leq -(1-\Omega)\boldsymbol{\sigma_0'}\|\boldsymbol{s}\|. \end{aligned} \tag{5.41}$$

Hence, the boundary layer $\bar{\theta}_2$ will be reached by the sliding manifold s in finite time.

$$\bar{\theta}_2 = \left\{\|s\| \leq \frac{\sigma}{\Omega\sigma_0'}\right\}. \tag{5.42}$$

Then, as mentioned earlier that the ultimate boundedness of s indicates that $\varepsilon_1^\star$ and $\varepsilon_2^\star$ are ultimately bounded. Then it follows from Definition 1 that the tracking error system in (5.11) is CUUB. This completes the proof. □

5.4 Numerical Simulation

An analysis of numerical simulations of car-like vehicles has been conducted to verify the effectiveness of the proposed controller. Our controller can be implemented for any configuration of the networked control systems. For example, Figure 5.1 illustrates a configuration for a team of one leader and three followers, where L represents the leader, and F1-F3 represents the three followers. In the simulation, none of the followers has a direct connection with the leader except F1, which sends faded state information to F2 and F3 and receives complete state information from the leader. Hence, we have

$$A = \begin{bmatrix} 0 & 0 & 0 \\ 1 & 0 & 0 \\ 1 & 0 & 0 \end{bmatrix}, L_m = \begin{bmatrix} 0 & 0 & 0 \\ -1 & 1 & 0 \\ -1 & 0 & 1 \end{bmatrix},$$

and the diagonal matrix between the leader and follower is given by B = diag$(1, 0, 0)$.

The initial states of the leader and followers are chosen as $p_L(0)$ = (-0.6, -0.2, 0), $p_1(0)$ = (-0.8,

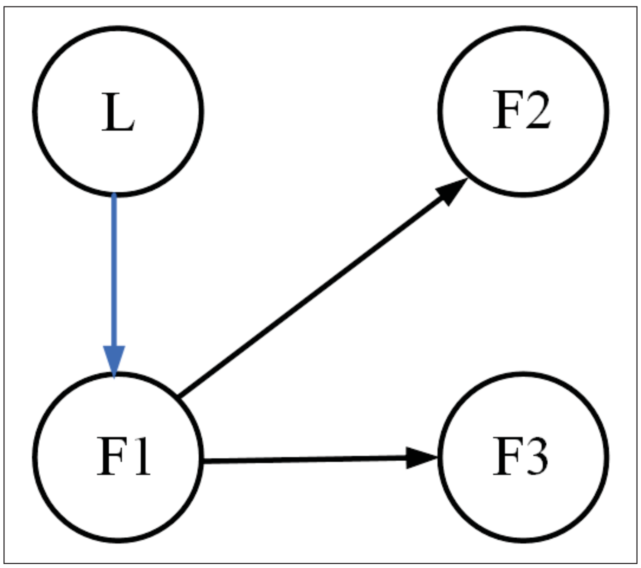

Figure 5.1 Communication topology

0.7, 0)^T, $p_2(0)$ = (-0.8, -0.6, 0)^T, $p_3(0)$ = (-0.3, -0.4, 0)^T, $v_l(0)$ = 0.26 $\frac{m}{s}$, $v_1(0)$ = 0.48 $\frac{m}{s}$, $v_2(0)$ = 1.4 $\frac{m}{s}$ and $v_3(0)$ = 0.22 $\frac{m}{s}$. The parameters of the sliding mode control (5.16) are chosen as $K_1 = 5$, $K_2 = 3$, $K_3 = 0.5$, $K_4 = 0.5$, $\mu = 2.5$, $\kappa = 0.002$ and $\xi = 0.0035$. Followers are affected by the following disturbance $d_i = 0.1sin(0.1it + \frac{i}{3}\pi)$. The identical parameters of the vehicles are given in Table 5.1.

In the simulation, follower 1 is subjected to a fading channel phenomenon from time $t = 0$ to the end of the mission. As a result, follower 2 and follower 3 only receive faded state information during the time of operation. In addition, follower 2 is exposed to the left actuator fault of $\gamma_i = 0.30$ and $\vartheta_i = 0.5 + 0.2e^{-0.1t}$ (N.m) from time $t = 0$ to the end of the mission as well.

Table 5.1 Physical parameters of vehicles

Parameters	Values	Unit
m_c	2.5	(Kg)
m_w	0.23	(Kg)
L	0.2	(m)
$2W$	0.1	(m)
I_{bzz}	0.015	(kg m^2)
I_{wzz}	0.002	(kg m^2)

Figures 5.2-5.6 show the capability of the proposed controller (5.16) in manipulating the states of the system (5.3) under the influence of the imposed faults. Figure 5.2 illustrates how the followers travel along number 8-shaped trajectories while tracking the leader's trajectory. It can be seen that the tracking and the formation are achieved successfully after a short time of starting the operation. This clearly can be observed from Figure 5.3 that the followers achieve the consensus on a common value on the x-axis while keeping the same distance from the leader. Moreover, the followers achieve a consensus and keep the same distance between each other and the leader on the y-axis. In addition, Figures 5.4-5.6 show the achievement of the consensus on the orientation, linear, and steering velocities. Figures 5.7 and 5.8 show the position and velocity tracking errors. It is obvious that the error states remain in the vicinity of zero. These results reveal the effectiveness of the proposed controller in handling the faded state information and actuator fault problems with the presence of disturbances and confirm the theoretical conclusion in Theorem 5 and Theorem 6.

Remark 2. *In this study, the real-time experiments were not conducted due to the closure of the NAV Lab for renovation works since the end of May 2022.*

5.5 Conclusion and Future Work

This study investigates cooperative control for networked systems with fading channels, actuator faults, and external disturbances. Based on the NFTSC approach, a novel control scheme is proposed in which all followers synchronize the leader with tracking errors convergent to a small

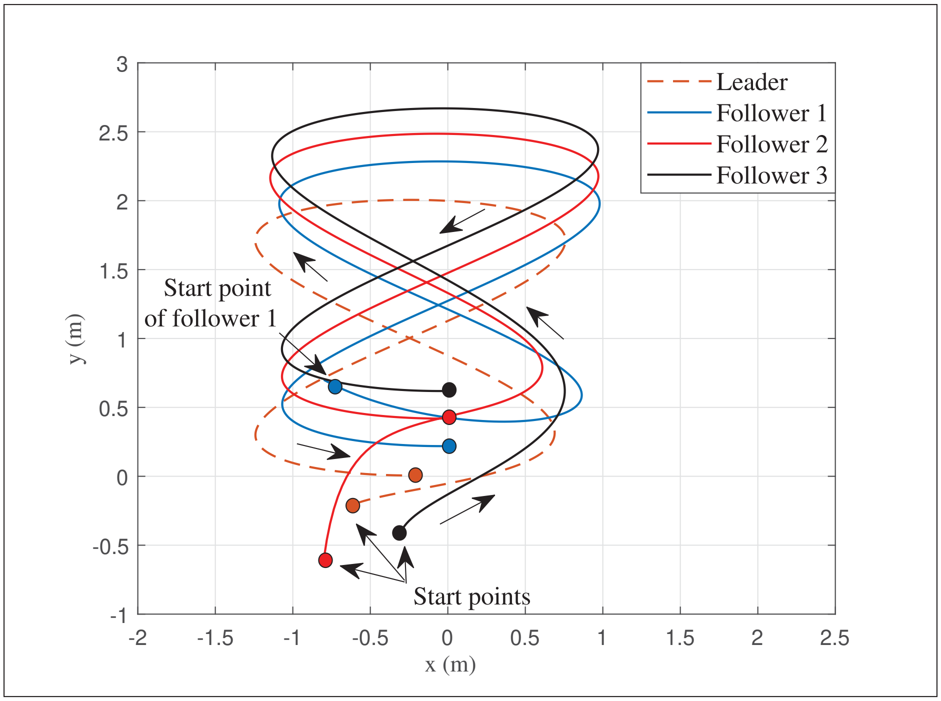

Figure 5.2 Actual trajectories of the leader and followers

area around the origin. Further, the tracking errors are shown to be uniformly bounded within a finite period of time. It has been demonstrated that the proposed adaptive sliding mode control can function effectively without prior knowledge of uncertainties or disturbances in the system. For future research, the cooperative control problem with the communication and actuator issues over dynamic communication networks is worthy of further investigation.

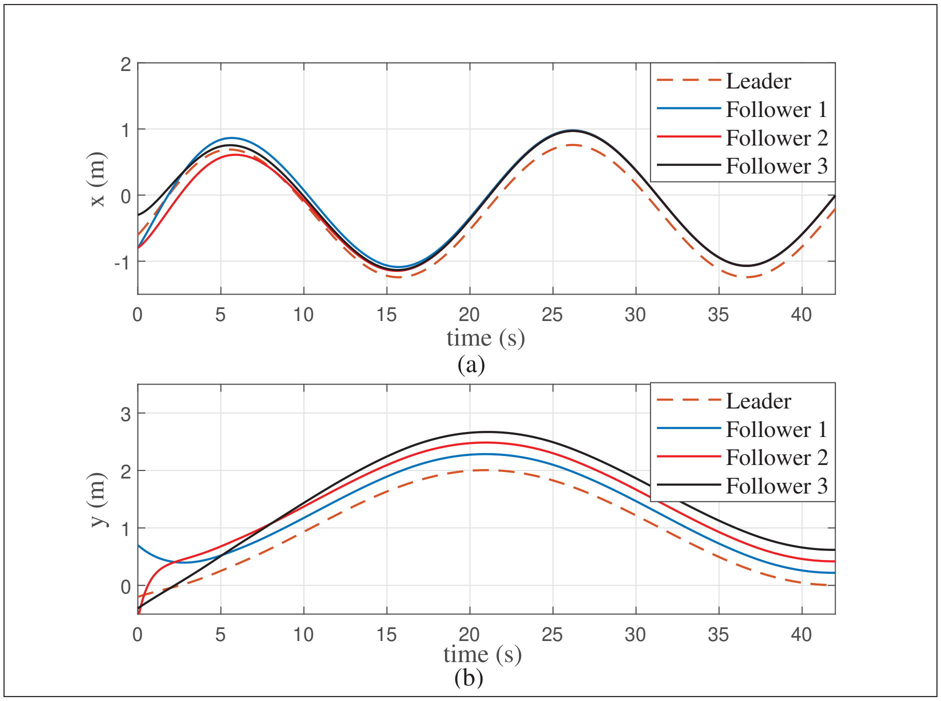

Figure 5.3 Consensus of positions. (a) Trajectories tracking on the x-axis. (a) Trajectories tracking on the y-axis

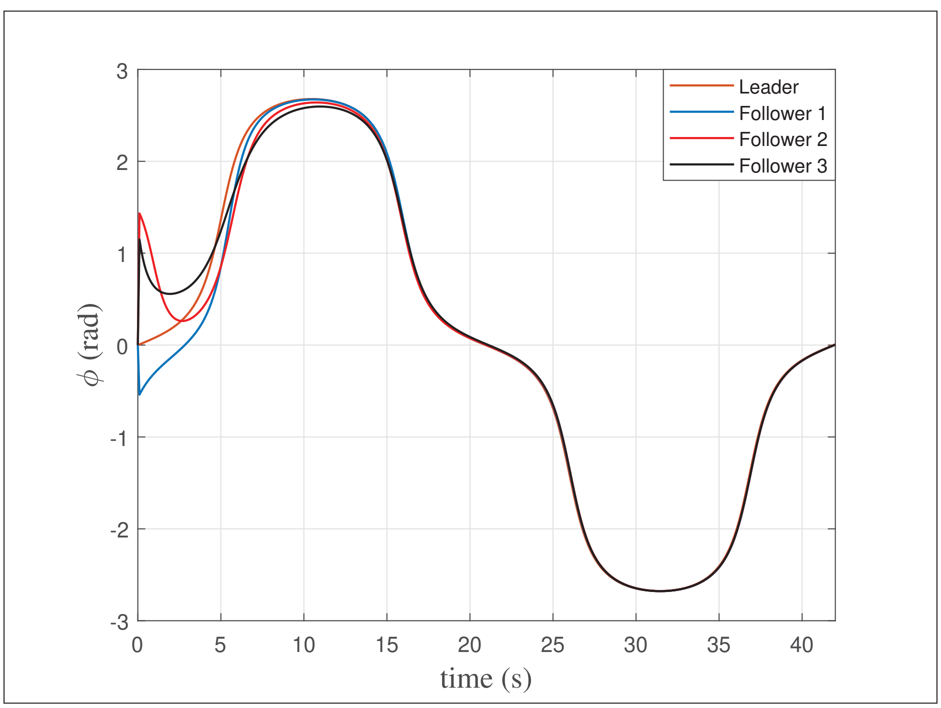

Figure 5.4 Consensus of orientations

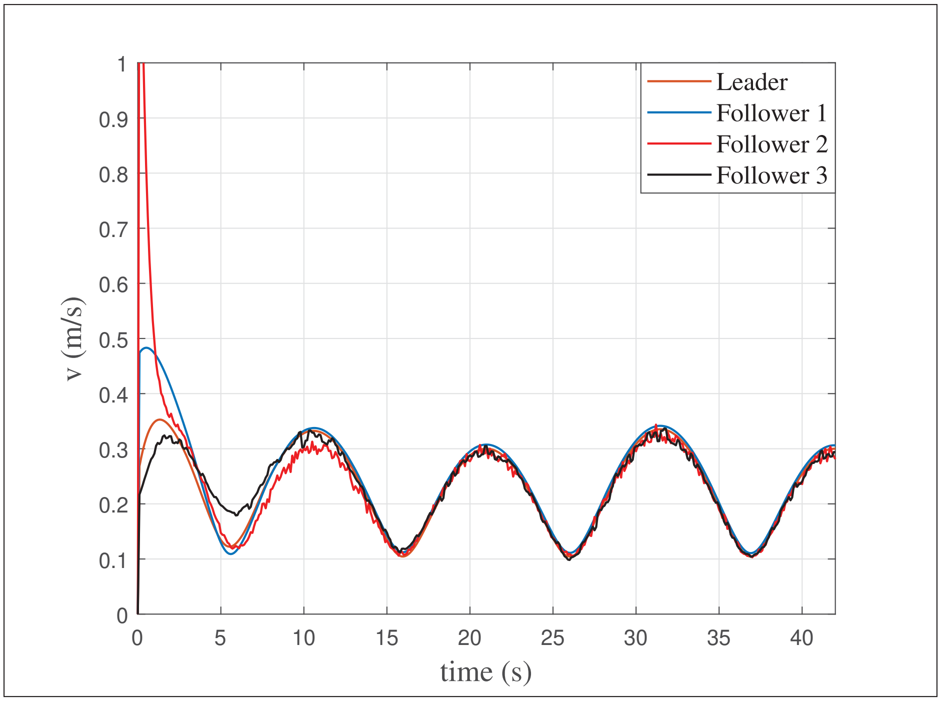

Figure 5.5 Consensus of linear velocities

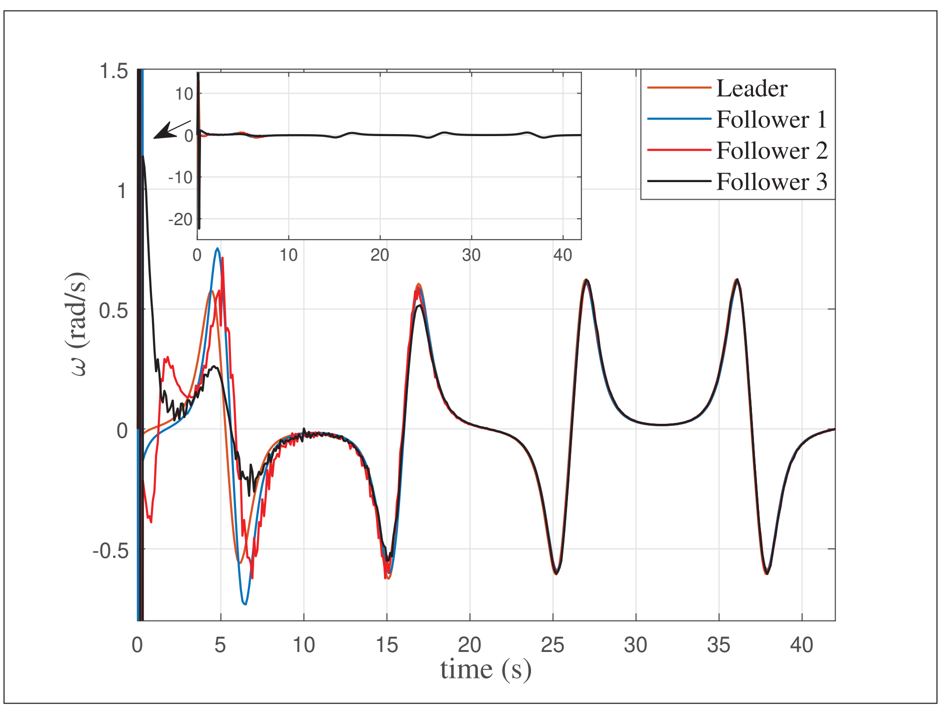

Figure 5.6 Consensus of steering velocity

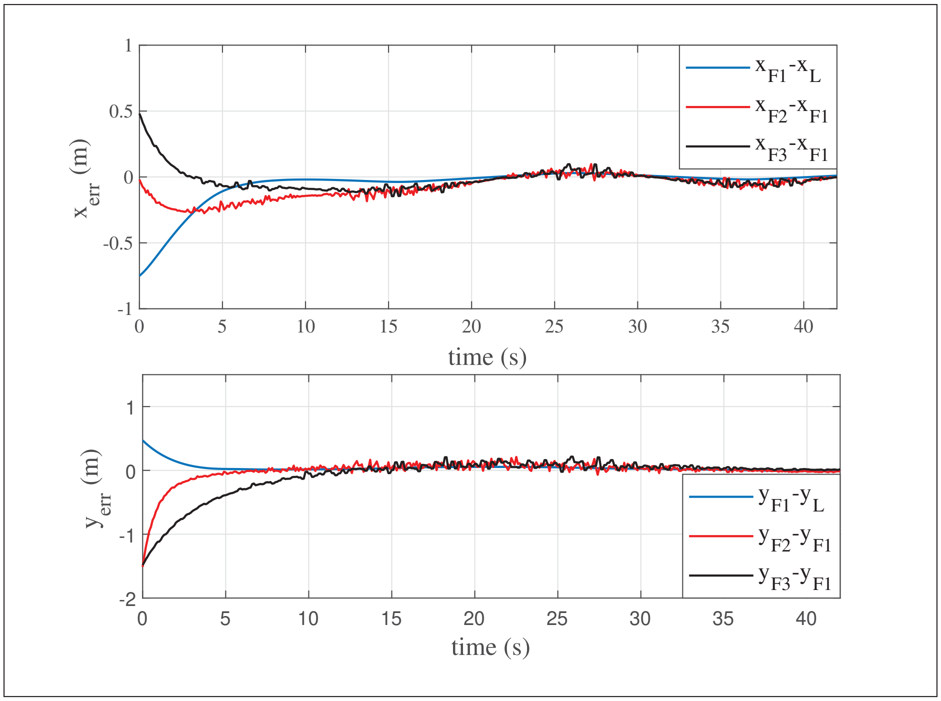

Figure 5.7 Position tracking errors

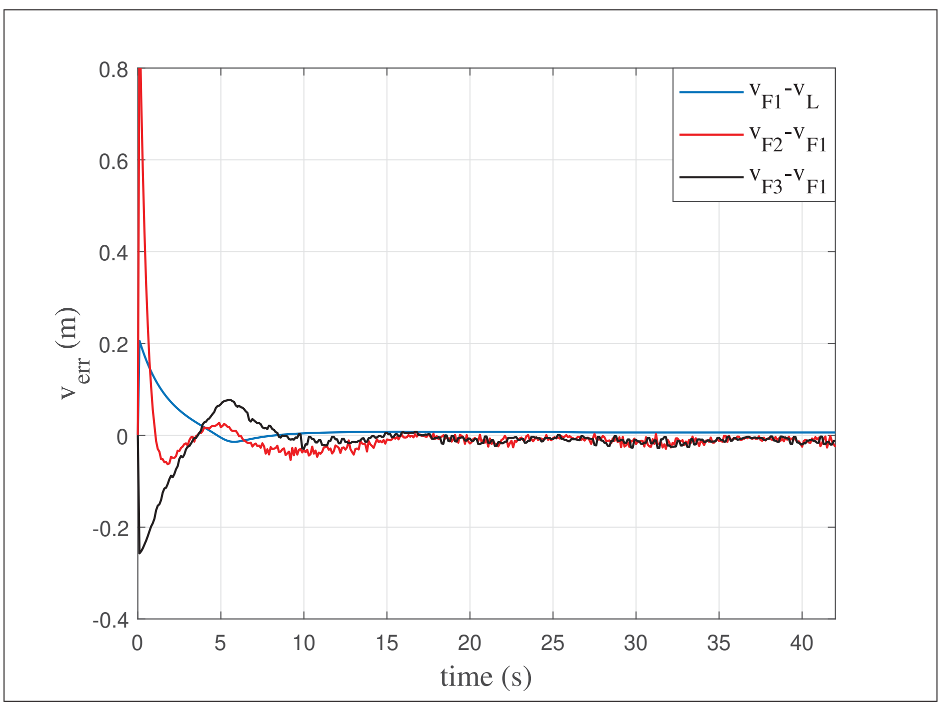

Figure 5.8 Linear velocities tracking errors

CHAPTER 6

CONCLUSIONS AND RECOMMENDATIONS

This thesis presents fault-tolerant cooperative control approaches for a team of car-like vehicles to achieve cooperative missions in fault-free and fault conditions. Two faults are investigated in our research work: (i) the actuator faults (ii) fading communication channels. Considering the limitations of the existing studies in addressing such fault conditions, three approaches have been developed in this research to compensate for the effects of these faults on the performance of the vehicles and guarantee the completion of the cooperative tasks. The successful implementation of the developed algorithms is regarded as an important aspect of the overall contribution.

In Chapter 3, a Distributed Fault-Tolerant Formation Control (DFTFC) scheme for a team of car-like vehicles is introduced to overcome the impact of the actuator problems. In the design of the DFTFC, we consider the dynamics of the actual vehicles and address both the partial and severe actuator faults problem. Moreover, we provide solutions to the re-assignment formation problem for healthy vehicles in the presence of one or more vehicles with severe/complete actuator faults. Our proposed DFTFC can reduce the computation load due to the implementation of the control algorithm in a distributed manner by each vehicle and provides an overall reliable system against the sudden changes that may occur to the actuators during the formation mission, regardless of the severity of the faults. The DFTFC scheme is designed based on a High-Order Sliding Mode (HOSM) observer to detect and isolate additive actuator faults, which are superimposed on the control signals, and the super-twisting algorithm to compensate for the impact of such actuator faults. The rigorous proofs are provided to guarantee the efficacy of the proposed DFTFC in the presence of faults under investigation. In our study, we divided the methodology into two stages. Stage 1: Designing a distributed formation controller based on the virtual vehicle approach under fault-free conditions, and Stage 2: Designing a distributed fault-tolerant formation controller for the entire system with the assumption that a partial or severe actuator fault conditions may occur in any one of the team members during the team mission. The severity level of the fault can be defined as presented by (Kamel *et al.*, 2018). In the partial fault condition, the proposed controller allows the faulty vehicle to accommodate the fault and continue the mission with the rest of the healthy ones. While in the severe fault condition, the controller excludes the faulty one from the formation and notifies the rest of the team members to reconfigure their formation to a specific pattern and continue functioning for the rest of the mission. The main contribution of this study can be summarized as follows: (i) Comparing to recently reported results in (Xu *et al.*, 2019; Yazdjerdi & Meskin, 2020; Khodabandeh *et al.*, 2021; Li *et al.*, 2023), our proposed DFTFC is more realistic to be implemented in real vehicles, and it provides a faster response to the occurrence of faults and better performance in handling both partial and severe actuator faults. In addition, it is faster in converging the vehicles to their reference trajectories after the occurrence of the faults, as demonstrated in the videos of our experimental results in (NAV Lab YouTube Channel, 2022). (ii) None of the recently reported studies solved the reconfiguration of the team formation in the presence of severe/complete actuator faults in any vehicle. In this study, we addressed this limitation and proposed a re-assignment task mechanism based on the Simplex algorithm. This algorithm is integrated with the DFTFC to ensure the convergence of the team to the desired formation pattern. As mentioned earlier, the faulty vehicle with severe faults is excluded by the DFTFC, and with the developed re-assignment algorithm, the remaining vehicles are assigned to their desired positions p_i^v. The theoretical analysis for the implementation of the re-assignment algorithm with the DFTFC has been carefully analyzed in Section 3.3. The pseudocode for the proposed DFTFC algorithm with the re-assignment task mechanism is introduced in Section 3.4. (iii) In contrast to the existing studies, the proposed DFTFC scheme is implemented in real car-like vehicles to validate the efficacy of the proposed controller in the presence of actuator fault conditions.

Chapter 4 addresses the Fault-Tolerant Cooperative Control (FTCC) problem for leader-follower networks in the presence of actuator faults and fading channels. First, we design the FTCC under the effect of a fading channel using sliding mode control. The tracking variables cannot be properly calculated with fading channel conditions. To overcome this issue, the information exchanged over the fading channel is utilized to evaluate the error of tracking variables. Using this strategy not only increases the precision of the controller's design but also provides a practical solution to the consistency problem of leader-follower networks with channel fading.

Second, we develop an FTCC approach under the influence of fading channels and actuator faults. Specifically, the multiplicative and additive actuator faults are considered in this study. The FTCC for such fault cases is designed based on the Integral Terminal Sliding Mode (ITSM) technique, which is known for its responsiveness, robustness, and stability in unknown conditions. The main contributions of this study can be summarized as follows: (i) This work introduces the first results for a team of car-like vehicles subject to simultaneous actuator faults and faded neighborhood communication information. In real applications, numerous factors will interfere with the transmission of information between agents. As a result, agents will not be able to receive precise information from neighbors but will only receive fading information. This study deals with this phenomenon as a random weakening amplitude of real state information and is expressed as a multiplicative random fading variable with a value between 0 and 1. (ii) The fading channel's effect and the vehicle dynamics' nonlinearity are carefully analyzed, providing guidelines for the fault-tolerant control design. (iii) The proposed methodology is implemented in real vehicles using the latest Quanser self-driving car (QCar) platform to validate the controller's performance in the presence of faults under investigation.

Chapter 5 discusses the cooperative control problem for a team of car-like vehicles with fading channels, actuator faults, and external disturbances. It is assumed that some followers cannot directly access the leader's states over a directed graph. A Non-singular Fast Terminal Sliding Mode Control (NFTSMC) is employed in the proposed control to speed up the consensus tracking and convergence of the entire system. This controller is developed to handle both the multiplicative and additive actuator faults as well as the multiplicative randomness of the fading channel. First, the adaptive fault-tolerant cooperative control is developed considering the presence of fading channels and external disturbances. Second, the adaptive fault-tolerant cooperative control is proposed, taking into consideration the influence of fading channels, actuator faults, and external disturbances. This controller is based on NFTSMC in order to overcome the singularity in the consensus tracking problem and provide fast convergence rates.

The main contributions of this study are as follows: (i) To the best of the authors' knowledge, the problem of the simultaneous occurrence of the fading channel and actuator faults for networked systems has not been reported. This study introduces the first results of the cooperative control problem, considering the effect of fading channel and actuator fault with the presence of external disturbances. (ii) In contrast to the existing adaptive fault-tolerant control strategies, in our developed adaptive control, the adaptive mechanism is able to modify the gain of sliding mode control automatically. This provides an advantage over a constant control gain in that the sliding mode control can function properly without prior knowledge of uncertainties and disturbances in the system. (iii) As compared to existing fault-tolerant control methods, our developed control has a simple structure and can be readily implemented in practice.

The performance measure of the three works in this thesis is evaluated by analyzing the capability of the vehicles to track their desired trajectories in fault-free and fault conditions. The analysis includes the time of the convergence rate to the reference trajectory and the error norms that provide more information about the performance of the developed controllers. However, it is worth mentioning that for the implementation of the proposed approaches in real-time experiments, we need to consider some physical limitations that can not be expressed by the mathematical models. For example, motors have some limited speed and are controlled by mathematics and algorithms with no physical limitations. Therefore, it is important to take into consideration this limitation when executing the proposed controllers in real vehicles.

Finally, we conclude that the proposed fault-tolerant cooperative control algorithms are capable of providing good performance for networked control systems in the presence of actuator faults, fading channels, and external disturbances. Furthermore, they can guarantee the successful completion of team cooperative missions in fault-free and fault conditions.

For future research, some challenging issues will need to be addressed. Considering that our proposed algorithms are designed for systems navigating in a known environment, there is a need to address the fault-tolerant control problem for systems performing cooperative tasks in more complex and unknown environments. Further, the cooperative control problem involving communication and actuator faults over dynamic communication networks is of great interest.

LIST OF REFERENCES

Aldana, C. I., Munguía, R., Cruz-Zavala, E. & Nuño, E. (2019). Pose consensus of multiple robots with time-delays using neural networks. *Robotica*, 37(5), 883–905.

Alshorman, A. M., Alshorman, O., Irfan, M., Glowacz, A., Muhammad, F. & Caesarendra, W. (2020). Fuzzy-based fault-tolerant control for omnidirectional mobile robot. *Machines*, 8(3), 55.

Andreasson, M., Dimarogonas, D. V., Sandberg, H. & Johansson, K. H. (2014). Distributed control of networked dynamical systems: Static feedback, integral action and consensus. *IEEE Transactions on Automatic Control*, 59(7), 1750–1764.

Azizi, S. M. & Khorasani, K. (2011). Cooperative actuator fault accommodation in formation flight of unmanned vehicles using relative measurements. *International Journal of Control*, 84(5), 876–894.

Balch, T. & Arkin, R. C. (1998). Behavior-based formation control for multirobot teams. *IEEE Transactions on Robotics and Automation*, 14(6), 926–939.

Balch, T. & Hybinette, M. (2000). Social potentials for scalable multi-robot formations. *Proceedings 2000 ICRA. Millennium Conference. IEEE International Conference on Robotics and Automation. Symposia Proceedings (Cat. No. 00CH37065)*, 1, 73–80.

Beard, R. W., Lawton, J. & Hadaegh, F. Y. (2001). A coordination architecture for spacecraft formation control. *IEEE Transactions on Control Systems Technology*, 9(6), 777–790.

Blanke, M., Kinnaert, M., Lunze, J., Staroswiecki, M. & Schröder, J. (2006). *Diagnosis and fault-tolerant control*. Springer.

Boskovic, J. D., Prasanth, R. & Mehra, R. K. (2007). Retrofit fault-tolerant flight control design under control effector damage. *Journal of guidance, control, and dynamics*, 30(3), 703–712.

Bu, X., Yu, W., Yu, Q., Hou, Z. & Yang, J. (2021). Event-triggered model-free adaptive iterative learning control for a class of nonlinear systems over fading channels. *IEEE Transactions on Cybernetics*, 52(9), 9597–9608.

Cai, J., Wen, C., Su, H. & Liu, Z. (2013). Robust adaptive failure compensation of hysteretic actuators for a class of uncertain nonlinear systems. *IEEE Transactions on Automatic Control*, 58(9), 2388–2394.

Cai, Y., Zhang, H., Zhang, J. & He, Q. (2020). Distributed bipartite leader-following consensus of linear multi-agent systems with input time delay based on event-triggered transmission mechanism. *ISA Transactions*, 100, 221–234.

Cao, W., Yan, J., Yang, X., Luo, X. & Guan, X. (2023). Communication-aware formation control of AUVs with model uncertainty and fading channel via integral reinforcement learning. *IEEE/CAA Journal of Automatica Sinica*, 10(1), 159–176.

Carvalho Leite, A., Schäfer, B. & de OLiveira e Souza, M. L. (2012). Fault-tolerant control strategy for steering failures in wheeled planetary rovers. *Journal of Robotics*, 2012.

Cepeda-Gomez, R. & Perico, L. F. (2015). Formation control of nonholonomic vehicles under time delayed communications. *IEEE Transactions on Automation Science and Engineering*, 12(3), 819–826.

Chamseddine, A., Zhang, Y. & Rabbath, C. A. (2012). Trajectory planning and re-planning for fault tolerant formation flight control of quadrotor unmanned aerial vehicles. *2012 American Control Conference (ACC)*, pp. 3291–3296.

Chang, C.-F. & Tsai, C.-C. (2014). Formation stabilization of nonholonomic multi-robot systems using relative distance measurements. *2014 IEEE International Conference on System Science and Engineering (ICSSE)*, pp. 1–6.

Chen, G., Song, Y. & Lewis, F. L. (2016). Distributed fault-tolerant control of networked uncertain Euler–Lagrange systems under actuator faults. *IEEE Transactions on Cybernetics*, 47(7), 1706–1718.

Chen, Y. & Sun, J. (2016). Distributed optimal control for multi-agent systems with obstacle avoidance. *Neurocomputing*, 173, 2014–2021.

Daigle, M. J., Koutsoukos, X. D. & Biswas, G. (2007). Distributed diagnosis in formations of mobile robots. *IEEE Transactions on Robotics*, 23(2), 353–369.

Das, A. K., Fierro, R., Kumar, V., Ostrowski, J. P., Spletzer, J. & Taylor, C. J. (2002). A vision-based formation control framework. *IEEE Transactions on Robotics and Automation*, 18(5), 813–825.

Davila, J., Fridman, L. & Levant, A. (2005). Second-order sliding-mode observer for mechanical systems. *IEEE Transactions on Automatic Control*, 50(11), 1785-1789. doi: 10.1109/TAC.2005.858636.

De La Cruz, C. & Carelli, R. (2006). Dynamic modeling and centralized formation control of mobile robots. *IECON 2006-32nd Annual Conference on IEEE Industrial Electronics*, pp. 3880–3885.

Defoort, M., Floquet, T., Kokosy, A. & Perruquetti, W. (2008). Sliding-mode formation control for cooperative autonomous mobile robots. *IEEE Transactions on Industrial Electronics*, 55(11), 3944–3953.

Dehshalie, M. E., Menhaj, M. B. & Karrari, M. (2019). Fault-tolerant cooperative control for affine multi-agent systems: An optimal control approach. *Journal of the Franklin Institute*, 356(3), 1360–1378.

Deng, C. & Yang, G.-H. (2019). Distributed adaptive fault-tolerant control approach to cooperative output regulation for linear multi-agent systems. *Automatica*, 103, 62–68.

Derafa, L., Benallegue, A. & Fridman, L. (2012). Super twisting control algorithm for the attitude tracking of four rotors UAV. *Journal of the Franklin Institute*, 349(2), 685–699.

Do, K. & Pan, J. (2007). Nonlinear formation control of unicycle-type mobile robots. *Robotics and Autonomous Systems*, 55(3), 191–204.

Dong, X., Xi, J., Lu, G. & Zhong, Y. (2014). Formation control for high-order linear time-invariant multiagent systems with time delays. *IEEE Transactions on Control of Network Systems*, 1(3), 232–240.

Egerstedt, M. & Hu, X. (2001). Formation constrained multi-agent control. *IEEE Transactions on Robotics and Automation*, 17(6), 947–951.

Egerstedt, M., Hu, X. & Stotsky, A. (2001). Control of mobile platforms using a virtual vehicle approach. *IEEE Transactions on Automatic Control*, 46(11), 1777–1782.

Elia, N. (2005). Remote stabilization over fading channels. *Systems & Control Letters*, 54(3), 237–249.

Eterno, J. S., Weiss, J. L., Looze, D. P. & Willsky, A. (1985). Design issues for fault tolerant-restructurable aircraft control. *1985 24th IEEE Conference on Decision and Control*, pp. 900–905.

Fagiolini, A., Babboni, F. & Bicchi, A. (2009). Dynamic distributed intrusion detection for secure multi-robot systems. *2009 IEEE International Conference on Robotics and Automation*, pp. 2723–2728.

Fax, J. A. & Murray, R. M. (2004). Information flow and cooperative control of vehicle formations. *IEEE Transactions on Automatic Control*, 49(9), 1465–1476.

Feng, Y. & Zheng, W. X. (2019). Adaptive tracking control for nonlinear heterogeneous multi-agent systems with unknown dynamics. *Journal of the Franklin Institute*, 356(5), 2780–2797.

Ferrari, R. M., Parisini, T. & Polycarpou, M. M. (2009). Distributed fault diagnosis with overlapping decompositions: An adaptive approximation approach. *IEEE Transactions on Automatic Control*, 54(4), 794–799.

Fujimori, A., Teramoto, M., Nikiforuk, P. N. & Gupta, M. M. (2000). Cooperative collision avoidance between multiple mobile robots. *Journal of Robotic Systems*, 17(7), 347–363.

Gautam, A. & Mohan, S. (2012). A review of research in multi-robot systems. *2012 IEEE 7th International Conference on Industrial and Information Systems (ICIIS)*, pp. 1–5.

Ghasemi, A., Askari Marnani, J. & Menhaj, M. (2017). Fault detection and isolation of multi-agent systems via complex Laplacian. *AUT Journal of Modeling and Simulation*, 49(1), 95–102.

Ghommam, J., Mehrjerdi, H., Saad, M. & Mnif, F. (2010). Formation path following control of unicycle-type mobile robots. *Robotics and Autonomous Systems*, 58(5), 727–736.

Guanghua, W., Deyi, L., Wenyan, G. & Peng, J. (2013). Study on formation control of multi-robot systems. *2013 Third International Conference on Intelligent System Design and Engineering Applications*, pp. 1335–1339.

Guy, S. J., Chhugani, J., Kim, C., Satish, N., Lin, M., Manocha, D. & Dubey, P. (2009). Clearpath: highly parallel collision avoidance for multi-agent simulation. *Proceedings of the 2009 ACM SIGGRAPH/Eurographics Symposium on Computer Animation*, pp. 177–187.

Hadi, B., Khosravi, A. & Sarhadi, P. (2021). A review of the path planning and formation control for multiple autonomous underwater vehicles. *Journal of Intelligent & Robotic Systems*, 101, 1–26.

Hu, B. (2021). Stochastic stability analysis for vehicular networked systems with state-dependent bursty fading channels: A self-triggered approach. *Automatica*, 123, 109352.

Hu, J., Zhang, Y. & Rakheja, S. (2021). Adaptive trajectory tracking for car-like vehicles with input constraints. *IEEE Transactions on Industrial Electronics*, 69(3), 2801–2810.

Huang, J., Farritor, S. M., Qadi, A. & Goddard, S. (2006). Localization and follow-the-leader control of a heterogeneous group of mobile robots. *IEEE/ASME Transactions on Mechatronics*, 11(2), 205–215.

Isermann, R. (2005). *Fault-diagnosis systems: An introduction from fault detection to fault tolerance*. Springer Science & Business Media.

Isermann, R. & Raab, U. (1993). Intelligent actuators—Ways to autonomous actuating systems. *Automatica*, 29(5), 1315–1331.

Ji, M., Zhang, Z., Biswas, G. & Sarkar, N. (2003). Hybrid fault adaptive control of a wheeled mobile robot. *IEEE/ASME Transactions on Mechatronics*, 8(2), 226–233.

Jin, X.-Z., Zhao, Z. & He, Y.-G. (2018). Insensitive leader-following consensus for a class of uncertain multi-agent systems against actuator faults. *Neurocomputing*, 272, 189–196.

Jin, X.-Z., Zhao, Y.-X., Wang, H., Zhao, Z. & Dong, X.-P. (2019). Adaptive fault-tolerant control of mobile robots with actuator faults and unknown parameters. *IET Control Theory & Applications*, 13(11), 1665–1672.

Ju, Y., Tian, X., Liu, H. & Ma, L. (2021). Fault detection of networked dynamical systems: A survey of trends and techniques. *International Journal of Systems Science*, 52(16), 3390–3409.

Kamel, M. A., Yu, X. & Zhang, Y. (2018). Fault-tolerant cooperative control design of multiple wheeled mobile robots. *IEEE Transactions on Control Systems Technology*, 26(2), 756-764. doi: 10.1109/TCST.2017.2679066.

Kamel, M. A., Ghamry, K. A. & Zhang, Y. (2017). Real-time fault-tolerant cooperative control of multiple UAVs-UGVs in the presence of actuator faults. *Journal of Intelligent & Robotic Systems*, 88, 469–480.

Kamel, M. A., Yu, X. & Zhang, Y. (2020). Formation control and coordination of multiple unmanned ground vehicles in normal and faulty situations: A review. *Annual Reviews in Control*, 49, 128–144.

Kanjanawanishkul, K. (2011). Formation control of mobile robots: Survey. *Journal of Engineering and Innovation*, 4(1), 50–64.

Khatib, M. & Chatila, R. (1995). An extended potential field approach for mobile robot sensor-based motions. *Proc. International Conference on Intelligent Autonomous Systems (IAS'4)*.

Khatib, O. (1986). Real-time obstacle avoidance for manipulators and mobile robots. In *Autonomous robot vehicles* (pp. 396–404). Springer.

Kheirandish, M., Yazdi, E. A., Mohammadi, H. & Mohammadi, M. (2023). A fault-tolerant sensor fusion in mobile robots using multiple model Kalman filters. *Robotics and Autonomous Systems*, 161, 104343.

Khodabandeh, S., Kharrati, H. & Hashemzadeh, F. (2021). Control for leader-follower consensus of multi-agent systems with actuator faults using decentralized robust fault-tolerant control. *Iranian Journal of Science and Technology, Transactions of Electrical Engineering*, 45, 529–541.

Khoo, S., Xie, L. & Man, Z. (2009). Robust finite-time consensus tracking algorithm for multirobot systems. *IEEE/ASME Transactions on Mechatronics*, 14(2), 219–228.

Kostić, D., Adinandra, S., Caarls, J., van de Wouw, N. & Nijmeijer, H. (2010). Saturated control of time-varying formations and trajectory tracking for unicycle multi-agent systems. *49th IEEE Conference on Decision and Control (CDC)*, pp. 4054–4059.

Kostic, D., Adinandra, S., Caarls, J. & Nijmeijer, H. (2010). Collision-free motion coordination of unicycle multi-agent systems. *Proceedings of the 2010 American Control Conference*, pp. 3186–3191.

Kumar, U. & Sukavanam, N. (2008). Backstepping based trajectory tracking control of a four wheeled mobile robot. *International Journal of Advanced Robotic Systems*, 5(4), 38.

Lafferriere, G., Williams, A., Caughman, J. & Veerman, J. (2005). Decentralized control of vehicle formations. *Systems & Control Letters*, 54(9), 899–910.

Lamiraux, F. & Lammond, J.-P. (2001). Smooth motion planning for car-like vehicles. *IEEE Transactions on Robotics and Automation*, 17(4), 498–501.

Lawton, J. R., Beard, R. W. & Young, B. J. (2003). A decentralized approach to formation maneuvers. *IEEE Transactions on Robotics and Automation*, 19(6), 933–941.

Lechevin, N., Rabbath, C. & Earon, E. (2007). Towards decentralized fault detection in uav formations. *2007 American Control Conference*, pp. 5759–5764.

Lee, G. & Chwa, D. (2018). Decentralized behavior-based formation control of multiple robots considering obstacle avoidance. *Intelligent Service Robotics*, 11, 127–138.

Leonard, N. E. & Fiorelli, E. (2001). Virtual leaders, artificial potentials and coordinated control of groups. *Proceedings of the 40th IEEE Conference on Decision and Control*, 3, 2968–2973.

Lewis, M. A. & Tan, K.-H. (1997). High precision formation control of mobile robots using virtual structures. *Autonomous Robots*, 4(4), 387–403.

Li, J. & Niu, Y. (2019). Sliding mode control subject to rice channel fading. *IET Control Theory & Applications*, 13(16), 2529–2537.

Li, W., Niu, Y. & Cao, Z. (2022). Event-triggered sliding mode control for multi-agent systems subject to channel fading. *International Journal of Systems Science*, 53(6), 1233–1244.

Li, X., Xiao, J. & Cai, Z. (2005). Backstepping based multiple mobile robots formation control. *2005 IEEE/RSJ International Conference on Intelligent Robots and Systems*, pp. 887–892.

Li, Y., Dong, S., Li, K. & Tong, S. (2023). Fuzzy adaptive fault tolerant time-varying formation control for nonholonomic multirobot systems with range constraints. *IEEE Transactions on Intelligent Vehicles*.

Liu, Y. & Passino, K. M. (2006). Cohesive behaviors of multiagent systems with information flow constraints. *IEEE Transactions on Automatic Control*, 51(11), 1734–1748.

Liu, Z., Zhang, Y., Yuan, C., Ciarletta, L. & Theilliol, D. (2019). Collision avoidance and path following control of unmanned aerial vehicle in hazardous environment. *Journal of Intelligent & Robotic Systems*, 95, 193–210.

Lu, M., Wu, J., Zhan, X., Han, T. & Yan, H. (2022). Consensus of second-order heterogeneous multi-agent systems with and without input saturation. *ISA Transactions*, 126, 14–20.

Mariottini, G. L., Morbidi, F., Prattichizzo, D., Pappas, G. J. & Daniilidis, K. (2007). Leader-follower formations: Uncalibrated vision-based localization and control. *Proceedings 2007 IEEE International Conference on Robotics and Automation*, pp. 2403–2408.

Meng, D., Jia, Y. & Du, J. (2014). Robust consensus tracking control for multiagent systems with initial state shifts, disturbances, and switching topologies. *IEEE Transactions on Neural Networks and Learning Systems*, 26(4), 809–824.

Mengji, S., Kaiyu, Q. & Li, P. (2014). Consensus of multiple mobile robot systems with directed topologies and nonuniform time delays. *2014 International Conference on Mechatronics and Control (ICMC)*, pp. 787–790.

Mesbahi, M. & Hadaegh, F. Y. (1999). Formation flying control of multiple spacecraft via graphs, matrix inequalities, and switching. *Proceedings of the 1999 IEEE International Conference on Control Applications*, 2, 1211–1216.

Meskin, N. & Khorasani, K. (2009a). Actuator fault detection and isolation for a network of unmanned vehicles. *IEEE Transactions on Automatic Control*, 54(4), 835–840.

Meskin, N. & Khorasani, K. (2009b). Fault detection and isolation of discrete-time Markovian jump linear systems with application to a network of multi-agent systems having imperfect communication channels. *Automatica*, 45(9), 2032–2040.

Monteiro, S. & Bicho, E. (2010). Attractor dynamics approach to formation control: theory and application. *Autonomous Robots*, 29(3), 331–355.

Moreno, J. A. & Osorio, M. (2008). A Lyapunov approach to second-order sliding mode controllers and observers. *2008 47th IEEE Conference on Decision and Control*, pp. 2856–2861.

Muñoz, F., Espinoza, E. S., González-Hernández, I., Salazar, S. & Lozano, R. (2019). Robust trajectory tracking for unmanned aircraft systems using a nonsingular terminal modified super-twisting sliding mode controller. *Journal of Intelligent & Robotic Systems*, 93, 55–72.

Murray, R. M. & Sastry, S. S. (1993). Nonholonomic motion planning: Steering using sinusoids. *IEEE Transactions on Automatic Control*, 38(5), 700–716.

Naseri, K., Vu, M. T., Mobayen, S., Najafi, A. & Fekih, A. (2022). Design of linear matrix inequality-based adaptive barrier global sliding mode fault tolerant control for uncertain systems with faulty actuators. *Mathematics*, 10(13), 2159.

Nguyen, N. T. & Nguyen, N. T. (2018). *Model-reference adaptive control*. Springer.

Niu, X., Liu, Y. & Man, Y. (2019). Finite-time consensus tracking for multi-agent systems with inherent uncertainties and disturbances. *International Journal of Control*, 92(6), 1415–1425.

Olfati-Saber, R. & Murray, R. M. (2004). Consensus problems in networks of agents with switching topology and time-delays. *IEEE Transactions on automatic control*, 49(9), 1520–1533.

Panagi, P. & Polycarpou, M. M. (2011). Decentralized fault tolerant control of a class of interconnected nonlinear systems. *IEEE Transactions on Automatic Control*, 56(1), 178-184. doi: 10.1109/TAC.2010.2089650.

Panagou, D., Stipanović, D. M. & Voulgaris, P. G. (2015). Distributed coordination control for multi-robot networks using Lyapunov-like barrier functions. *IEEE Transactions on Automatic Control*, 61(3), 617–632.

Pane, Y. P., Fuady, S. & Mutijarsa, K. (2013). Overtaking in centralized multi robot formation control based on pedestrian behavior. *2013 UKSim 15th International Conference on Computer Modelling and Simulation*, pp. 271–276.

Patton, R. J., Kambhampati, C., Casavola, A., Zhang, P., Ding, S. & Sauter, D. (2007). A generic strategy for fault-tolerance in control systems distributed over a network. *European Journal of Control*, 13(2-3), 280–296.

Pei, H., Zhang, J., Zhang, Y., Pei, X., Feng, S. & Li, L. (2023). Fault-tolerant cooperative driving at signal-free intersections. *IEEE Transactions on Intelligent Vehicles*, 8(1), 121–134.

Qiao, W. & Sipahi, R. (2015). Consensus control under communication delay in a three-robot system: Design and experiments. *IEEE Transactions on Control Systems Technology*, 24(2), 687–694.

Qu, G. & Shen, D. (2019). Stochastic iterative learning control with faded signals. *IEEE/CAA Journal of Automatica Sinica*, 6(5), 1196–1208.

Qu, G., Shen, D. & Yu, X. (2021). Batch-based learning consensus of multiagent systems with faded neighborhood information. *IEEE Transactions on Neural Networks and Learning Systems*.

Ren, C.-E. & Chen, C. P. (2015). Sliding mode leader-following consensus controllers for second-order non-linear multi-agent systems. *IET Control Theory & Applications*, 9(10), 1544–1552.

Ren, H., Peng, Y., Deng, F. & Zhang, C. (2018). Impulsive pinning control algorithm of stochastic multi-agent systems with unbounded distributed delays. *Nonlinear Dynamics*, 92, 1453–1467.

Ren, W. (2007). Multi-vehicle consensus with a time-varying reference state. *Systems & Control Letters*, 56(7-8), 474–483.

Ren, W. & Beard, R. W. (2004a). Decentralized scheme for spacecraft formation flying via the virtual structure approach. *Journal of Guidance, Control, and Dynamics*, 27(1), 73–82.

Ren, W. & Beard, R. W. (2004b). Formation feedback control for multiple spacecraft via virtual structures. *IEE Proceedings-Control Theory and Applications*, 151(3), 357–368.

Ren, W. & Beard, R. W. (2005). Consensus seeking in multiagent systems under dynamically changing interaction topologies. *IEEE Transactions on Automatic Control*, 50(5), 655–661.

Ren, Y., Wang, Q. & Duan, Z. (2021). Optimal distributed leader-following consensus of linear multi-agent systems: A dynamic average consensus-based approach. *IEEE Transactions on Circuits and Systems II: Express Briefs*, 69(3), 1208–1212.

Reynolds, C. W. (1987). Flocks, herds and schools: A distributed behavioral model. *Proceedings of the 14th Annual Conference on Computer Graphics and Interactive Techniques*, pp. 25–34.

Reynolds, C. W. (1999). Steering behaviors for autonomous characters. *Game Developers Conference*, 1999, 763–782.

Reynolds, C. W. (2000). Interaction with groups of autonomous characters. *Game Developers Conference*, 2000, 83.

Rezaee, H. & Abdollahi, F. (2013). A decentralized cooperative control scheme with obstacle avoidance for a team of mobile robots. *IEEE Transactions on Industrial Electronics*, 61(1), 347–354.

Rubio, F., Valero, F. & Llopis-Albert, C. (2019). A review of mobile robots: Concepts, methods, theoretical framework, and applications. *International Journal of Advanced Robotic Systems*, 16(2), 1729881419839596.

Sadowska, A., den Broek, T. v., Huijberts, H., van de Wouw, N., Kostić, D. & Nijmeijer, H. (2011). A virtual structure approach to formation control of unicycle mobile robots using mutual coupling. *International Journal of Control*, 84(11), 1886–1902.

Sanchez, J. & Fierro, R. (2003). Sliding mode control for robot formations. *Proceedings of the 2003 IEEE International Symposium on Intelligent Control*, pp. 438–443.

Semsar-Kazerooni, E. & Khorasani, K. (2010). Team consensus for a network of unmanned vehicles in presence of actuator faults. *IEEE Transactions on Control Systems Technology*, 18(5), 1155-1161. doi: 10.1109/TCST.2009.2032921.

Shankar, S., Darbha, S. & Datta, A. (2002). Design of a decentralized detection of interacting LTI systems. *Mathematical Problems in Engineering*, 8(3), 233–248.

Shen, D. (2017). Data-driven learning control for stochastic nonlinear systems: Multiple communication constraints and limited storage. *IEEE Transactions on Neural Networks and Learning Systems*, 29(6), 2429–2440.

Shen, D. & Qu, G. (2019). Performance enhancement of learning tracking systems over fading channels with multiplicative and additive randomness. *IEEE Transactions on Neural Networks and Learning Systems*, 31(4), 1196–1210.

Shen, D. & Xu, J.-X. (2018). Distributed learning consensus for heterogenous high-order nonlinear multi-agent systems with output constraints. *Automatica*, 97, 64–72.

Shen, D. & Yu, X. (2020). Learning tracking over unknown fading channels based on iterative estimation. *IEEE Transactions on Neural Networks and Learning Systems*, 33(1), 48–60.

Shen, Q., Jiang, B., Shi, P. & Zhao, J. (2014). Cooperative adaptive fuzzy tracking control for networked unknown nonlinear multiagent systems with time-varying actuator faults. *IEEE Transactions on Fuzzy Systems*, 22(3), 494-504. doi: 10.1109/TFUZZ.2013.2260757.

Shtessel, Y., Edwards, C., Fridman, L. & Levant, A. (2014). *Sliding Mode Control and Observation*. Springer, New York.

Stancu, A., Codres, E. & Puig, V. (2016). A fault hiding approach for the sliding mode fault-tolerant control of a non-holonomic mobile robot. *2016 3rd conference on control and fault-tolerant systems (SysTol)*, pp. 7–14.

Sun, D., Wang, C., Shang, W. & Feng, G. (2009). A synchronization approach to trajectory tracking of multiple mobile robots while maintaining time-varying formations. *IEEE Transactions on Robotics*, 25(5), 1074–1086.

Tanner, H. G. & Kumar, A. (2005). Towards decentralization of multi-robot navigation functions. *Proceedings of the 2005 IEEE International Conference on Robotics and Automation*, pp. 4132-4137. doi: 10.1109/ROBOT.2005.1570754.

Tanner, H. G., Pappas, G. J. & Kumar, V. (2004). Leader-to-formation stability. *IEEE Transactions on Robotics and Automation*, 20(3), 443–455.

NAV Lab YouTube Channel. (2022). QCar experiments for distributed fault-tolerant control designs. Retrieved from: https://www.youtube.com/watch?v=14bSpO3e0T0.

Thumati, B. T., Dierks, T. & Sarangapani, J. (2012). A model-based fault tolerant control design for nonholonomic mobile robots in formation. *The Journal of Defense Modeling and Simulation*, 9(1), 17–31.

Wang, F., Zhang, Y., Zhang, L., Zhang, J. & Huang, Y. (2020). Finite-time consensus of stochastic nonlinear multi-agent systems. *International Journal of Fuzzy Systems*, 22, 77–88.

Wang, G., Wang, C., Cai, X. & Ji, Y. (2018). Distributed leaderless and leader-following consensus control of multiple Euler-Lagrange systems with unknown control directions. *Journal of Intelligent & Robotic Systems*, 89, 439–463.

Wang, Q. & Wang, J. (2018). Fully distributed fault-tolerant consensus protocols for Lipschitz nonlinear multi-agent systems. *IEEE Access*, 6, 17313–17325.

Wang, X. (2020). Active fault tolerant control for unmanned underwater vehicle with actuator fault and guaranteed transient performance. *IEEE Transactions on Intelligent Vehicles*, 6(3), 470–479.

Wang, X., Zeng, Z. & Cong, Y. (2016). Multi-agent distributed coordination control: Developments and directions via graph viewpoint. *Neurocomputing*, 199, 204-218. doi: https://doi.org/10.1016/j.neucom.2016.03.021.

Wei, L., Chen, W.-H., Luo, S. & Huang, G. (2022). Impulsive average-consensus of multi-agent systems with time-delays. *Journal of the Franklin Institute*, 359(2), 1544–1568.

West, D. B. (2001). *Introduction to graph theory*. Prentice hall Upper Saddle River.

Wu, L.-B., Yang, G.-H. & Ye, D. (2014). Robust adaptive fault-tolerant control for linear systems with actuator failures and mismatched parameter uncertainties. *IET Control Theory & Applications*, 8(6), 441–449.

Wu, X. & Huang, Y. (2022). Adaptive fractional-order non-singular terminal sliding mode control based on fuzzy wavelet neural networks for omnidirectional mobile robot manipulator. *ISA Transactions*, 121, 258–267.

Wu, Z.-G., Xu, Y., Lu, R., Wu, Y. & Huang, T. (2017). Event-triggered control for consensus of multiagent systems with fixed/switching topologies. *IEEE Transactions on Systems, Man, and Cybernetics: Systems*, 48(10), 1736–1746.

Xiao, B., Yin, S. & Gao, H. (2017). Reconfigurable tolerant control of uncertain mechanical systems with actuator faults: A sliding mode observer-based approach. *IEEE Transactions on Control Systems Technology*, 26(4), 1249–1258.

Xiao, F. & Wang, L. (2006). State consensus for multi-agent systems with switching topologies and time-varying delays. *International Journal of Control*, 79(10), 1277–1284.

Xu, D., Zhang, X., Zhu, Z., Chen, C. & Yang, P. (2014a). Behavior-based formation control of swarm robots. *Mathematical Problems in Engineering*, 2014.

Xu, K. & Song, P. (2010). A coordination framework for weakly centralized mobile robot teams. *The 2010 IEEE International Conference on Information and Automation*, pp. 77–82.

Xu, L., Zheng, J., Xiao, N. & Xie, L. (2018). Mean square consensus of multi-agent systems over fading networks with directed graphs. *Automatica*, 95, 503–510.

Xu, L.-X., Wang, Y.-L., Wang, X. & Peng, C. (2022). Decentralized event-triggered adaptive control for interconnected nonlinear systems with actuator failures. *IEEE Transactions on Fuzzy Systems*, 31(1), 148–159.

Xu, M., Yang, P., Huang, Y., Shu, Q. & Wang, Y. (2019). Fault-tolerant consensus control of second-order multi-agent system based on sliding mode control theory. *The Journal of Engineering*, 2019(15), 555–560.

Xu, Q., Yang, H., Jiang, B., Zhou, D. & Zhang, Y. (2014b). Fault tolerant formations control of UAVs subject to permanent and intermittent faults. *Journal of Intelligent & Robotic Systems*, 73(1-4), 589–602.

Xu, Y., Sun, J., Wu, Z.-G. & Wang, G. (2021). Fully distributed adaptive event-triggered control of networked systems with actuator bias faults. *IEEE Transactions on Cybernetics*, 52(10), 10773–10784.

Yaghoubi, Z. & Talebi, H. A. (2020). Cluster consensus for nonlinear multi-agent systems. *Journal of Intelligent & Robotic Systems*, 100(3-4), 1069–1084.

Yan, X.-G. & Edwards, C. (2008). Robust decentralized actuator fault detection and estimation for large-scale systems using a sliding mode observer. *International Journal of control*, 81(4), 591–606.

Yang, H., Staroswiecki, M., Jiang, B. & Liu, J. (2011). Fault tolerant cooperative control for a class of nonlinear multi-agent systems. *Systems & Control Letters*, 60(4), 271–277.

Yazdjerdi, P. & Meskin, N. (2020). Fault tolerant controller schemes for single and multiple mobile robots. *Soft Computing in Condition Monitoring and Diagnostics of Electrical and Mechanical Systems: Novel Methods for Condition Monitoring and Diagnostics*, 3–56.

Yoshioka, C. & Namerikawa, T. (2008). Formation control of nonholonomic multi-vehicle systems based on virtual structure. *IFAC Proceedings Volumes*, 41(2), 5149–5154.

Yu, D. & Ji, X. Y. (2018). Finite-time containment control of perturbed multi-agent systems based on sliding-mode control. *International Journal of Systems Science*, 49(2), 299–311.

Yu, H., Chen, X., Chen, T. & Hao, F. (2019a). Event-triggered bipartite consensus for multiagent systems: A Zeno-free analysis. *IEEE Transactions on Automatic Control*, 65(11), 4866–4873.

Yu, Z., Qu, Y. & Zhang, Y. (2018). Distributed fault-tolerant cooperative control for multi-UAVs under actuator fault and input saturation. *IEEE Transactions on Control Systems Technology*, 27(6), 2417–2429.

Yu, Z., Qu, Y. & Zhang, Y. (2019b). Fault-tolerant containment control of multiple unmanned aerial vehicles based on distributed sliding-mode observer. *Journal of Intelligent & Robotic Systems*, 93, 163–177.

Yu, Z., Zhang, Y., Jiang, B. & Yu, X. (2021). Fault-tolerant time-varying elliptical formation control of multiple fixed-wing UAVs for cooperative forest fire monitoring. *Journal of Intelligent & Robotic Systems*, 101, 1–15.

Yu, Z. & Zhang, W. (2023). Almost sure consensus of stochastic nonlinear multi-agent systems via event-triggered control. *Nonlinear Dynamics*, 111(4), 3469–3478.

Zhang, B., Sun, X., Liu, S., Lv, M. & Deng, X. (2021). Event-triggered adaptive fault-tolerant synchronization tracking control for multiple 6-DOF fixed-wing UAVs. *IEEE Transactions on Vehicular Technology*, 71(1), 148–161.

Zhang, H. & Lewis, F. L. (2012). Adaptive cooperative tracking control of higher-order nonlinear systems with unknown dynamics. *Automatica*, 48(7), 1432–1439.

Zhang, M., Shen, Y., Wang, Q. & Wang, Y. (2010). Dynamic artificial potential field based multi-robot formation control. *2010 IEEE Instrumentation & Measurement Technology Conference Proceedings*, pp. 1530–1534.

Zhang, T. & Li, J. (2017). Iterative learning control for multi-agent systems with finite-leveled sigma-delta quantization and random packet losses. *IEEE Transactions on Circuits and Systems I: Regular Papers*, 64(8), 2171–2181.

Zhang, X. (2010). Decentralized fault detection for a class of large-scale nonlinear uncertain systems. *Proceedings of the 2010 American Control Conference*, pp. 5650–5655.

Zhang, X. & Zhang, Q. (2011). Distributed fault detection and isolation in a class of large-scale nonlinear uncertain systems. *IFAC Proceedings Volumes*, 44(1), 4302–4307.

Zhang, X., Polycarpou, M. M. & Parisini, T. (2001). Integrated design of fault diagnosis and accommodation schemes for a class of nonlinear systems. *Proceedings of the 40th IEEE Conference on Decision and Control (Cat. No. 01CH37228)*, 2, 1448–1453.

Zhang, X. & Quan, Y. (2022). Fractional non-singular fast terminal sliding mode control based on disturbance observer. *Int. J. Innov. Comput. Inf. Control*, 18(1), 93–104.

Zhang, Y., Yang, X., Wei, P. & Liu, P. X. (2020). Fractional-order adaptive non-singular fast terminal sliding mode control with time delay estimation for robotic manipulators. *IET Control Theory & Applications*, 14(17), 2556–2565.

Zhang, Y. & Chamseddine, A. (2012). Fault tolerant flight control techniques with application to a quadrotor UAV testbed. *Automatic Flight Control Systems-Latest Developments*, 5, 119–150.

Zhang, Y. & Jiang, J. (2003). Fault tolerant control system design with explicit consideration of performance degradation. *IEEE Transactions on Aerospace and Electronic Systems*, 39(3), 838–848.

Zhang, Y. & Jiang, J. (2006). Issues on integration of fault diagnosis and reconfigurable control in active fault-tolerant control systems. *IFAC Proceedings Volumes*, 39(13), 1437–1448.

Zhang, Y. & Jiang, J. (2008). Bibliographical review on reconfigurable fault-tolerant control systems. *Annual Reviews in Control*, 32(2), 229-252.

Zhang, Y. & Mehrjerdi, H. (2013). A survey on multiple unmanned vehicles formation control and coordination: Normal and fault situations. *2013 International Conference on Unmanned Aircraft Systems (ICUAS)*, pp. 1087–1096.

Zhang, Z., Chen, S. & Zheng, Y. (2019). Leader-following scaled consensus of second-order multi-agent systems under directed topologies. *International Journal of Systems Science*, 50(14), 2604–2615.

Zhou, K., Doyle, J. C., Glover, K. et al. (1996). *Robust and optimal control*. Prentice hall New Jersey.

Zhu, L., Li, X., Huang, D., Dong, H. & Cai, L. (2023). Distributed cooperative fault-tolerant control of high-speed trains with input saturation and actuator faults. *IEEE Transactions on Intelligent Vehicles*, 8(2), 1241–1251.

Zohar, I., Ailon, A. & Guterman, H. (2012). Tracking Controllers for Single and Group of Unmanned Aerial Vehicles Under Various Wind Conditions. *Proceedings of International Conference on Intelligent Unmanned Systems*, 8.

Zou, Y., Su, X., Li, S., Niu, Y. & Li, D. (2019). Event-triggered distributed predictive control for asynchronous coordination of multi-agent systems. *Automatica*, 99, 92–98.

Zuo, Z., Zhang, J. & Wang, Y. (2014). Adaptive fault-tolerant tracking control for linear and Lipschitz nonlinear multi-agent systems. *IEEE Transactions on Industrial Electronics*, 62(6), 3923–3931.

Zuo, Z. & Tie, L. (2016). Distributed robust finite-time nonlinear consensus protocols for multi-agent systems. *International Journal of Systems Science*, 47(6), 1366–1375.